5. Development of compression-coated pulsatile release (PR) formulations

Now-a-day, the growth of compression coating technology is steadily intensifying in the field of PR formulations. The technology offers several advantages like isolation of incompatible ingredients, protection of light/acid/moisture sensitive drugs, continuous and solvent-less processing etc (1, 2). The technology can be efficiently employed for designing of chronotherapeutic PR dosage forms to target the drug release at specific site or predetermined time (3-6).

5.1. QbD enabled development of PR compression-coated tablets (CCTs) of prednisone (PRS)

5.1.1. PRS drug profile (7-13)

PRS is a well-known corticosteroid which is used for the treatment of a number of chronic and acute disorders such as RA, BA, congenital adrenal hyperplasia, allergic rhinitis, hepatitis, systemic lupus erythematosus, allograft rejection and several infectious, hematological, neurological, cardiac, metabolic, GI, dermal as well as malignant diseases and numerous inflammatory conditions.

Physicochemical characteristics (7-9, 12)

Molecular Formula: $C_{21}H_{26}O_5$

Chemical Name: 17α,21-dihydroxypregna-1,4-diene-3,11,20-trione.

Structure:
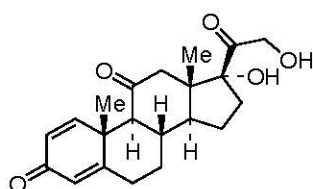
Molecular weight: 358.4 g/mol

Appearance: White to almost white, crystalline powder

Solubility: Practically insoluble in water, slightly soluble in ethanol and in methylene chloride.

Melting point: 233-235 °C with decomposition

Nature: Neutral

pKa: None

Log P: 1.5

Dose: 1-50 mg

BCS class: I (borderline)

Mechanism of action: PRS, having glucocorticoid receptor agonistic activity, metabolizes by hepatic microsomes to form prednisolone, an active metabolite. Prednisolone after entering into the cytoplasm, binds with the cytoplasmic receptors with high affinity which leads to inhibition of leucocyte infiltration at the inflammatory site and interfere with the release of inflammatory mediator. This results into the suppression of humoral immunity which leads to decrease in odemea and scar formation. Various other mediator such as Phospholipase A2, lipocortins that regulates the biosynthesis of potent inflammatory mediators like prostaglandins and leukotrienes can be efficiently inhibited through the several glucocorticoids including prednisolone (11).

Pharmacokinetics (7, 10)

Absorption: Rapidly and almost completely absorbed from GI tract.

Peak effect: 1–2 h

Duration of action: 1.25–1.5 days

Plasma half life: 3.4-3.8 h

Bioavailability: The systemic availability averages 80–100%. For very high oral doses (>50mg), slightly low between 62%-74% has been reported.

Protein binding: The drug binds to plasma proteins relatively low (<50%) which is non linear and dose dependent.

Permeability: Using artificial phospholipid membranes, a permeability coefficient of 0.3×10^{-6} cm/s has been reported.

Distribution: PRS follows dose-dependent nonlinear pharmacokinetics. The reported volume of distribution is 0.4–1 L/kg.

Metabolism and Excretion: More than 80 % of the PRS is converted to prednisolone by first-pass hepatic metabolism. The ratio of PRS to prednisolone is approximately 1:6 to 1:10. Negligible amounts of PRS and prednisolone are found unchanged in the urine. The plasma clearance of PRS ranged from 572 ml/min/1.73m^2 for the 5 mg oral dose to 2271 ml/min/1.73 m^2 for the 50 oral mg dose.

Indications and dosage: PRS is used over a wide range of dose. Low dose corticosteroid treatment includes doses up to 10 mg/day, with generally recommended amount at about 5–7.5 mg/day. The dosage has to be individualized and is highly variable relying upon the type and seriousness of the disease, and on patient response. There is no absolute highest dosage, however, frequency and intensity of side effects is

seen to increase with rise in dosage. PRS is not considered as a narrow therapeutic index drug and usually monitoring of blood levels is not necessary. However, severe diseases which need very high drug doses, it may be advisable to monitor the blood concentrations. Based on physico-chemical, pharmacokinetic and pharmacodynamic properties, it was suggested that, a false biowaiver decision is highly unlikely if the test product satisfies appropriate criteria of *in vitro* analysis (7, 11).

Drug withdrawal approach for long term corticosteroid therapy: A special contemplation should be given in PRS therapy is to take after proper withdrawal procedures in chronically treated patients with high drug doses. The strategy of withdrawal relies on duration of treatment and possibility of the disease to relapse. The patients who have received systemic corticosteroids for over three weeks at high doses, the withdrawal should be gradual so as to permit the HPA axis to recover (14). Sudden withdrawal of systemic corticosteroid, which has continued for up to 3 weeks, might be suitable if the disease is implausible to relapse (15, 16) and unlikely to lead HPA-axis inhibition (17). However, low-dose corticosteroid treatment can usually be ended without dose tapering procedure (7). So, the proposed lower dose formulation can also be helpful to replace the higher dose therapy assisting dose tapering approach.

Contraindications: PRS is contraindicated in systemic fungal infections (13).

Adverse Effects: Corticosteroid therapy has number of adverse effects such as adrenal suppression, dermal thinning, growth suppression, Cushing's syndrome, hypertension, cataracts and muscle weakness. Chronic use of corticosteroid can also result in immunologic attenuation with loss of delayed-type sensitivity, reduced immunoglobulin G (IgG) levels without alteration in functional antibody response, potential for reactivation of latent tuberculosis infection, and possible increased risk for infection, especially the development of severe varicella (18). Further, psychologic disturbances, peptic ulcer disease, aseptic necrosis of bone, atherosclerosis and diabetes mellitus can also occur. Apart from them, PRS therapy also leads to electrolyte and fluid disturbances including sodium retention, congestive heart failure in susceptible patients, hypokalemic alkalosis, hypertension and potassium loss (13). Since high-dose systemic corticosteroids can be immunosuppressive, such treatment requires appropriate steps to monitor and prevent the infection (18-20). Hence, when a Glucocorticoid therapy is needed, a balance between adverse effects and therapeutic

benefits is attempted, and administration of minimal effective dose for shortest duration of time is recommended to avoid the adverse effects (21).

Corticotherapy timing according to biological rhythms to optimize treatment goals: Knowledge of the circadian rhythm of the HPA axis is important to optimize the impact of synthetic corticosteroids, whether they are employed to treat BA, RA or any other cortico-dependent diseases like substitution therapy for Addison's disease. The dosing of synthetic corticosteroids late in the afternoon or evening, by whatever route of delivery, inhibits pituitary production of ACTH during consequent 24-hour spans, resulting in adrenocortical suppression (22). The release of glucocorticoids varies notably over the 24 hour span; the peak plasma level usually occurs at very beginning of the day while lowest is at early to mid-sleep span (i.e. around 12 midnight). The rational timing of corticosteroid dosing should be at daily peak of cortisol secretion. Thus, in diurnally active individuals, a morning dosing of corticosteroids has proven to be best tolerated as compared to other treatment times (i.e. evening or afternoon) which produces neither adrenal inhibition nor suppression of the adrenocortical circadian rhythmicity (22).

However, this approach while targeting to early morning chronological attacks (i.e. BA and RA) requires a bit higher amount of dose to extend its effects up to next morning; which in turn will enhance severe dose dependent side effects of corticosteroids. So, the compromised conventional therapy suggests night time IR dosing prior to sleep for targeting early morning attacks which however leads to HPA axis suppression. Instead of this compromised approach, designing of PR formulations which would release the drug at around 2-3 am, can be more beneficial in targeting the early morning chronological attacks. For instance, Arvidson *et al.* found that administration of low doses of prednisolone (5 or 7.5 mg daily) at 2 am was advantageous in the treatment of RA (23). In another study, hydrocortisone dosing during the usual sleep span at 3 am has proven to be most efficacious in the treatment of congenital adrenal hyperplasia (24). Thus, proposed PDDS of PRS can be considered as rather convincing approach for management of early morning chronological attacks.

5.1.2. Methods (PRS)

5.1.2.1. Analytical method for determination of PRS

5.1.2.1.1. Determination of PRS by UV spectrophotometry

Initially, UV spectrophotometric method was developed and validated for determination of PRS to be used in some preliminary trials.

5.1.2.1.1.1. Preparation of standard stock solutions of PRS

Accurately weighed quantity of drug (100 mg) was dissolved in 100 mL of methanol to obtain stock solution of 1000 µg/mL. An aliquot of 10 mL of this stock solution was further diluted to 100 mL with 50:50% v/v methanol:water to obtain working standard solution of 100 µg/mL.

5.1.2.1.1.2. Preparation of calibration curve of PRS

Varying concentrations of drug solutions (2-25 µg/mL) were prepared from 100 µg/mL working standard solution using water as a diluent. The solutions were analyzed by UV spectrophotometer (UV1700, Shimadzu, Kyoto, Japan) using 1 cm quartz cuvettes. The absorbance was measured at 242 nm and calibration curve was plotted for absorbance vs. concentration (µg/mL) as shown in Table 5.1. No interference of excipients was found at specified detection wavelength. The overlaid calibration spectra are depicted in Figure 5.1 and corresponding linearity curve, regression equation and correlation coefficient are depicted in Figure 5.2. Accuracy, precision and ruggedness were carried out as per International Conference on Harmonization (ICH) guidelines (25) and their respective results are depicted in Table 5.2, Table 5.3 and Table 5.4. The limit of detection (LOD) and limit of quantification (LOQ) were respectively determined using Eq. 5.1 and Eq. 5.2. Overall results of validation parameters are demonstrated in Table 5.5.

LOD = 3.3 (Standard Deviation (SD) of intercept) / slope   (5.1)

LOQ = 10 (SD of intercept) / slope   (5.2)

Table 5.1 Calibration curve and regression equation of PRS obtained using UV spectrophotometric method

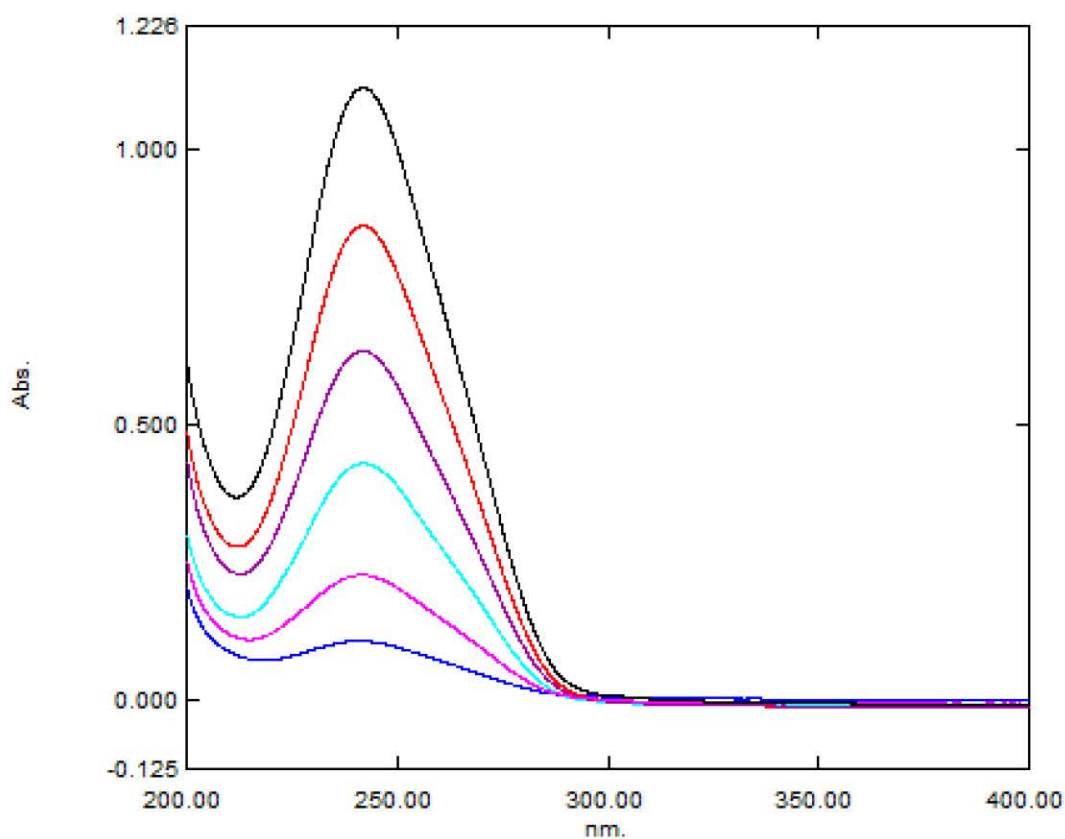| Concentration (µg/mL)	Abs at 242 nm (mean±SD; n=5)
2	0.10611±0.00185
5	0.22694±0.00140
10	0.44226±0.00233
15	0.65549±0.00085
20	0.88192±0.00148
25	1.11334±0.00105
Regression equation	
Slope	0.04377±0.00003
Intercept	0.00932±0.00166
Correlation coefficient	0.9996

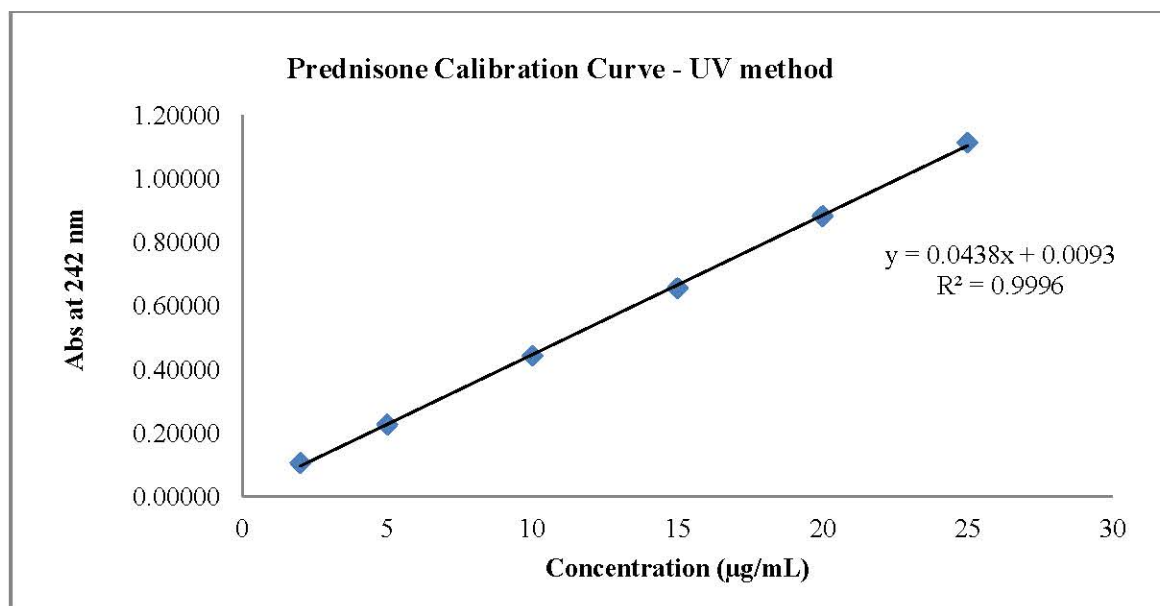Fig. 5.1 Overlaid UV spectra of 2-25 µg/mL PRS in water

Fig. 5.2 UV calibration curve of PRS (2-25 µg/mL)

Table 5.2 Accuracy data of PRS obtained using UV spectrophotometric method

Amount spiked (mg)	Amount recovered (mg) (mean±SD; n=3)	% recovery (mean± SD; n=3)	% recovery (range; n=3)	Average % recovery
5	4.99±0.05	99.8±1.06	98.7-100.8	
10	10.01±0.09	100.1±0.94	99.2-101.1	99.7
15	14.87±0.12	99.2±0.80	98.4-100.0	

Table 5.3 Precision data of PRS obtained using UV spectrophotometric method

Concentration (µg/mL)	Repeatability (% RSD; n=3)	Intra-day (% RSD; n=3)	Inter-day (% RSD; n=3)
5	0.66	0.98	1.31
10	0.42	0.71	0.95
15	0.31	0.40	0.75

Table 5.4 Ruggedness data of PRS obtained using UV spectrophotometric method

Concentration (µg/mL)	% RSD; n=2
5	1.45
10	1.24
15	0.91

Table 5.5 Summary of validation parameters of PRS UV spectrophotometric method

Parameters	Results
Linearity range	2-25 µg/mL
Correlation coefficient	0.9996
Accuracy (% recovery)	98.4-101.1 %
Precision (% RSD; n=3)	
Repeatability	0.31-0.66 %
Intra-day	0.40-0.98 %
Inter-day	0.75-1.31 %
Ruggedness (% RSD; n=2)	0.91-1.45 %
LOD	0.125 µg/mL
LOQ	0.380 µg/mL

5.1.2.1.2. Determination of PRS by RP-HPLC method

The RP-HPLC method was further developed for determination of PRS in various formulation trials. The chromatographic conditions and various parameters are enlisted in Table 5.6.

5.1.2.1.2.1. Preparation of standard stock solutions of PRS

Accurately weighed quantity of drug (100 mg) was dissolved in 100 mL of methanol to obtain the stock solution of 1000 µg/mL. An aliquot of 10 mL of this stock solution was further diluted to 100 mL with mobile phase to obtain working standard solution of 100 µg/mL.

### 5.1.2.1.2.2. Preparation of calibration curve of PRS

Varying concentrations of drug solutions (1-20 µg/mL) were prepared from 100 µg/mL working standard solution using mobile phase as diluent. The solutions were analyzed with Kromasil C18 column using an isocratic HPLC coupled with UV detector (LC-20AT/SPD-20A, Shimadzu, Kyoto, Japan). The samples were injected through a Rheodyne 7725 injector valve fixed with 20 µL loop. The mobile phase was vacuum filtered through 0.22 µm nylon membrane filter followed by degassing with an ultrasonicator prior to use. The detection was performed at 240 nm and calibration curve was plotted for area vs. concentration (µg/mL) as shown in Table 5.7. The data acquisition and integration was performed using Spinchrome software (Spincho Biotech, Vadodara, India). The system suitability criteria complied with United States Pharmacopoeia (USP) limits (26). The overlaid calibration chromatograms are depicted in Figure 5.3 and corresponding linearity curve, regression equation and correlation coefficient are depicted in Figure 5.4. Accuracy, precision and ruggedness were carried out as per ICH guidelines (25) and their results are respectively depicted in Table 5.8, Table 5.9 and Table 5.10. The LOD and LOQ were determined using Eq. 5.1 and Eq. 5.2 respectively. Overall summary of validation results are depicted in Table 5.11.

Table 5.6 Chromatographic conditions for determination of PRS

Stationary phase:	C18, 250 mm, 4.6 mm, 5 µm
Mobile phase:	60:5:35 % v/v/v mixture of 10 mM phosphate buffer: methanol: acetonitrile
Flow rate:	1 mL/min
Detection wavelength:	240 nm
Temperature:	≈ 25°C
Injection volume:	20 µL
Retention time:	6.52±0.04 min
Asymmetry factor:	1.212±0.011
Theoretical plates:	14589±125.12

Table 5.7 Calibration curve and regression equation of PRS obtained using HPLC method

Concentration (µg/mL)	Area (mV.s) (mean±SD; n=5)
1	33.432±0.593
2	65.834±1.035
5	153.782±1.186
10	320.433±1.998
15	465.716±1.452
20	629.021±2.830
Regression equation	
Slope	31.268±0.098
Intercept	1.840±0.541
Correlation coefficient	0.9997
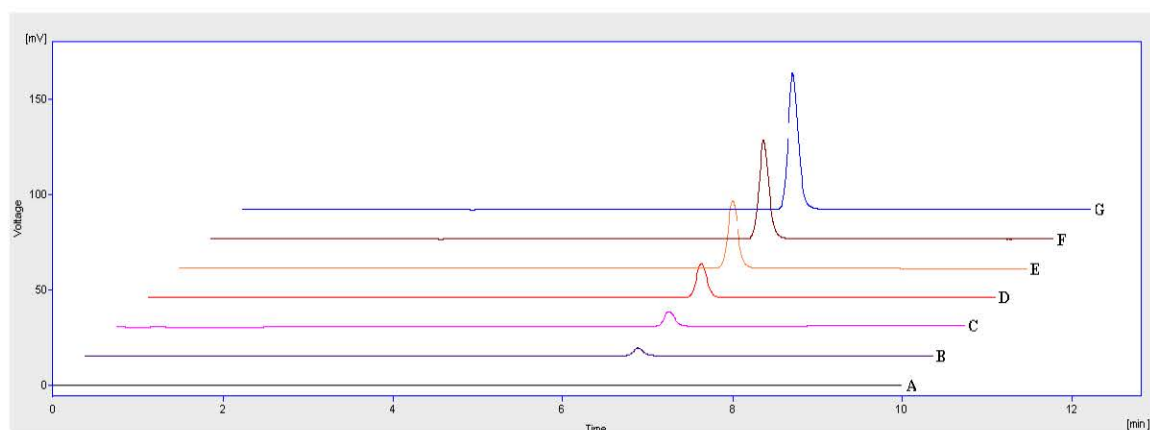
Fig. 5.3 Overlain HPLC chromatograms of 1-20 µg/mL PRS; (A) blank, (B) 1 µg/mL, (C) 2 µg/mL, (D) 5 µg/mL, (E) 10 µg/mL, (F) 15 µg/mL and (G) 20 µg/mL
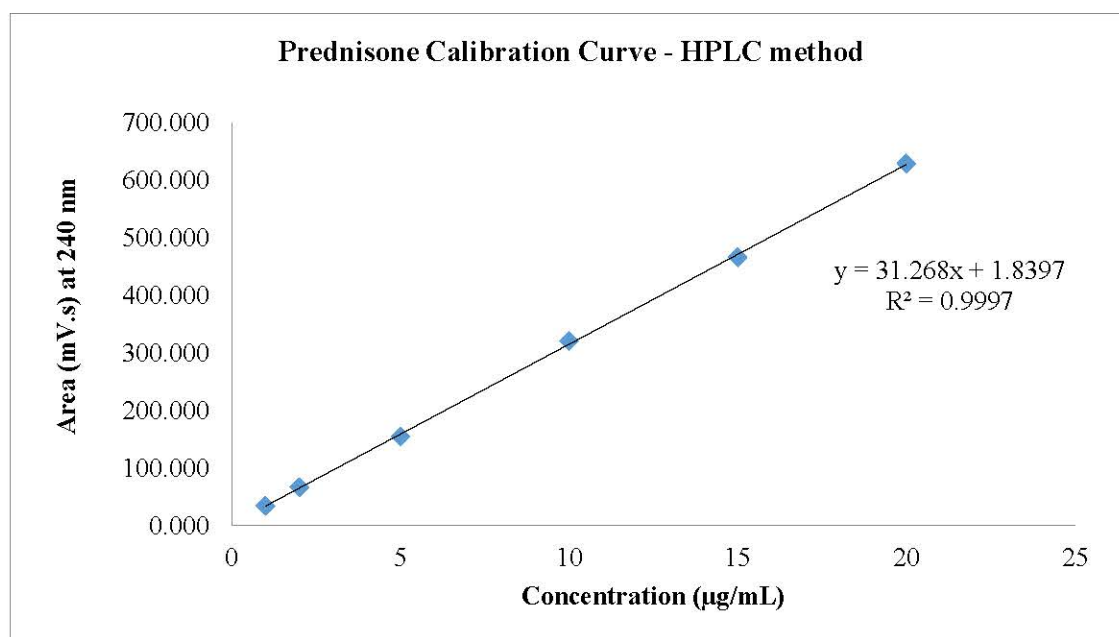
Fig. 5.4 HPLC calibration curve of PRS (1-20 µg/mL)

Table 5.8 Accuracy data of PRS obtained using HPLC method

Amount spiked (mg)	Amount recovered (mg) (mean±SD; n=3)	% recovery (mean±SD; n=3)	% recovery (range; n=3)	Average % recovery
5	4.97±0.04	99.4±0.80	98.6-100.2	
10	10.08±0.06	100.8±0.59	100.1-101.2	99.7
15	14.83±0.06	98.9±0.43	98.4-99.2	

Table 5.9 Precision data of PRS obtained using HPLC method

Concentration (µg/mL)	Repeatability (% RSD; n=3)	Intra-day (% RSD; n=3)	Inter-day (% RSD; n=3)
5	0.26	0.76	1.12
10	0.18	0.59	0.45
15	0.12	0.13	0.38

Table 5.10 Ruggedness data of PRS obtained using HPLC method

Concentration (µg/mL)	% RSD; n=2
5	0.83
10	0.64
15	0.53

Table 5.11 Summary of validation parameters of PRS HPLC method

Parameters	Results
Linearity range	1-20 µg/mL
Correlation coefficient	0.9997
Accuracy (% recovery)	98.4-101.2 %
Precision (% RSD; n=3)	
Repeatability	0.12-0.26 %
Intra-day	0.13-0.76 %
Inter-day	0.38-1.12 %
Ruggedness (% RSD; n=2)	0.53-0.83 %
LOD	0.057 µg/mL
LOQ	0.173 µg/mL

5.1.2.2. Establishment of Quality Target Product Profile (QTPP)

The template for target product profile (TPP) has been provided by United States Food and Drug Administration (USFDA) guidance that elucidates the parts of TPP for new drug applications (27). The target product quality profile is enlisted as the quality properties that a drug product ought to possess so as to fulfil the objectives set in TPP as quantitative attributes (28). ICH Q8 (R2) reiterates the TPP as QTPP (29). The QTPP is a vital element of QbD approach and forms the basis for systematic product development (30). ICH defines QTPP as *"A prospective summary of the quality characteristics of a drug product that ideally will be achieved to ensure the desired quality, taking into account safety and efficacy of the drug product"* (29). Thus, by beginning with the end in mind, it is possible to obtain a robust formulation with an acceptable control strategy that ensures desired performance of the drug product. For systemic development of a product, the QTPP elements should be explicitly defined before initiating development activities. The QTPP for desired PR formulation is depicted in Table 5.12.

Table 5.12 QTPP of desired PR formulation

QTPP element	Target	Justification
Dosage form	Compression-coated tablet for time-controlled pulsatile release	Tablet – commonly accepted unit solid oral dosage form; Compression coating – to achieve desired lag time for time-controlled release; solvent-less and continuous processing, favourable in terms of formulation stability and productivity.
Route of administration	Oral	Dosage form designed to administer orally; most acceptable route of administration
Dose	Lower dose (5 mg)	Drug is only released when required – this approach requires relatively lower amount of dose. Lower dose minimises metabolic load, dose dependent side effects as well as long term drug withdrawal effects.
Quality drug product attributes	Drug release: 4-6 h of lag time followed by sharp burst release i.e. >85% within 30 min	Administration of the formulation before going to bed will restrict the drug release for 4-6 h followed by burst release to have peak effect explicitly in the early morning hours.
	Physical attributes	No physical defects like chipping, capping, lamination etc.
	Assay: 95-105 %; Content uniformity: 90-110 %; weight variation: ±5%	Meeting the quality standards.
	Stability: Short term (3 months) stability on accelerated (40°C/75% RH) and long term (25°C/60% RH) conditions.	Minimum time period (at least 3 months) decided to study stability of optimized formulation.
Container closure system	Suitable for storage and stability of formulation	To maintain product quality and integrity up to target shelf life.

5.1.2.3. Identification of Critical Quality Attributes (CQAs) and their Risk assessment

Risk based compliance is an imperative FDA initiative for current Good Manufacturing Practice (cGMP) for 21st century (31). ICH Q9 guidance document has introduced the concept of quality risk management for communicating, evaluating, reviewing and controlling the risks to the quality of drugs throughout product life cycle (32). According to ICH *"A CQA is a quality attribute (a physical, chemical, biological or microbiological property or characteristic) that must be controlled (directly or indirectly) to ensure the product meets its intended stability, safety, efficacy and performance"* (32). The CQAs relies upon type of the formulation, dosage form designed, employed methodology of production etc.; and selected amongst several possible options. Subsequently, formulation and process development typically carried out by employing empirical prior knowledge and small scale feasibility studies. The identification of CQAs is carried out using QTPP elements based on the severity of harm caused by the product falling outside the acceptable range for that attribute.

5.1.2.4. Risk assessment by Failure Mode and Effects Analysis (FMEA)

An overall risk of the formulation or process variables can be assessed using an FMEA technique (32). The FMEA analysis helps to gather current knowledge in a systemic way and permits the information on risk assessment to be stored for future use. In this technique, the failure modes are ranked for the management of risk according to three priorities – i.e. seriousness of failure or their consequences, how frequently they occur and how easily they can be detected. The relative risk for each critical formulation or process attribute was ranked according to its priority and risk priority number (RPN) was calculated using Eq. 5.3 as mentioned below (33, 34). The attributes with major impact on the drug product quality ought to be studied in detail whereas the attributes with minor impact do not require further investigation.

$$RPN = [S] \times [O] \times [D] \qquad (5.3)$$

Where S is the severity of failure, which is a measure of how severely the effect would cause to a failure mode – can be ranked as 1 (negligible or no effect), 2 (minor), 3 (serious), 4 (critical) and 5 (catastrophic). The parameter O is the probability of occurrence or the likelihood of an event to occur – can be ranked as 1 (improbable to occur), 2 (remote), 3 (occasional), 4 (probable) and 5 (frequent). The parameter D is the

detectability of failure that is the ease with which a failure mode can be detected – can be ranked as 1 (easily detectable or absolutely certain), 2 (highly detectable), 3 (moderately detectable), 4 (remotely detectable) and 5 (hard to detect or absolutely uncertain).

5.1.2.5. Drug-excipient compatibility

Drug-excipient compatibility was investigated using Differential Scanning Calorimetry (DSC) and Fourier Transform Infra-Red (FT-IR) spectroscopy study.

5.1.2.5.1. DSC study

DSC was used for investigating any incompatibility between drug and excipients. Pure drug and physical mixture of drug and excipients were crimped in a standard aluminum pan and heated from 40°C to 300°C at a heating rate of 10°C/min under continuous purging of dry nitrogen at 40 mL/min. DSC thermograms were obtained using an automatic thermal analyzer (DSC-60, Shimadzu, Kyoto, Japan). Temperature calibration was carried out using indium as standard. An empty pan, sealed in the same way as sample, was used for reference.

5.1.2.5.2. FTIR study

FTIR study was further undertaken in order to examine any chemical interaction between drug and excipients. The FTIR (Alpha-T, Bruker Optik, Mumbai, India) spectra of pure drug and physical mixture of drug and excipients were analyzed using KBr disk method. In brief, the procedure involved mixing of 2% w/w of sample with dry KBr; homogenous mixing by grinding into mortar; which was finally compressed with a hydraulic press at 10000 psi to obtain a disk. Each disk was scanned using FTIR instrument (16 scans at 4 mm/s speed with a resolution of 2 cm^{-1} over range of 400–4000 cm^{-1} wave number) to obtain the characteristic peaks.

5.1.2.6. Preparation of PRS core tablets

The core tablet was prepared by direct compression method as per the composition shown in Table 5.13. Since sharp burst release after specific lag time was the main target of final formulation, the core tablets were meant to be fast disintegrating with help of classical swelling excipients chosen meticulously. An accurately weighed quantity of PRS, microcrystalline cellulose (MCC), lactose monohydrate and sodium

starch glycolate (SSG) were sifted through ASTM #36 and further blended at 15 rpm for 10 min. Subsequently, colloidal SiO_2 was sifted through ASTM #60 and blended at 15 rpm for 5 min. Finally, magnesium stearate (MgSt) was sifted through ASTM #60 and blended at 15 rpm for 5 min. The homogeneous blend was processed for tablet compression using an eight station automatic rotary tablet press (JM-8, General Machinary Co., Mumbai, India) equipped with standard concave punches of 5.5 mm diameter to a target weight of 100 mg/tab and 4-6 kp hardness.

Table 5.13 List of ingredients and their respective concentrations employed for formulation of PRS core tablets

Ingredients	mg/tab (%w/w)
Drug	5 mg
MCC	38 mg
Lactose	53 mg
SSG	3 mg
Colloidal SiO_2	0.5 mg
MgSt	0.5 mg
Total weight	100 mg

5.1.2.7. Characterization of PRS core tablets

The core tablets were characterized for appearance, hardness, thickness, weight variation, friability, disintegration time, assay, content uniformity (CU) and drug release. The weight variation was carried out with twenty tablets using an electronic weighing balance (AX120, Shimadzu, Kyoto, Japan). The disintegration time was measured for six tablets using a disintegration test apparatus (VTD-DV, Veego Instruments Co., Mumbai, India). Tablet hardness was determined for six tablets using a dial type tablet hardness tester (Scientific Engineering Co., Delhi, India). Friability was analyzed using a friability test apparatus (VFT-2D, Veego Instruments Co., Mumbai, India) by rotating it at 25 rpm for 4 min. For assay, twenty units were powdered and weight equivalent to 20 mg of drug was analyzed using developed HPLC method. CU was determined using ten individual units. Drug release study was carried out using 500 mL of pH 6.8 USP phosphate buffer with USP type I (basket) apparatus (VDA-6DR, Veego Instruments Co., Mumbai, India) operated at 100 rpm agitation and $37\pm0.5°C$ temperature. Further, the dissolution was also performed in purified water keeping all other conditions constant. Moreover, the effect of apparatus change on drug

release was examined by performing the release studies using USP type II (paddle) apparatus with 500 mL of purified water as dissolution medium at 100 rpm agitation and 37±0.5°C temperature. All drug release studies were carried out using degassed dissolution medium. The release profile was obtained for six tablets at 5, 10, 15, 30, 45 and 60 min sampling intervals. At each point, 5 mL sample was withdrawn which was subsequently replaced with equivalent amount of fresh medium. The withdrawn samples were filtered through 0.45 μm membrane filter and analyzed for drug content using developed HPLC method.

5.1.2.8. Preparation of PRS CCTs

The most critical facet of a PR formulation is the lag time which can be scrupulously contrived by fabricating a rupturable outer coat, using the mixtures of water soluble and water insoluble materials, around a swellable core (35-38). Nonetheless, targeting early morning attacks with a PR formulation necessitates a robust time-controlled lag time which must not be easily affected by biological variations especially those induced through variations in pH. Hence, it was foremost decided to develop the outer coat using pH-independent excipients solely.

Predominantly, ethylcellulose (EC) was selected as pH-independent water insoluble material to fabricate the rupturable outer coat (39). As per the stated purpose, i.e. compression, free flowing and directly compressible EC grade, Aqualon EC N10, was opted for the study. Here, preliminary studies were conducted for the selection of optimal lubricant, glidant and hydrophilic additive. For the same, various blends were prepared and compression coating was performed on previously devised core tablets as per below mentioned procedure.

Initially, EC and hydrophilic additive were individually sifted through ASTM#36 and blended at 15 rpm for 10 min to obtain a homogenous mass. The mass was further blended with glidant (sifted through ASTM#60) at 15 rpm for 5 min and finally blended with lubricant (sifted through ASTM#60) at 15 rpm for 5 min. Such homogeneous blends were processed for compression coating on previously formulated core tablets. The compression was accomplished on rotary tablet press equipped with 9.0 mm standard concave punches using two equal halves of 240 mg blend to obtain the final CCT of 340 mg. Sequentially, half of the blend (120 mg) was added into die cavity followed by core tablet placement at the centre which was, in turn, covered with

remaining half (120 mg) of blend and finally compressed at 13 kp target hardness (range 11.5-14.5 kp).

5.1.2.9. Characterization of PRS CCTs

The CCTs were characterized for appearance, weight variation, thickness, hardness, friability, assay, and drug release. The weight variation, hardness, thickness, friability, and assay were determined in the same manner as mentioned for the core tablets. Initial formulation development and optimization of lag time was carried out using 500 mL of 0.1 N hydrochloric acid (HCl) for first 2 h followed by pH 6.8 phosphate buffer as dissolution medium with basket apparatus operated at 100 rpm agitation and 37.0±0.5°C temperature. The optimized formulation was further evaluated at different dissolution conditions such as multi-media, change in apparatus, change in agitation intensity and biorelevant dissolution testing since it was reviewed that change in dissolution medium, apparatus and/or agitation intensity may also affect drug release profile (40). The multi-media dissolutions were carried out using purified water, 0.1 N HCl, pH 4.5 acetate buffer, and pH 6.8 phosphate buffer. The effect of apparatus change was examined by switching to paddle apparatus operated at 100 rpm agitation with 500 mL of purified water as dissolution medium. Further, the effect of change in agitation intensity was tested with paddle apparatus operated at 50 rpm agitation using 500 mL of purified water. Next, three biorelevant media, i.e. fasted state simulated gastric fluid (FaSSGF), fasted state simulated intestinal fluid (FaSSIF), and fed state simulated intestinal fluid (FeSSIF), were employed to check the performance of the optimized formulation in biorelevant conditions. All three biorelevant media were prepared from simulated intestinal fluid (SIF) powder (QMB Innovation Centre, London, UK), a marketed available product containing bile salts and phospholipids. Moreover, the optimized formulation was assessed for alcohol-induced dose dumping study at five different levels i.e. 5%, 10%, 20%, 30%, and 40% v/v ethanol in 0.1 N HCl for first 2 h followed by pH 6.8 phosphate buffer. Both, biorelevant and alcohol-induced dose dumping studies were carried out with 500 mL media volume using paddle apparatus operated at 100 rpm agitation and 37.0±0.5°C temperature. The dissolution profile was obtained using six dosage units and the data was recorded at every 1 h of repeated interval up to complete release of drug. In each case, the time to rupture the outer coating was observed visually and noted down. After rupture of outer coat (visual observation), additional data points were taken at every 15 min of repeated

interval up to complete release of drug to examine burst release pattern after lag time. Here, lag time was considered as the time up to which the release was less than 5%. At each point, 5 mL sample was withdrawn and equivalent amount of fresh medium was replaced. Each withdrawn samples were filtered through a 0.45 μm membrane filter and analyzed by an RP-HPLC method. Scanning electron microscopy (SEM) images (JSM-5610LV, Jeol Ltd., Tokyo, Japan) were taken to examine the surface characteristics of CCTs. Many times, polymer cross linking upon stability may also alter the release behaviour of a formulation (40). Hence, the optimized CCTs were subjected to curing study by exposing them at 60°C for 24 h in hot air oven and subsequently analyzed for appearance, hardness, assay, and drug release testing.

5.1.2.10. Packaging and stability study (PRS CCTs)

The optimized formulation was subjected to short term stability testing according to ICH guidelines (41). Forty CCTs along with a silica bag were packed into high density polyethylene bottles with induction cap sealing. The sealed bottles were subjected to accelerated (40±2°C/75±5% RH) and long term (25±2°C/60±5% RH) stability studies for three months. The samples were periodically withdrawn at 0, 30, 60, and 90 days interval and examined for appearance, hardness, assay, and drug release.

5.1.3. Results and discussion (PRS)

5.1.3.1. QTPP

The QTPP elements of desired time-controlled PR formulation with their respective justifications are stated in Table 5.12. The key feature was 4-6 h of lag time followed by sharp burst release i.e. >85% within 30 min. The time-controlled lag time was attempted through the help of the outer coat made from pH-independent excipients whereas sharp burst release was sought by formulating fast dissolving IR core. The QTPP elements made the basis for determining CQAs which were the prerequisites for establishing risk assessment matrix.

5.1.3.2. Identification of CQAs and their risk assessment

Overall formulation/process parameters were divided in two parts i.e. core tablet elements and coating elements and CQAs were identified as demonstrated in Table 5.14. The CQAs were further assessed for risk based matrix analysis to understand the impact of formulation variables and unit operations on drug product quality attributes. Here, the assessment was carried out to determine which formulation/process components have high risk of impact on drug product attributes (28, 32). Table 5.15 demonstrates initial risk assessment matrix for identification of impact of formulation variables on drug product attributes whereas Table 5.16 demonstrates initial risk assessment matrix for identification of impact of unit operations on drug product attributes. The justifications for initial risk assessment of formulation variables are depicted in Table 5.17 whereas those of process variables are depicted in Table 5.18.

Table 5.14 Identification of CQAs for desired compression-coated PR formulation

Quality attribute of the drug products		Target	Is it a CQA?	Justification
Core tablet elements				
Physical Attributes	Appearance	No physical defects	No	Core tablet will be covered by secondary coating – not critical
	Odor	No unpleasant odor	No	Core tablet will be covered by secondary coating – not critical
	Friability of core tablets	Not more than 0.5% w/w	No	Target has been set to meet compendial standards; friability will not impact patient safety or efficacy – not critical
	Core tablet Hardness	Depending upon drug release profile and excipients	Yes	Core tablet hardness may affect lag time/burst release of final CCT and thereby affect product safety or efficacy – critical
Assay		95% -105% of the label claim	Yes	Changes in the formulation or process variables may affect assay; which in turn can affect safety/efficacy – critical
CU		90% -110% of the label claim	Yes	Variability in CU affects safety/efficacy; since dose is low (5 mg) – critical
Drug release		>85% within 30 min	Yes	It will ensure burst release pattern after completion of lag time; both formulation and process variables can greatly impact the dissolution profile; failure to meet this specification will directly impact patient safety and/or efficacy – critical
Coating elements				
Physical Attributes	Appearance	No physical defects	No	Color, shape and appearance are set to ensure patient acceptability and not directly linked to patient safety and/or efficacy – not critical
	Odor	No unpleasant odor	No	Odor is linked to patient acceptability and have no impact on safety/efficacy; neither drug nor excipients have unpleasant odor – not critical
	Friability of final CCT	Not more than 0.5% w/w	No	Target has been set to meet compendial standards; friability will not impact patient safety/efficacy – not critical
	CCT Hardness	Depends on CCT release profile and excipients	Yes	Tablet hardness modulates drug release profile which further affects product safety and/or efficacy – critical

Assay	95% -105% of the label claim	No	Drug is incorporated in the core formula for which assay is considered as a CQA; further, compression coating with inert excipients will not impact assay of the final CCT – not critical
CU	90% -110% of the label claim	No	Same as assay, CU is also considered as CQA for core tablets; further compression coating with inert excipients will not affect CU of the final CCT – not critical
Drug release	4-6 h of lag time followed by burst release i.e. >85% within 30 min	Yes	Both formulation and process variables can highly affect the dissolution profile. Hence, it will be observed throughout the formulation development and optimization; failure to meet this specification will directly affect patient safety and/or efficacy – critical

Table 5.15 Initial risk analysis matrix for identification of impact of formulation ingredients on drug product attributes

Core tablet elements				
CT CQAs[*]	Fillers	Super-disintegrant	Glidant	Lubricant
CT Hardness	Medium	Low	Low	Medium
Assay	Low	Low	Low	Low
CU	Low	Low	Low	Low
CT release profile	Low	High	Low	Medium
Coating elements				
CCT CQAs[#]	Core tablet attributes	Hydrophilic pore former	Coating weight	Glidant	Lubricant
CCT Hardness	Low	Low	Low	Low	Medium
CCT release profile	High	High	High	High	High

CT CQAs[*] Core Tablet critical quality attributes; CCT CQAs[#] Compression-coated tablet critical quality attributes

Table 5.16 Initial risk analysis matrix for identification of impact of unit operations on drug product attributes

Core tablet elements				
CT CQAs[*]	Sifting	Blending	Compression	Compression coating
CT Hardness	Low	Low	High	Medium
Assay	Low	Medium	Medium	Low
CU	Low	Medium	Medium	Low
CT release profile	Low	Medium	High	Medium
Coating elements				
CCT CQAs[#]	Sifting	Blending	Compression	
CCT Hardness	Low	Low	High	
CCT release profile	Low	Low	High	

CT CQAs[*] Core Tablet critical quality attributes; CCT CQAs[#] Compression-coated tablet critical quality attributes

Table 5.17 Justifications for initial risk assessment of formulation variables on drug product attributes

Formulation variable	Drug product CQA	Risk category	Justification	Proposed action
Fillers (core)	CT Hardness	Medium	Filler type and its concentration can impact tablet compactability and its hardness. Associated risk is medium.	Appropriate filler type and its concentration to be selected to achieve optimum hardness.
	Assay	Low	Fillers affect flow properties of the blend which in turn can impact core tablet Assay/CU. However, in order to have proper flow, free flowing fillers which are suitable for direct compression process would only be selected. Associated risk is low.	No action required
	Content uniformity (CU)	Low		
	CT drug release profile	low	Fillers can impact compactability/ tablet hardness and thereby dissolution. However, since the target was fast dissolving IR core, the fillers would be selected with typical swellable/soluble properties which would result in a rapidly disintegrating tablet with fast dissolving release profile. Associated risk is low.	No action required
Super disintegrant (core)	CT Hardness	Low	The quantity of super-disintegrant would be quite low. Hence, its impact on tablet hardness is low.	No action required
	Assay	Low	Since the level of super-disintegrant to be used would be low, its effect on flow properties would be minimal. Thus it is unlikely to impact assay/CU and associated risk is low.	No action required
	CU	Low		

	CT drug release profile	High	The type and amount of super-disintegrant highly impact tablet disintegration time and thereby drug release profile. The risk is high.	Optimum amount of super-disintegrant is to be selected so as to achieve desired lag time and burst release profile.
Glidant (core)	CT Hardness	Low	In general, commonly used glidants at their recommended concentration levels do not have much effect on tablet hardness. The risk is low.	No action required
	Assay	Low	The role of glidant is to improve the flow property and/or blend uniformity which will resolve the assay/CU problem if it's there. In addition, the excipients were also selected with free flowing nature. Hence, associated risk of failure is low.	No action required
	CU	Low		
	CT drug release profile	low	In general, commonly used glidants do not hamper drug release profile; associated risk of failure is low.	No action required
Lubricant (core)	CT Hardness	Medium	The lubricant like MgSt has the property to decrease tablet hardness at higher concentration level. Associated risk is medium.	Appropriate type and concentration of lubricant would be selected.
	Assay	Low	The amount of lubricant would be too low to have any impact on blend uniformity. Hence, its effect on assay or CU is low.	No action required
	CU	Low		
	CT drug release profile	Medium	The hydrophobic lubricant like MgSt is known for retarding the release profile if used at higher concentration. Associated risk is medium.	Proper selection would be carried out without hampering drug release profile.
Core tablet attributes	CCT Hardness	Low	The CCT hardness is rather controlled by outer coat ingredients and compression parameters than core tablet	No action required

			attributes. Risk of failure is low.	
	CCT drug release profile	High	Core tablet super-disintegrant amount and core tablet hardness govern its swelling behaviour and thereby CCT rupturing time or lag time. Further CCT burst release profile also depends on core tablet release profile. Associated risk is high.	Impact of critical core tablet elements on CCT release profile would be properly investigated and appropriate actions would be taken if required.
Hydrophilic pore former (coat)	CCT Hardness	Low	The CCT hardness is mainly controlled by compression parameters. The amount of hydrophilic pore former would be relatively low and so its impact on CCT hardness would also be low. Associated risk is low.	No action required
	CCT drug release profile	High	The desired lag time of PR CCT would be obtained through proper combination of hydrophobic and hydrophilic excipients. Apt selection of hydrophilic pore former and its concentration is the key to achieve desired release profile. Risk of failure is high.	Appropriate type and amount of hydrophilic pore former to be selected through thorough assessment and statistical optimization.
Coating weight	CCT Hardness	Low	During compression, change in fill weight may lead to weight variation which in turn can alter tablet hardness. However if the weight variation would be controlled within its specification limits, associated risk can be considered as low.	No action required
	CCT drug release profile	High	Increase in coating weight increases the lag time and vice versa. Associated risk of failure is high.	The coating weight would be optimized using a statistical design in order to obtain desired release profile.

Glidant (coat)	CCT Hardness	Low	The tablet hardness is mainly controlled by compression parameters. Commonly used glidants do not have much impact on tablet hardness. The risk is low.	No action required
	CCT drug release profile	High	The drug release profile may, sometimes, be hastened by type and/or amount of glidant used. Considering lag time as a critical attribute, the risk of failure is considered high.	Appropriate type and concentration of glidant to be selected which would be best suited for achieving desired quality traits.
Lubricant (coat)	CCT Hardness	Medium	The lubricants like MgSt have the property to decrease tablet hardness if used at higher concentration. Associated risk is medium.	Appropriate type and amount of lubricant would be selected.
	CCT drug release profile	High	The type and concentration of lubricant can alter the drug release profile. Since the target was to achieve stringent lag time, the associated risk of failure is high.	Appropriate type and amount of lubricant to be selected by thorough investigation.

Table 5.18 Justifications for initial risk assessment of unit operations on drug product attributes.

Process variable	Drug product CQA	Risk category	Justification	Proposed action
Sifting (core)	CT Hardness	Low	The purpose of sifting is to obtain homogeneous sized particles in order to facilitate mixing process. Sifting is a rather simple process and moreover all excipients would be chosen from free flowing and directly compressible grades; which would not create any problem of tablet hardness, assay, CU or release profile. Associated risk of failure is low.	No action required
	Assay	Low		
	CU	Low		
	CT drug release profile	low		
Blending (core)	CT Hardness	Low	The purpose of mixing/blending is to prepare homogeneous blend which would thereafter be employed for tablet compression. The effect of blending on tablet hardness is low.	No action required
	Assay	Medium	Improper mixing or blending time would result in non-compliance of assay and/or CU results. Associated risk of failure can be considered as medium.	Proper blending speed and time would be selected in order to obtain homogeneous blend.
	CU	Medium		
	CT drug release profile	Medium	Sometime excessive blending with lubricant like MgSt may slow down drug release profile. Associated risk is medium.	Proper blending speed and time would be selected to lower the risk.
Compression (core)	CT Hardness	High	It is the compression process which determines tablet hardness. Even minor change in compression force alters hardness. Risk of failure is high.	Appropriate machine settings to be done to obtain desired hardness.

	Assay	Medium	In general, deviations in assay and CU are the outcomes of blend non-uniformity and/or weight variation. Both of these issues can be ruled out by adequate blending process and proper flow. However, sometimes segregation is observed during compression process which may lead to assay/CU failure. Associated risk can be considered as medium.	Appropriate adjustment of machine settings to be done.
	CU	Medium		
	CT drug release profile	High	The compression process directly controls tablet hardness which subsequently modulates drug release profile. Associated risk is high.	Appropriate hardness would be set so as to obtain desired release profile.
Compression coating	CT Hardness	Medium	Compression to an already formed tablet may increase the tablet hardness which can also affect other core tablet attributes. Associated risk is medium.	The risk will be evaluated and appropriate action would be taken if required.
	Assay	Low	Compression coating with inactive ingredients will not affect the assay and/or CU results of an already formed core tablet. The risk is low.	No action required
	CU	Low		
	CT drug release profile	Medium	Compression to an already formed core tablet may increase its hardness and thereby can slow down its release profile which in turn may result in failure to get burst release profile. Associated risk is medium.	The risk will be evaluated and appropriate action would be taken if required.
Sifting (coat)	CCT Hardness	Low	Sifting procedure removes higher sized particles and subsequently assists mixing/blending process to produce a homogeneous blend. However, sifting would not	No action required
	CCT drug release profile	Low		

		■	directly impact tablet hardness or release profile. Associated risk is low.	
Blending (coat)	CCT Hardness	Low	Here, all excipients would be chosen with free flowing and directly compressible grades. Hence, blending/mixing process would not be a major concern and further its effect on tablet hardness or release profile would be negligible. Associated risk is low.	No action required
	CCT drug release profile	Low		
Compression (coat)	CCT Hardness	High	It is the compression process which determines tablet hardness. Change in compression force highly affects tablet hardness. Associated risk is high.	Appropriate machine setting would mitigate the risk.
	CCT drug release profile	High	The compression force determines tablet hardness and thereby controls release profile. Associated risk of failure is high.	The hardness would be set in accordance with desired release profile.

5.1.3.3. Evaluation of PRS core tablets

The physical appearance of core tablets was found to be satisfactory. The tablets had hardness of 4-6 kp, friability less than 0.5% and disintegration time less than 30 s. The tablet thickness was found to be 3.8-3.9 mm. The weight variation, assay and CU results were found within their respective specification limits. The release studies demonstrated >85% drug release within 15 min with all tested dissolution conditions and therefore the core tablet was construed as fast dissolving IR tablet (i.e. >85% release within 30 min). The dissolution profile of PRS core obtained using basket apparatus, 100 rpm, pH 6.8 phosphate buffer, 500 mL, $37\pm0.5°C$ is depicted in Figure 5.5.
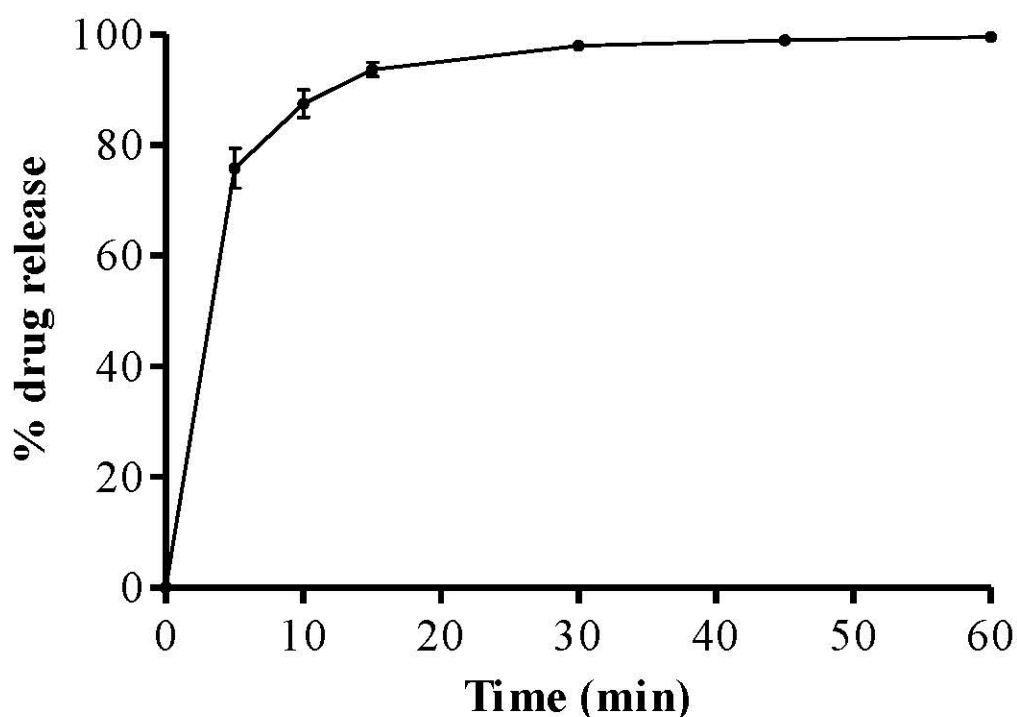
Fig. 5.5 Drug release profile of PRS core tablet in pH 6.8 phosphate buffer; basket apparatus; 100 rpm; 500 mL; $37.0\pm0.5°C$ [mean$\pm$SD; n=6]

5.1.3.4. Evaluation of PRS CCTs

5.1.3.4.1. Selection of lubricant and glidant

Since early days of tablet manufacturing, lubricants and glidants are the imperative ingredients of compression process which are particularly required for smooth manufacturing process. Though they are needed in a fairly petite amount, they require an apt contemplation otherwise they can overwhelm the effect of actual release controlling polymers (42, 43). Their precise selection can troubleshoot critical issues like sticking, capping, weight variation, CU etc., while improper choice can adversely affect desired quality profile (42-45). Academic and small scale laboratory research, many-a-times, target predefined release profile with austere focus on rate controlling excipients without considering the effects of so called trivial elements (i.e. lubricant/glidant) of compression physics. As such, the adverse effects of lubricants and glidants on tablet hardness, friability, disintegration time and drug release profile are well-known with a large number of literature available for the same (42, 43, 46, 47). However, no specific study was found for the influence of lubricants and glidants on lag time of PR CCTs. Hence, the study was conducted to investigate the impact of several lubricants and glidants on lag time of EC based CCTs. The selections were made from diverse classes based on their use and popularity. The concentration levels were basically selected in the common working range of glidants and lubricants (39).

For exclusively getting effects of individual ingredient, the study was designed by changing only one factor at a time (OFAT) while keeping other parameters constant. Throughout the study, all other critical factors such as core tablet, coating weight and tablet hardness were kept constant. Typically, individual blends of EC were prepared with various concentrations of lubricant and/or glidant which were further processed for compression coating of previously formulated core tablets. The combined effect of some selected glidant and lubricant was also examined in similar manner since they are generally engaged to render flow-enhancing and anti-adherent properties respectively.

Figure 5.6 summarizes the comparative data of lag time for various studied lubricants and glidants. Here, the lag time of each CCT, prepared with various lubricated blends, was compared with the lag time of unlubricated EC CCT. The results revealed that each selected lubricants and glidants significantly reduced (p value<0.001) the lag time of EC based CCTs when analyzed by one way Analysis of

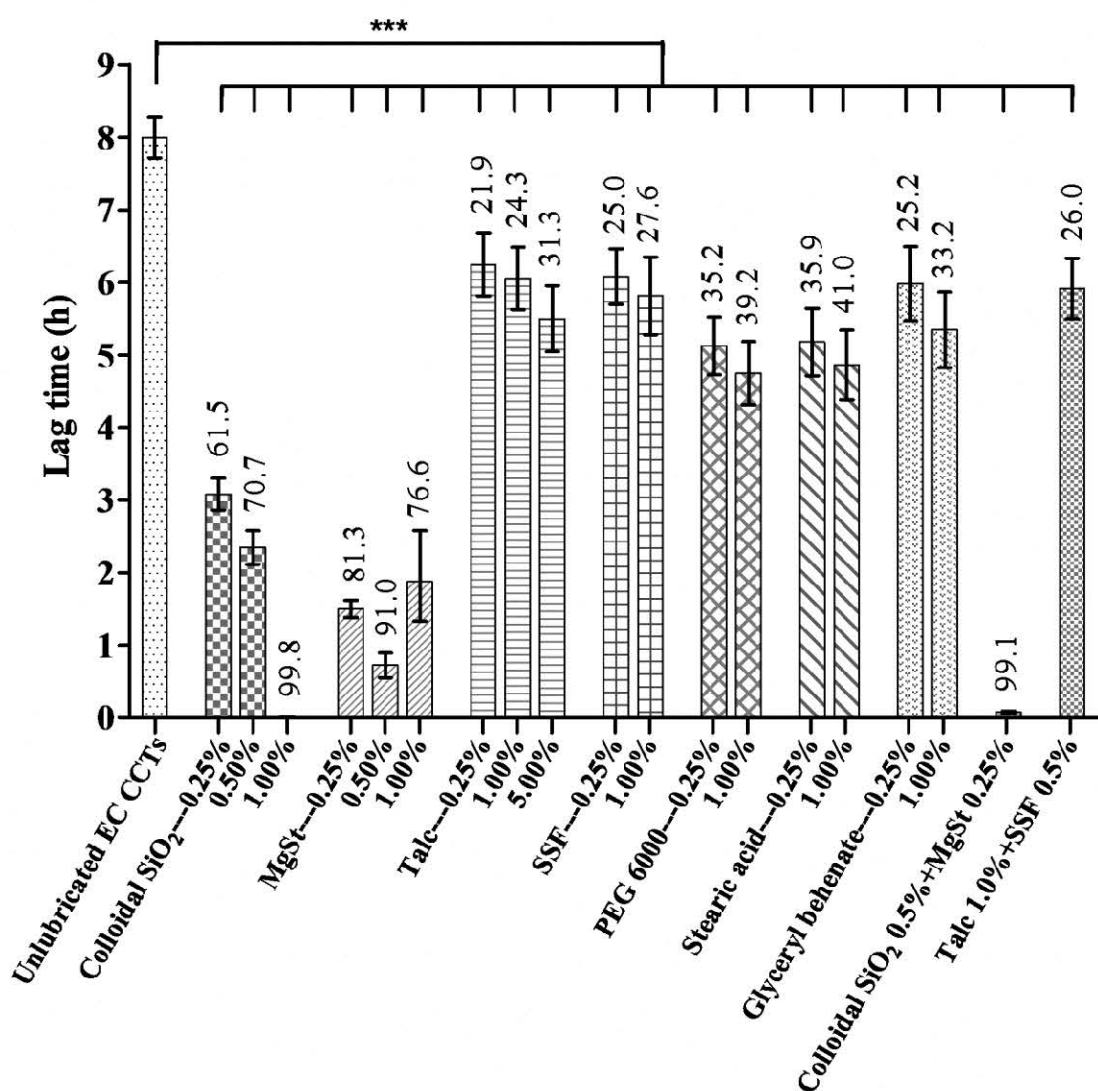Variance (ANOVA) with Bonferroni's multiple comparison test (GraphPad Prism Version 5.00, La Jolla, CA).

Fig. 5.6 Effect of type and amount of lubricants and/or glidants on lag time of compression-coated EC tablets [mean±SD; n=6]; numeric values above the error bars represent mean % reduction in lag time in comparison to Unlubricated EC CCTs; ***p value<0.001 when compared with Unlubricated EC CCTs.

In all cases, no drug release was found unless the outer coat ruptured followed by >85% drug release within 15 min of rupturing. The illustrative dissolution profile for the same is depicted in Figure 5.7. Since no batch exhibited sustained/premature release, the lag time and the time to rupture outer coat remained same in all cases.
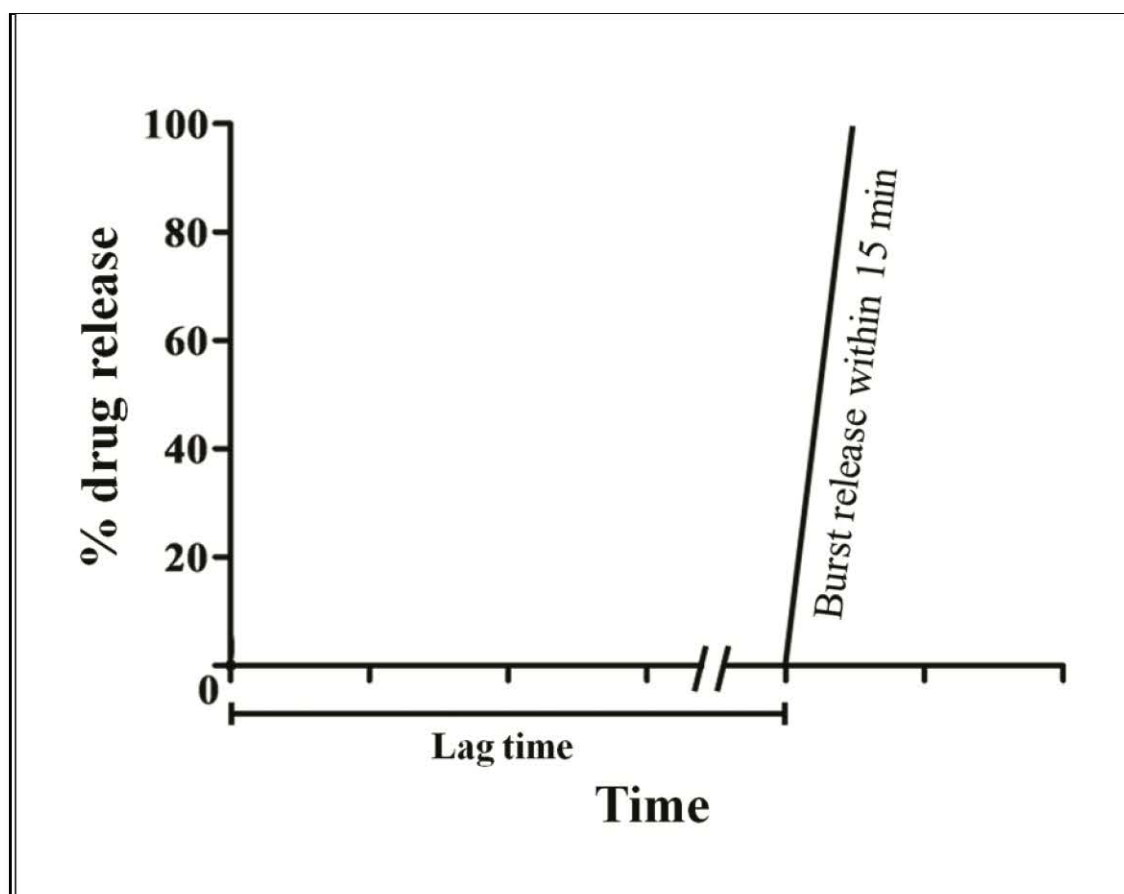
Fig. 5.7 Typical dissolution pattern of CCTs depicting distinct lag time followed by burst release profile

Further, the SEM analysis was carried out for some selected batches to examine the surface characteristics of some lubricated and unlubricated CCTs. As depicted in Figure 5.8, the images displayed the differences in surface characteristics of lubricated and unlubricated CCTs. The unlubricated CCT surfaces seem to be clean whereas lubricated CCTs depicted the appearance of lubricant/glidant on their surfaces as marked in dotted circles.
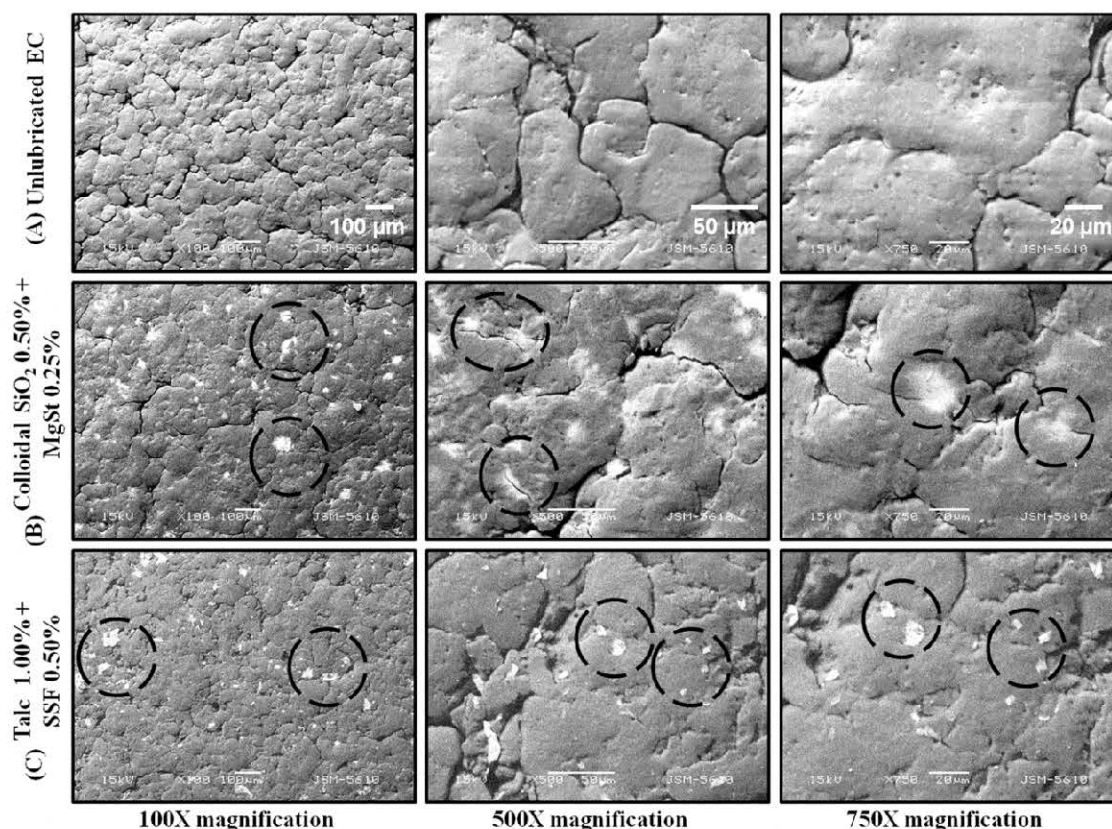
Fig. 5.8 The SEM images of CCTs prepared from (A) unlubricated EC; (B) colloidal SiO$_2$ (0.50% w/w) and MgSt (0.25% w/w) lubricated blend; and (C) talc (1.00% w/w) and sodium stearyl fumarate (SSF) (0.50% w/w) lubricated blend

Unlubricated EC CCTs: The lag time of unlubricated EC CCTs was found to be 8.00±0.28 h (mean±SD; n=6). Here, it was anticipated that the small pores between the compressed EC particles assisted slow penetration of dissolution medium to the core tablet through capillary action. When aqueous medium came in contact with the hydrophilic core, the swellable excipients gradually started swelling which built up internal pressure on surrounding coat layer. As coating layer did not possess any swelling properties, at specific time (i.e. 8.00±0.28 h) when core pressure overcame the strength of outer shell, it ruptured.

Lubricated EC CCTs: Figure 5.6 evidently shows that each selected lubricant and glidant, even at concentration as low as 0.25% w/w, significantly reduced the lag time of EC based CCTs. Here, except MgSt, the mean lag time of each lubricated CCT was found to be decreased with increase in the concentration of lubricant/glidant. Hence, it can be corroborated that it is the basic property of any lubricant/glidant which was responsible for reducing the lag time. Apparently, lubricant/glidant inherently

possess tendency to coat larger particles (here EC particles) to a greater or lesser extent depending on its type, concentration and/or surface covering potential (42, 43). Since strong bonds are formed between clean surfaces (48), it can be inferred that the surface covering of EC particles with lubricant/glidant leads to weakening of inter-particulate bonding between them (42). Now, if EC particles could not strongly consolidate with each other, the resultant coating matrix would contain relatively more interruptions and so aqueous medium would require relatively less time to travel through coat layer. Consequently, the necessary core pressure required to rupture the outer coat was achieved in a rather short time – ultimately reducing the lag time. Further, SEM images also confirmed the presence of lubricants and glidants on CCT surfaces (Figure 5.8). Typically, the CCTs of Colloidal SiO_2-MgSt lubricated blend depicted numerous areas of fine layering throughout its surface whereas talc-SSF lubricated CCTs displayed randomly spotted distinct particles. Hence, it can be anticipated that the lubrication with talc-SSF pair would be less hindering to inter-particulate EC bonding than lubrication with Colloidal SiO_2-MgSt pair; which was clearly evident from their drastic difference in lag times (Figure 5.6). Thus, it was construed that the surface covering property of a lubricant/glidant was responsible for the reduction in lag time of EC based CCTs. That's why the most popular glidant-lubricant combination, i.e. colloidal SiO_2-MgSt, which have very high surface covering potential (39, 49), exhibited most detrimental effects on lag time. Figure 5.9 is the representative diagram explaining the by and large effects of glidants/lubricants on the lag time of compression-coated EC tablets.
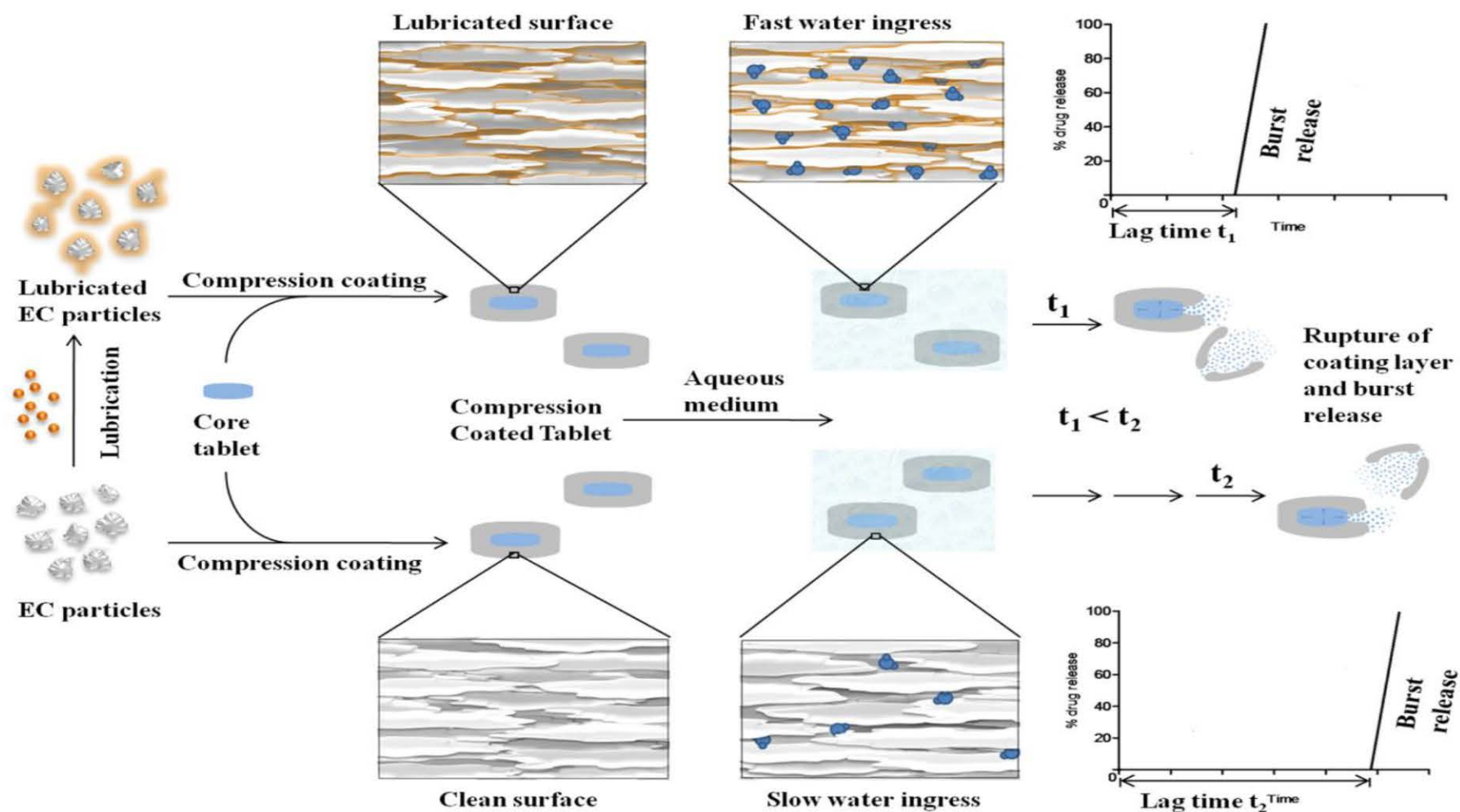
Fig. 5.9 A holistic diagram illustrating the effect of lubricants/glidants on lag time of compression-coated EC tablets

Individual results of each lubricant and glidant are separately discussed as mentioned below.

Colloidal SiO$_2$ lubricated CCTs: The colloidal SiO$_2$ is one of the most popular glidant in solid oral formulations with fine particle size and hydrophilic nature (39, 50). Large surface area and highly polar silanol groups of colloidal SiO$_2$ are, in fact, responsible for its high affinity for water molecules (50, 51). According to the literature, fine sized silica particles increases drug release by adsorbing on poorly soluble drugs and thereby providing them a larger surface area in contact with the dissolution medium (48, 50, 52). Hence, it was anticipated that this hydrophilic glidant would make the EC surface rather hydrophilic through which the aqueous medium can get ingress across the compressed coat and generate the core pressure more quickly; resulting in bursting of the CCTs with shorter lag time. The CCTs of 0.25% w/w and 0.50% w/w SiO$_2$ exhibited the lag time of 3.08±0.22 h and 2.35±0.23 h respectively; and the % reductions in lag time, as compared to unlubricated CCTs, were respectively found to be 61.5% and 70.7% (Figure 5.6). However, at the concentration of 1.00% w/w SiO$_2$, the CCTs astonishingly converted into fast disintegrating tablets with disintegration time even in less than 60 s i.e. no lag time. This would be due to the fast wicking action of hydrophilic colloidal SiO$_2$ which thereby instigated very fast ingress of aqueous medium through the outer coat. The snapshot images of the same are demonstrated in Figure 5.10 (A). Figure 5.10 (B) portrays the photographs of CCT before and after drug release study. Notably, all CCTs (with each selected lubricant and glidant) exhibited similar rupturing behaviour as illustrated in Figure 5.10 but with varying individual lag time as per its outer shell composition.
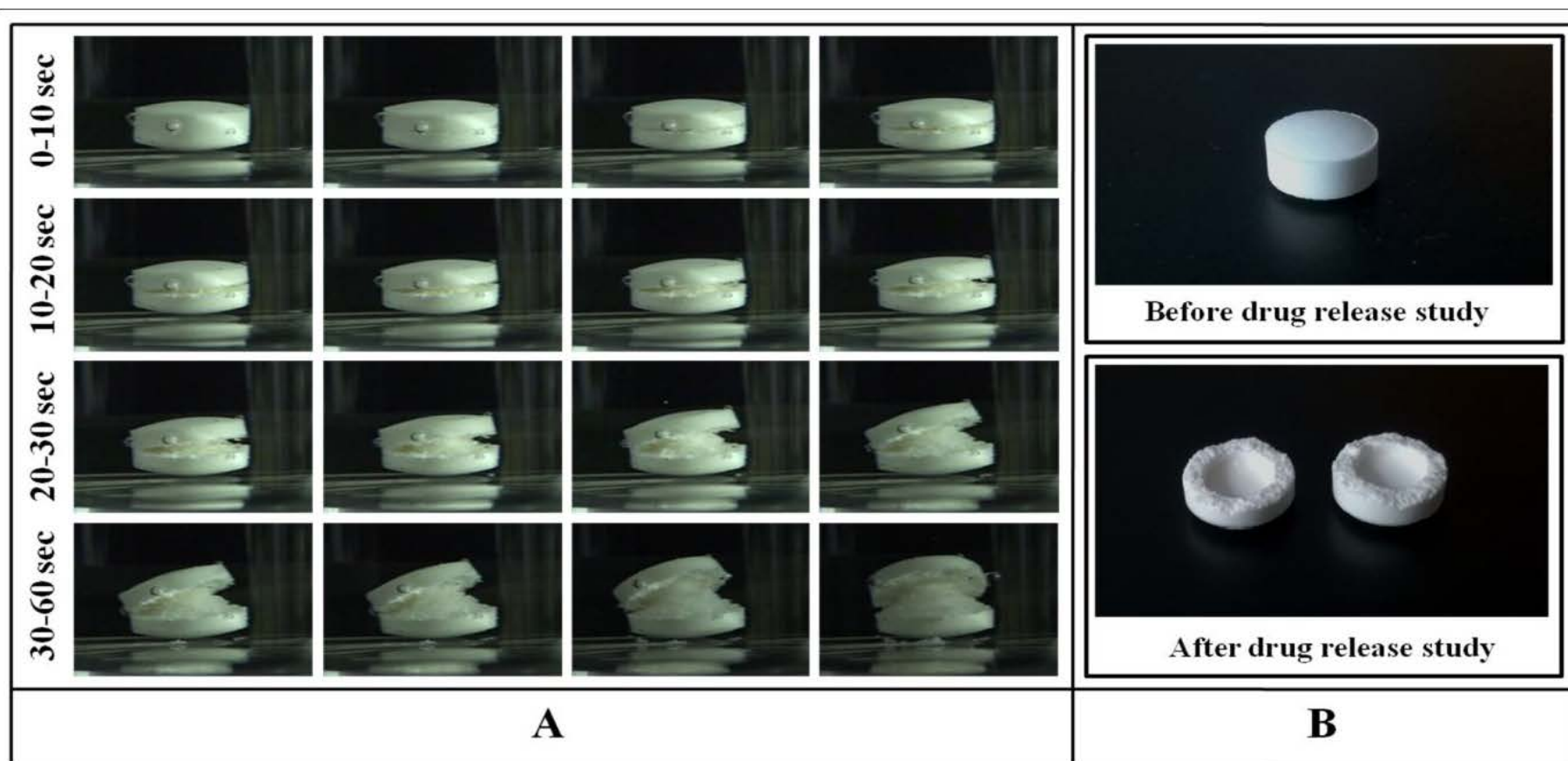
Fig. 5.10 (A) The photographs showing fast rupturing of 1.00% w/w colloidal SiO_2 lubricated CCT, (B) the photographs of CCT before and after drug release study

Magnesium stearate (MgSt): The surface covering property of MgSt is so powerful that, sometimes, even a slight increase in its concentration or a little extended blending time can result in decrease in tablet hardness, prolongation of disintegration time and/or retardation of drug release profile (42, 43, 47). The reduction in hardness is associated with its fine surface covering or film forming properties around the large particles, whereas, the retardation of drug release profile and prolongation of disintegration time is the outcome of its highly hydrophobic nature. However, opposite finding was observed here i.e. shortening of disintegration time and hastening of release profile of CCTs (Figure 5.6) because of surface coverage of EC particles by fine MgSt particles. Typically, the lower concentration, i.e. 0.25% w/w MgSt, resulted in 1.5±0.12 h of lag time (81.3% reduction), whereas 0.50% w/w MgSt depicted 0.72±0.17 h lag time (91.0 % reduction) (Figure 5.6). Here, even though the compression was executed at relatively higher compression force in order to achieve the target hardness, the lag time was considerably shorter. Noticeably, the maximum achievable hardness with 1.00% w/w MgSt lubricated CCTs was mere 5-6 kp which was distinctly shorter from desired hardness range. The observation was, prominently, in line with reported MgSt properties i.e. weaker compacts were formed and decrease in the bonding was observed as the level of MgSt in the tablet increased (42, 48, 53, 54). However, despite of less hardness, the mean lag time of 1.00% w/w MgSt lubricated CCTs (1.88±0.49 h; 76.6% reduction) was found to be greater than 0.50% as well as 0.25% lubricated CCTs (Figure 5.6). Thus, at lower selected levels, i.e. 0.25% and 0.50% w/w MgSt, the mean lag time decreased with increase in the concentration whereas at higher level, i.e. 1.00% w/w MgSt, the mean lag time slightly increased (Figure 5.11) despite of having less hardness. The reason might be the increase in hydrophobicity of outer coat (42) (for 1.00% MgSt batch) which eventually decreased water ingress rate in comparison to 0.50% as well as 0.25% w/w MgSt lubricated CCTs. On the whole, lubrication with MgSt drastically reduced the lag time irrespective of its concentration used. Besides, the variability in lag time was also increased with increase in MgSt concentration. Altogether, it can be said that most pernicious and dramatic effects on lag time were observed with MgSt lubricated CCTs.
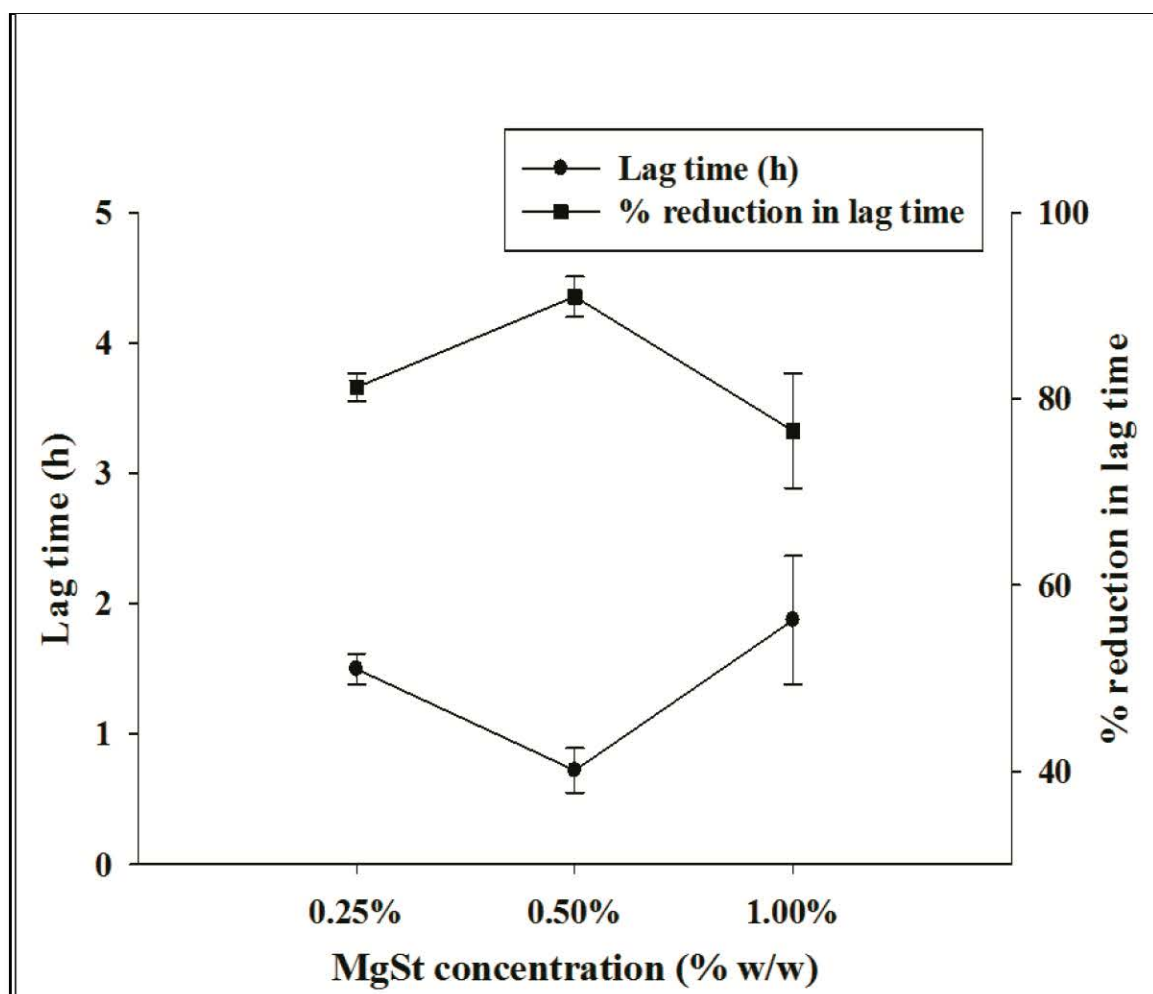
Fig. 5.11 Effect of MgSt concentration on lag time of compression-coated EC tablets [mean±SD; n=6]

Combined effect of colloidal SiO₂ and MgSt: The combined effect of colloidal SiO_2 and MgSt, was analyzed from the batch containing 0.50% w/w colloidal SiO_2 and 0.25% w/w MgSt. The CCTs ruptured within 3-6 min with 99.1% reduction in lag time (Figure 5.6). Here, the collective effects of hydrophilic colloidal SiO_2 (imparting wicking action) and hydrophobic MgSt (rigorously limiting inter-particulate bonding) ended up in fast disintegrating IR tablets without any lag time. Thus, the most favourable glidant-lubricant combination (colloidal SiO_2 and MgSt) was found to be incompetent for developing EC based PR CCTs.

Other selected lubricants: As shown in Figure 5.6, all other lubricants (i.e. talc, SSF, glyceryl behenate, PEG 6000 and stearic acid) at each studied concentration, also significantly reduced the lag time (p value <0.001) in comparison to unlubricated CCTs. However, % reduction in lag time for all other lubricants was significantly lesser

than that of colloidal SiO_2 or MgSt lubricated CCTs (p value <0.001); and ranged from 21-41% for all other lubricants at their studied concentrations. Thus, they are found to be relatively less injurious than either of colloidal SiO_2 or MgSt. Hence, depending on feasibility or desired quality traits, anyone amongst them can be employed in developing EC based PR CCTs. Typically, the lag time of combined talc (1.00% w/w) and SSF (0.50% w/w) lubricated CCTs was found to be 5.92±0.42 h exhibiting 26% reduction as compared to unlubricated CCTs. The results showed neither pronounced synergistic impact nor severely limited the lag time as observed in the case of colloidal SiO_2 and MgSt lubricated CCTs (Figure 5.6). Therefore, this combination was opted for further development of PR CCTs. Further it was found that the varying levels of talc (i.e. 0.25-5.00 %w/w) as well as SSF (i.e. 0.25-1.00 %w/w) in the outer coat did not significantly alter the lag time (p value >0.05) in stated concentration range. Since our working concentration level reasonably fall within these stated ranges, the risk of failure to achieve desired quality traits due to the selected glidant and lubricant (i.e. 1% w/w talc and 0.5% w/w SSF) was low.

5.1.3.4.2. Selection of hydrophilic additive

As stated earlier, the desired lag time of a PR formulation can be engineered by precise combination of hydrophobic (i.e. water insoluble EC) and hydrophilic (i.e. water soluble) excipient. Therefore, after selecting suitable glidant-lubricant pair, the study was undertaken for selection of proper hydrophilic material which can be a superior fit for fabricating PR formulations. Various hydrophilic excipients from diverse categories, such as freely water soluble fillers, polymeric binders like cellulosic, povidones and polyethylene glycols, etc. were explored to know their suitability for stated purpose.

The results of lag time for all selected hydrophilic additives at their respective concentrations are demonstrated in Figure 5.12. Here also, in all cases, no drug release was observed before rupturing of outer coat followed by >85% release within 15 min (Figure 5.7); and so lag time and time required to rupture the outer coat remained same.
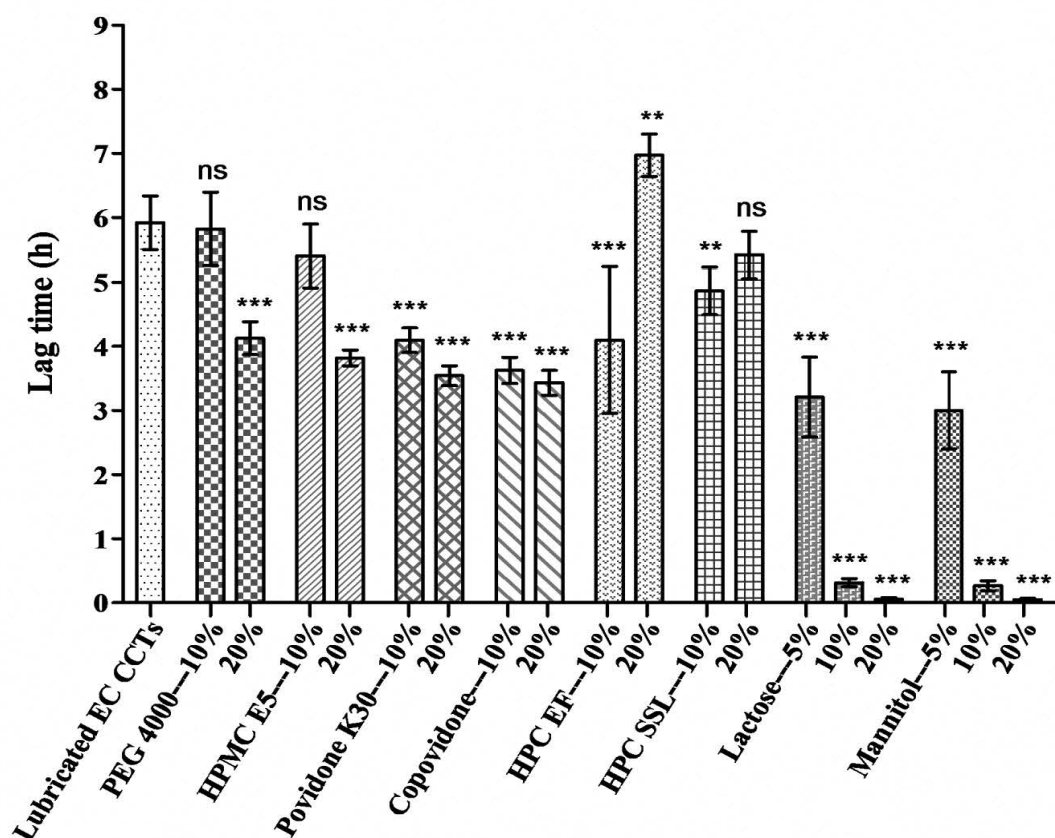
Fig. 5.12 Effect of several hydrophilic additives on lag time of compression-coated EC tablets [mean±SD; n=6]; ***p value<0.001; **p value<0.01; ns (not significant) p value>0.05 when compared with Lubricated EC CCTs

Freely water soluble hydrophilic fillers: The study revealed that freely water soluble fillers, i.e. lactose and mannitol, exhibited too drastic effect on lag time (Figure 5.12). Typically, at 10% w/w concentration, CCTs of lactose and mannitol depicted the lag time of 0.31±0.06 h and 0.27±0.08 h respectively, whereas at 20% concentration, both CCTs were ruptured within 5 min. Therefore, additional 5% w/w concentration was also evaluated to understand the impact of these two fillers at lower level. At 5% w/w concentration, the observed lag time for lactose and mannitol CCTs were 3.21±0.62 h and 3.00±0.60 h respectively with high variability in both cases. Both fillers, at all three levels, i.e. 5%, 10% and 20% w/w, significantly reduced the lag time (p value <0.001) of EC based CCTs (Figure 5.12). Thus, both fillers with nearly similar aqueous solubility demonstrated almost similar effect on lag time. Hence, it was corroborated that upon exposure to dissolution medium freely water soluble fillers rapidly dissolved out from the outer coat and thereby created pores facilitated quick

penetration of aqueous medium to the core tablet. Subsequently, generated core pressure abruptly ruptured the outer shell with very short lag time (at concentration of $\geq10\%$ w/w). Though the lower concentration (5% w/w) exhibited somewhat considerable lag time, the high variability in results limits its application. Thus, mere combination of EC and freely water soluble hydrophilic fillers was found to be inept for development of EC based PR CCTs.

Hydrophilic polymers with binding properties: As illustrated in Figure 5.12, various polymeric binders (i.e. HPMC E5, HPC EF, HPC SSL, povidone K30, copovidone and PEG 4000), at 10% and 20% w/w concentration, exhibited 2-8 h of lag time with more or less variability. Notably, except HPCs, the mean lag time of all other polymers at 10% w/w concentrations was relatively higher than that at 20% concentrations; whereas CCTs with HPC EF and HPC SSL demonstrated relatively lower lag time at 10% concentration than at 20% concentration. Since all CCTs were compressed at same hardness, it was deduced that the HPCs are relatively more efficient as dry binder amongst selected polymers. Further, the lag time of low molecular weight (MW) HPC (HPC SSL, 40000 Da) was relatively less variable than that of higher MW HPC (HPC EF, 80000 Da) at both studied concentration levels. It means that lower MW can be preferred over higher MW for development of robust PR CCTs. Moreover, each polymer at 10% concentration depicted relatively higher variability in lag time than that of 20% level (Figure 5.12) suggesting higher concentration level as more preferable over lower concentration level. Amongst all selected polymers, HPMC E5 typically exhibited most promising results in terms of lag time as well as variability and therefore opted for developing EC based PR CCTs.

5.1.3.4.3. Selection of HPMC MW grade

The results of the previous study exhibited that the outer coat with HPMC E5 was found to be rather promising for modulating the lag time of EC based CCTs (55). However, HPMCs are available in a wide range of viscosity or MW grades which possess different functional properties and thereby employed for different applications such as tablet binder, coating agent, control release matrix, bioadhesive, rheology controller etc. (39, 56). Normally, low MW HPMCs (generally $\leq$E50) are employed as tablet binder, whereas higher MW HPMCs (generally $\geq$K100LV) are useful as

controlled release agents (39, 57). However, for developing compression-coated PR formulations, which HPMC grade would be more efficient in combination with EC was a question and no available literature had an answer to the same. Hence, it was of common interest to carry out a comprehensive comparative assessment of various MW HPMCs in formulation of compression-coated PR tablets; and thus the present study was a desideratum to solve the selection perplexity. Here, five HPMC MW grades, i.e. E5, E15, E50, K100LV and K4M, were investigated at three different concentrations, i.e. 10% w/w, 20% w/w and 30% w/w in outer coat, to examine their effects on lag time of compression-coated EC tablets.

Here, several blends were prepared using EC and HPMC followed by lubrication with 1.0% w/w talc and 0.5% w/w SSF. In a similar way, plain EC (i.e. without HPMC; 0% level) was also blended with talc and SSF to prepare comparison batch. For exclusively assessing the effect of each HPMC grade, changing only OFAT design was adopted and except type and/or amount of HPMC in outer coat all other parameters such as core tablet, coating weight and tablet hardness were kept constant throughout the study. All CCTs were prepared as per the procedure described in section 5.1.2.8.

The release study revealed that the batch containing 30% w/w K4M in outer coat exhibited slight premature release (<5%) before the rupture of outer coat, whereas remaining batches depicted no drug release before the rupture of outer coat. As soon as the outer coat ruptured, >85% drug was released within 15 min for all CCTs. Figure 5.13 depicts the drug release profiles of CCTs obtained using paddle apparatus; 0.1 N HCl for first 2 h followed by pH 6.8 buffer; 500 mL; 100 rpm; 37±0.5°C; and corresponding lag time results are demonstrated in Figure 5.14. Here, the higher MW CCTs depicted significant swelling upon dissolution which made it difficult to figure out the exact rupturing time of tablet through visual observation if placed inside the basket apparatus. Hence, to facilitate visual observations the study was conducted with paddle apparatus instead of basket apparatus.
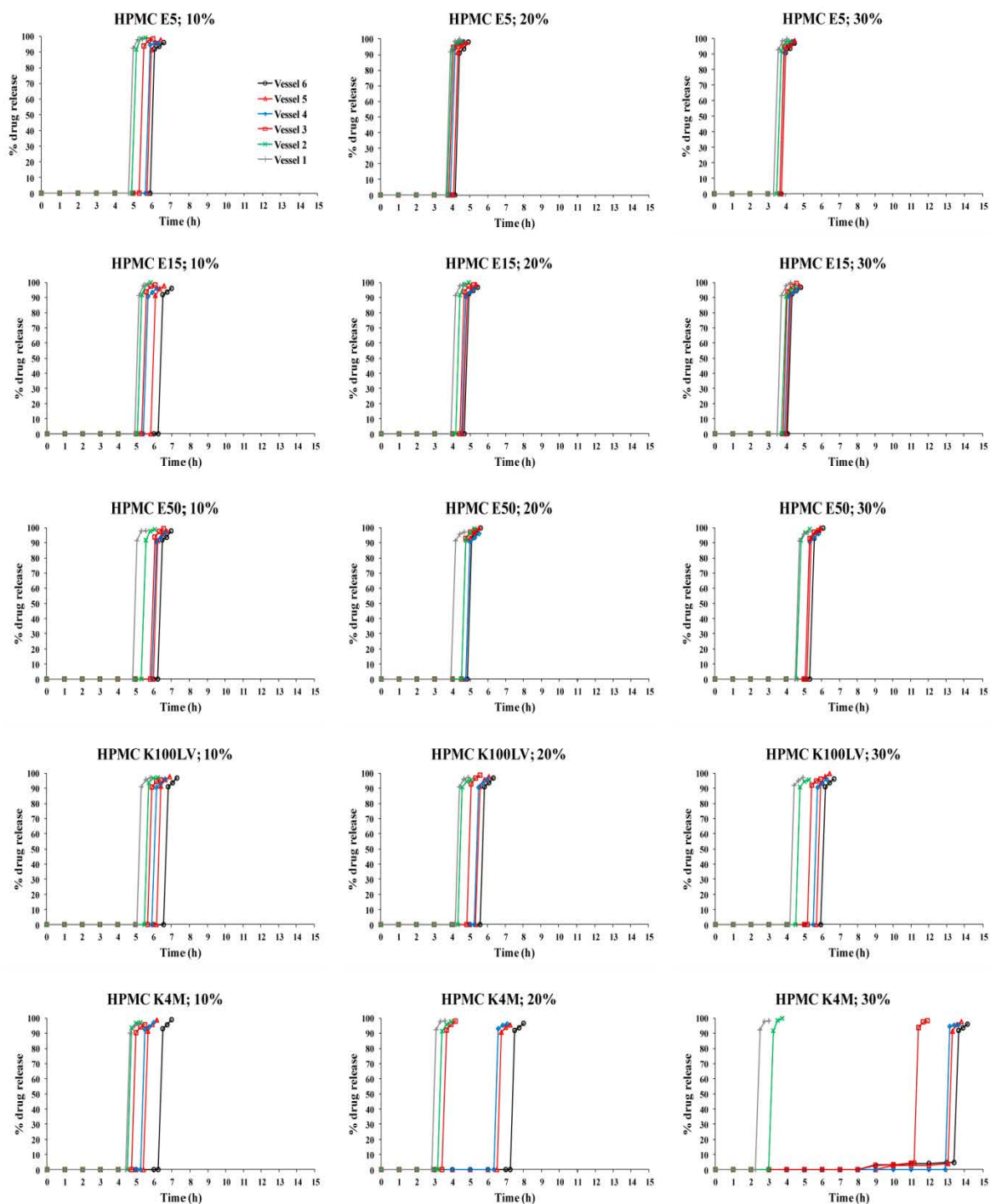
Fig. 5.13 Drug release profiles of six individual units of various EC based CCTs having different type and/or amount of HPMC in the outer coat

All CCTs exhibited distinct pattern of initial lag time followed by sharp burst release. Since premature release observed with 30% K4M CCTs was less than 5%, the lag time and time to rupture the outer coat remained same for all batches. Further, the CCTs of 20% w/w level of each HPMC grade were examined by SEM testing to observe the tablet surface before and after drug release study.
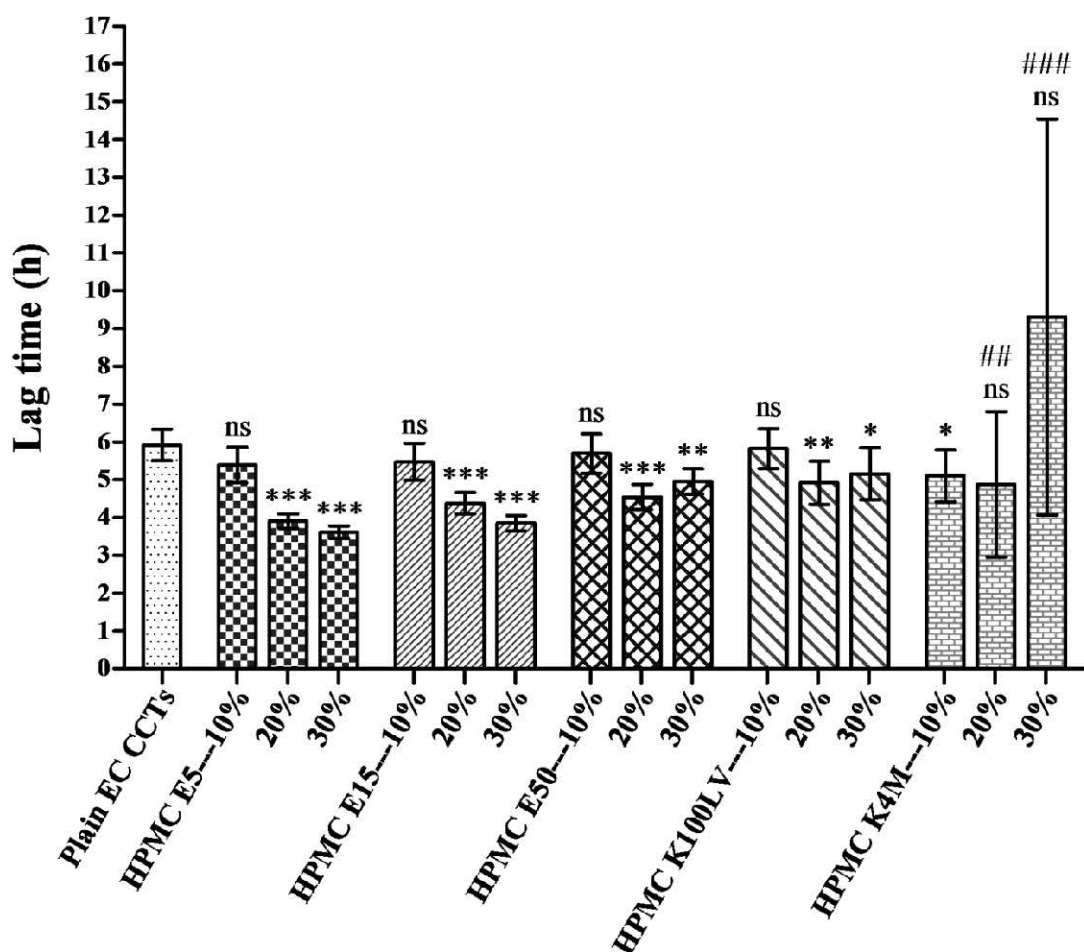
Fig. 5.14 Effect of type and amount of HPMC on lag time of EC based CCTs (mean±SD; n=6); *** *p value* <0.001, ** *p value* <0.01, * *p value* <0.05, ^{ns} *p value* >0.05 when compared with plain EC CCTs using t test; $^{###}$ and $^{##}$ depict significantly high variance with *p value* <0.001 and *p value* <0.01 respectively when compared with plain EC CCTs using F test

Plain EC CCTs (0% HPMC): Plain EC CCTs depicted lag time of 5.92±0.42 h followed by burst drug release (>85%) within 15 min of rupturing (Figure 5.14). Here, slow ingress of dissolution medium through small pores of the EC matrix led to gradual built up of core pressure on surrounding coat layer and as soon as the core pressure overcame strength of the outer coat, the CCTs ruptured.

HPMC E5: The lag time of lowest selected concentration (i.e. 10% w/w E5 CCTs) was found to be 5.39±0.47 h with no significant difference (p value >0.05) from plain EC CCTs. With increase in HPMC concentrations in outer coat i.e. 20% w/w and

30% w/w, the lag times were respectively reduced to 3.90±0.19 h and 3.61±0.16 h; both significantly lesser (p value <0.001) than plain EC CCTs (Figure 5.14). The % RSD of lag time for 10% w/w, 20% w/w and 30% w/w levels were respectively found to be 8.7%, 4.9% and 4.4%.

HPMC E15: The lag time of 10% w/w E15 CCTs was found to be 5.47±0.49 h with no significant difference (p value >0.05) from plain EC CCTs. With increase in HPMC concentrations i.e. 20% w/w and 30% w/w, the lag times were respectively reduced to 4.38±0.28 h and 3.85±0.21 h; both significantly lesser (p value <0.001) than plain EC CCTs (Figure 5.14). The % RSD of lag time for 10% w/w, 20% w/w and 30% w/w levels were respectively found to be 9.0%, 6.4% and 5.5%.

HPMC E50: The lag time of 10% w/w E50 CCTs was found to be 5.69±0.52 h with no significant difference (p value >0.05) from plain EC CCTs. With increase in HPMC concentrations i.e. 20% w/w and 30% w/w, the lag times were respectively found to be 4.54±0.34 h and 4.96±0.34 h; both significantly lesser (p value <0.001 and <0.01 respectively) than plain EC CCTs (Figure 5.14). The % RSD of lag time for 10% w/w, 20% w/w and 30% w/w levels were respectively found to be 9.1%, 7.5% and 6.9%.

HPMC K100LV: The lag time of 10% w/w K100LV CCTs was found to be 5.82±0.53 h with no significant difference (p value >0.05) from plain EC CCTs. With increase in HPMC concentrations i.e. 20% w/w and 30% w/w, the lag times were respectively found to be 4.92±0.57 h and 5.15±0.69 h; both significantly lesser (p value <0.01 and <0.05 respectively) than plain EC CCTs (Figure 5.14). The % RSD of lag time for 10% w/w, 20% w/w and 30% w/w levels were respectively found to be 9.1%, 11.6% and 13.4%.

HPMC K4M: The lag time of lowest selected concentration (i.e. 10% w/w K4M CCTs) was found to be 5.10±0.69 h which was significantly lesser (p value <0.05) from plain EC CCTs. Whereas with increase in HPMC concentrations i.e. 20% w/w and 30% w/w, the lag times were respectively found to be 4.88±1.92 h and 9.31±5.25 h; with no significant difference (p value >0.05 for both batches) from plain EC CCTs. However, the variances of 20% w/w and 30% w/w K4M CCTs were significantly higher (p value <0.01 and <0.001 respectively; F test) in comparison to plain EC CCTs, which was a distinct observation from other batches (Figure 5.14). The % RSD of lag time for 10%

w/w, 20% w/w and 30% w/w levels were respectively found to be 13.5%, 39.3% and 56.4%. Importantly, individual tablet rupturing times of six tested units of 20% w/w K4M CCTs were found to be 2.83, 3.17, 3.42, 6.33, 6.50 and 7.00 h, whereas those of 30% w/w K4M CCTs were found to be 2.25, 3.00, '*11.17*', 12.92, '*13.08*' and '*13.42*' h. Here, the values in '*italic*' depict slight premature release (<5%) before the rupture of outer coat. As premature release in all units were found to be below 5%, lag time and time to rupture outer coat remained same. The drug release profile of six individual units of HPMC K4M CCTs is depicted in Figure 5.13.

Figure 5.15 demonstrates the SEM images of CCTs for 20% w/w HPMC concentration of all selected MW grades before and after drug release study. The images displayed that the tablet surfaces which were fairly smooth and similar before dissolution turned rough due to generation of pores after dissolution and the surface roughness or pore sizes progressively increased with increase in HPMC MW in outer coat.

Thus, above results evidently corroborated that the addition of HPMCs in outer coat modulated the lag time of EC based CCTs depending on the MW and concentration of HPMC. However, to better illustrate individual effects of HPMC, the lag time of each batch was plotted against HPMC MW on log scale (Figure 5.16). The reported weight average MWs for HPMC E5, E15, E50, K100LV and K4M are 34500, 52000, 91300, 164000 and 400000 Da respectively (58) and reported nominal viscosities of their 2% w/v aqueous solutions are 5, 15, 50, 100 and 4000 mPa.s at 20°C respectively (39, 57). For HPMCs, aqueous viscosity and MW are proportional to each other and hence, the relationship can be extrapolated in either way (59). Say as, hydration of higher MW HPMCs results into gel formation by increasing the aqueous viscosity.
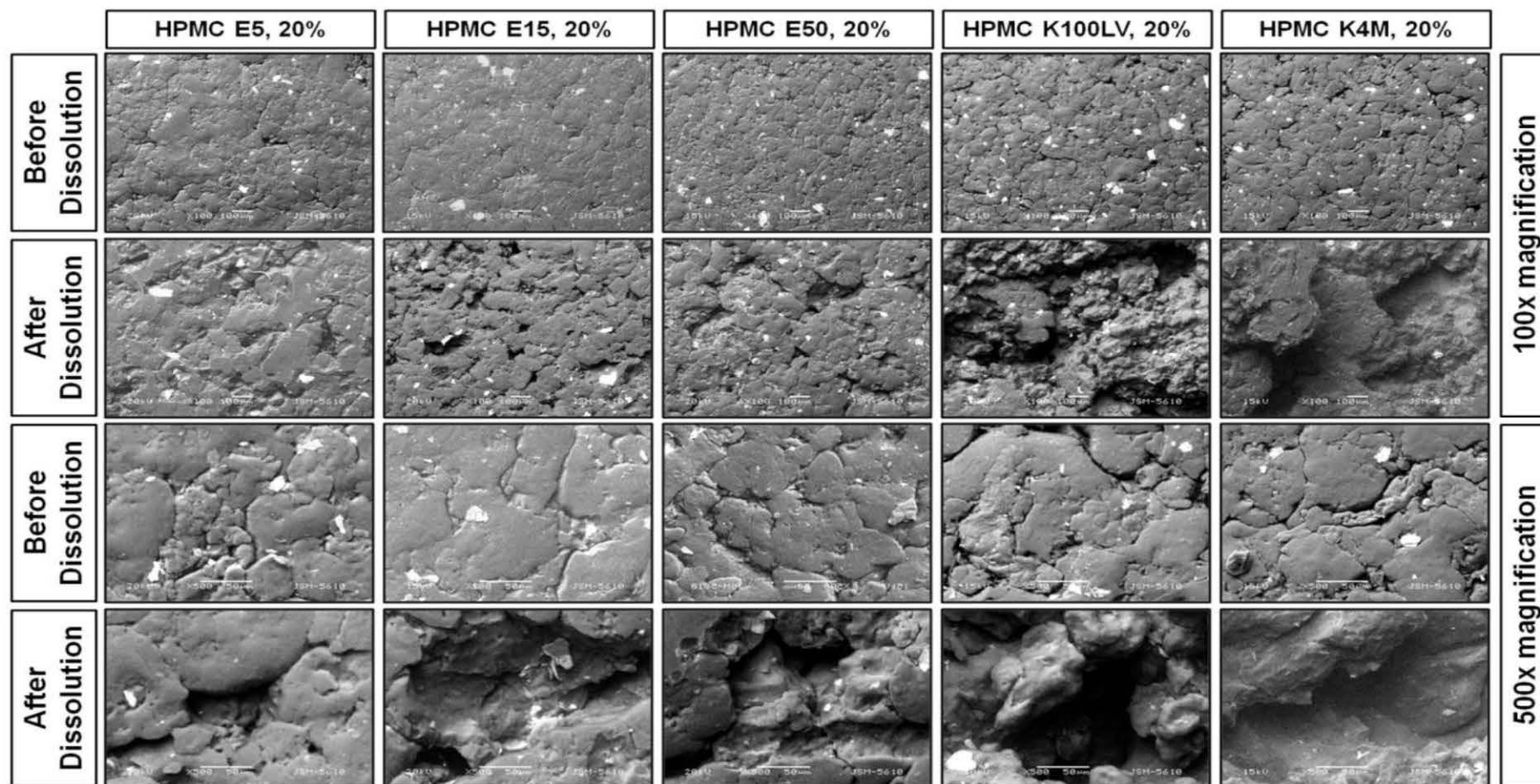
Fig. 5.15 The SEM images of several EC based CCTs, having different MW HPMC at 20% w/w concentration in outer coat, before and after drug release study
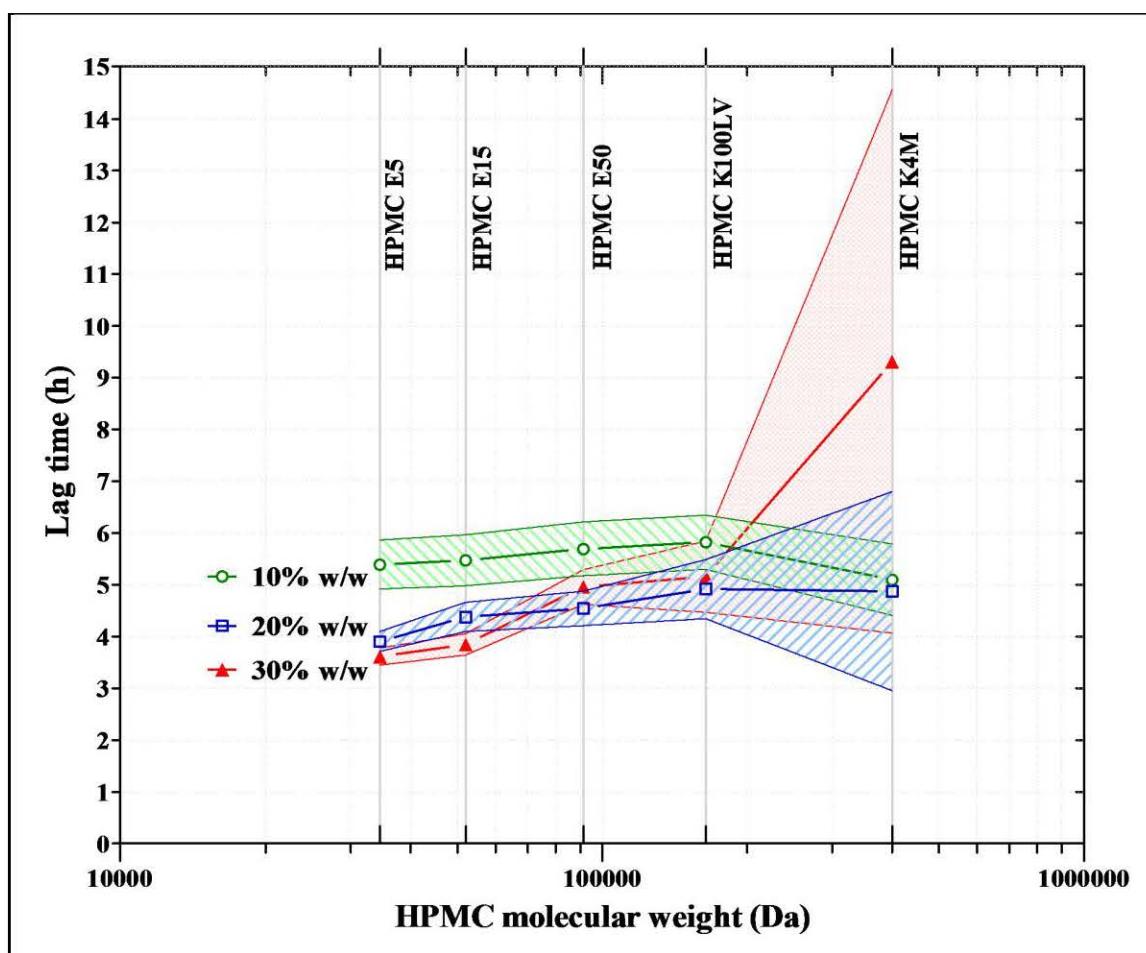
Fig. 5.16 Effect of HPMC MWs and their concentrations on lag time of EC based CCTs (mean±SD; n=6)

As shown in Figure 5.14 and Figure 5.16, the mean lag times of two low MW HPMC CCTs (E5 and E15) were found to be decreased with increase in HPMC concentrations. Hence, it can be postulated that these low MW grades would have predominantly acted as pore formers in the EC matrix and therefore, increase in their concentrations brought about an increase in water penetration through the outer coat leading to faster built up of core pressure which ultimately resulted shorter lag times than plain EC CCTs.

However, with other selected grades (E50, K100LV and K4M), the mean lag time initially decreased with increase in their concentration up to 20% w/w and thereafter increased for 30% w/w level (Figure 5.14). This infers that initial decrease in mean lag times up to 20% w/w concentration was the result of dominating pore forming properties, whereas further increase in lag time for 30% w/w level was the outcome of increased gelling phenomenon. Now, the gelling properties of HPMC do increase with

increase in their MWs as well as their concentrations (60). Hence, during dissolution, the outer coats of E50, K100LV and K4M CCTs (at 30% level) would have become elastic as a result of increased gelling phenomenon, whereas the outer coats of E5 and E15 CCTs which lacked such gelling properties remained brittle. Since elastic coat can evidently withstand relatively higher core pressure than brittle one, the mean lag times of E50, K100LV and K4M CCTs (at 30% level) were increased in contrast to E5 and E15 CCTs. Thus, with increase in HPMC MW, as gelling phenomenon dominated over pore forming phenomenon, the elasticity of outer coat was increased at higher HPMC concentration and eventually progressively decreasing trend of lag time (with increase in concentrations) was altered above E15 MW grade. The SEM images of CCTs obtained after drug release study displays progressive enhancement of surface roughness and pore size with increase in HPMC MW (Figure 5.15); which is also a direct indication of gradual increase in gelling phenomenon with increase in MW of HPMC.

Another crucial and seldom discussed aspect from the viewpoint of a formulation scientist is the dissolution variability. The variability in lag time was studied with change of HPMC MW and their concentration levels in outer coat layer. The higher two levels of highest selected MW grade, i.e. 20% w/w and 30% w/w K4M CCTs depicted significantly high variances in lag times when compared to plain EC CCTs; wherein higher concentration (30% w/w) showed higher variance than lower ones (20% w/w) (Figure 5.14). Now, to completely understand the variability behaviour, % RSD in lag time was plotted against HPMC MW on log scale for each batch (Figure 5.17). The plot revealed that for three lower MW grades (E5, E15 and E50), % RSD in lag time gradually decreased with increase in HPMC concentration, whereas for two higher MW grades (K100LV and K4M), % RSD increased with increase in their concentrations up to 30% w/w. For six tested dissolution units – E5, E15 and E50 CCTs showed <10% RSD at all studied concentrations, 10% w/w K100LV CCTs demonstrated <10% RSD, 20% w/w and 30% w/w K100LV CCTs and 10% w/w K4M CCTs exhibited 10-20% RSD, 20% w/w K4M CCTs depicted 30-40% RSD, and 30% w/w K4M CCTs depicted 50-60% RSD (Figure 5.17). Thus, it was observed that CCTs with low MW HPMCs (E5, E15 and E50), which governs the lag time by pore forming mechanism, demonstrated far less variability than that of higher ones. On the other hand, at 10% w/w concentration, higher MW (K100LV and K4M)

CCTs also demonstrated relatively less variability in lag time as the concentration was not sufficient to induce adequate gelling in the outer coat. However, as K4M concentration increased in the outer coat (i.e. 20% w/w and 30% w/w), the gelling phenomenon took dominance and resulted in significant enhancement in lag time variability. Thus, highly desired gelling properties of higher MW HPMC (K4M) for developing diffusion controlled sustained release (SR) matrix formulations were found undesirable (with regards to variability in lag time) for developing robust EC based PR CCTs. According to USP, *"dissolution results are considered highly variable if RSD is greater than 20% at time points of 10 min or less and greater than 10% RSD at later time points"* (26), Taking this into account, the lag times with <10% RSD obtained with low MW (E5, E15 and E50) CCTs can be considered appropriate according to USP, whereas the CCTs of higher concentrations of higher MW HPMC in outer coat, especially 20% w/w and 30% w/w K4M, demonstrated very high % RSD in lag time which were far beyond the USP recommended % RSD limits to be considered as highly variable (Figure 5.17). Therefore, the low MW HPMCs (E5, E15 and E50) which restricted the lag time variability within USP specification limits were found to be rather suitable for developing robust EC based PR CCTs.
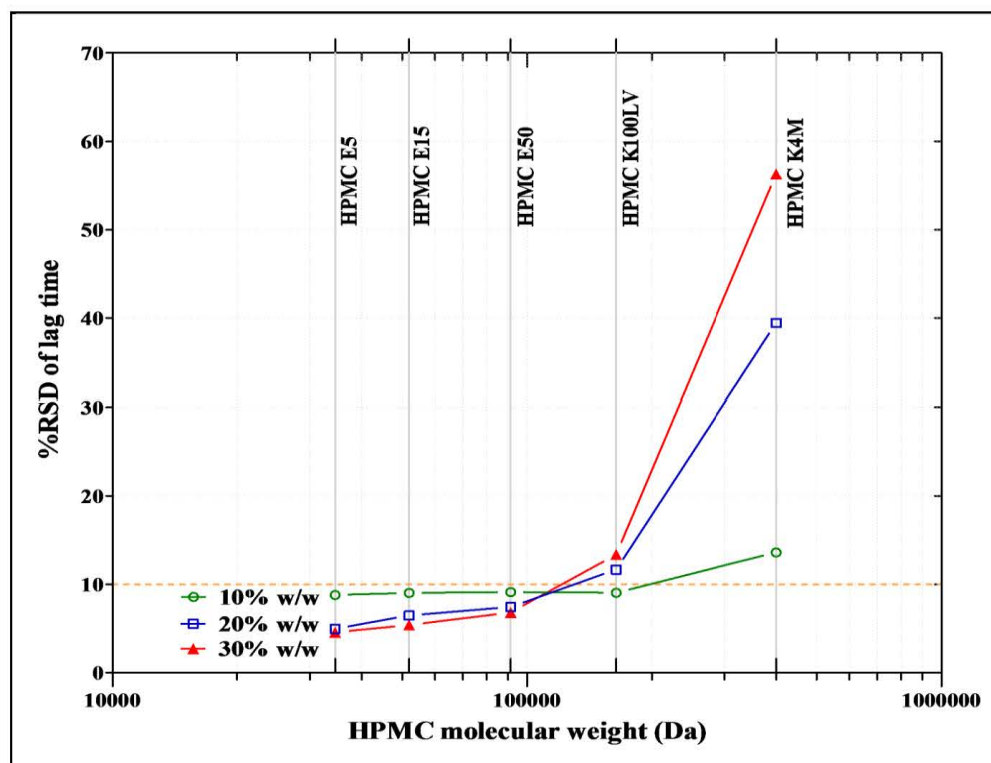

Fig. 5.17 Effect of HPMC MWs and their concentrations on lag time variability (% RSD; n=6) of EC based CCTs

Further, the patterns in the lag times of various CCTs were also found noteworthy. For example, the lag times of 30% w/w K100LV CCTs and 10% w/w K4M CCTs were found to be quite similar with no significant difference (p value >0.05). Likewise, 30% w/w E50 CCTs and 20% w/w K100LV CCTs also demonstrated fairly similar lag times with no significant difference (p value >0.05) (Figure 5.14). Thus, some of the CCTs of higher concentration of lower MW HPMCs were found to be equivalent to that of lower concentration of next higher MW HPMC. Thereby, it could be anticipated that the balance of pore forming and gelling properties between the above mentioned pairs would have a close resemblance. In other words, K4M CCTs at 10% w/w concentration generated similar gelling strength as that of K100LV CCTs at 30% w/w level. Thus, the stated lag time patterns also substantiate the dependence of gelling phenomenon on both, HPMC MW as well as their concentration in outer coat layer.

Importantly, except 10% w/w K4M CCTs, the lag times of all other 10% w/w CCTs (i.e. E5, E15, E50 and K100LV) did not significantly differ (p value >0.05) from plain EC CCTs (Figure 5.14). Here, despite of having higher gelling or binding strength (60), K4M CCTs at 10% level demonstrated shorter lag time than that of other MWs; which suggest comparatively faster ingress of dissolution medium for K4M CCTs than those of others at 10% w/w level. Hence, it can be inferred that the highest selected MW (K4M) augmented the aqueous medium ingress through the outer coat by providing wider diffusion path, however as 10% w/w concentration was not sufficient for providing adequate gelling/elasticity to the outer coat, the CCTs of 10% w/w K4M ruptured relatively earlier than those of other MW grades at the same concentration. On the other hand, higher concentration (30% w/w) of K4M in outer coat, which was able to impart sufficient elasticity to the outer coat, demonstrated higher mean lag time as well as variability (Figure 5.14 and Figure 5.16).

The lag times of individual units of two highly variable K4M batches (i.e. 20% w/w and 30% w/w) also demonstrated notably distinct patterns. Three out of six tested units of 20% w/w K4M CCTs depicted <4 h of lag time (i.e. 2.83, 3.17 and 3.42 h), whereas remaining three exhibited >6 h (i.e. 6.33, 6.50 and 7.00 h) (Figure 5.13). On the other hand, two out of six tested units of 30% w/w K4M CCTs showed <4 h of lag time (i.e. 2.25 and 3.00 h), whereas remaining four showed >11 h (i.e. 11.17, 12.92, 13.08 and 13.42 h) (Figure 5.13). Thus, in both batches, the lag times of some units

were far shorter than remaining ones. As stated earlier, the lower concentration (10% w/w) of K4M in outer coat resulted in shorter lag time due to relatively faster penetration of dissolution medium, whereas higher concentration (30% w/w) of K4M in outer coat resulted in higher mean lag time as well as variability owing to increased elasticity of the outer coat. Thus, pondering over the individual lag times, it was postulated that the CCTs with shorter lag times would have allowed faster ingress of aqueous medium through the outer coat and ruptured before complete hydration/gelation of outer coat HPMC could be accomplished, which in turn, would have made the outer coat elastic enough to withstand against core pressure. Nonetheless, if the outer coat survived the core pressure up to complete hydration of HPMC and converted into a sufficiently elastic/flexible layer, then the rupture would be governed by slow erosion of such elastic coat layer and in that case, CCT would rupture with considerably higher lag time. Besides, shorter lag times of 30% w/w K4M CCTs (2.25 and 3.00 h) were found slightly shorter than that of 20% w/w K4M CCTs (2.83, 3.17 and 3.42 h), whereas higher lag times of 30% w/w K4M CCTs (11.17, 12.92, 13.08 and 13.42 h) were found to be quite higher than that of 20% w/w K4M CCTs (6.33, 6.50 and 7.00 h) (Figure 5.13). This also signifies that it was relatively faster ingress of dissolution medium though the outer coat of 30% w/w K4M CCTs which ruptured couple of higher concentration (30% w/w) units slightly earlier than those with lower concentration (20% w/w) before complete hydration of HPMC could be possible; whereas after sufficient hydration of HPMC, more stronger gelling and elasticity of outer coat in 30% w/w K4M CCTs prolonged the rupturing time of remaining higher concentration (30% w/w) units in comparison to those with lower concentration (20% w/w). Thus, increase in concentration of higher MW HPMC (K4M) in outer coat resulted in increased lag time variability.

The last critical point is the premature release (<5%) observed with 30% w/w K4M CCTs (highest selected concentration of highest MW HPMC) before the rupturing of outer coat. Here, three (i.e. with lag times of '*11.17*', '*13.08*' and '*13.42*' h) out of four higher rupturing units (with lag times of 11.17, 12.92, 13.08 and 13.42 h) demonstrated slight premature release whereas units with shorter rupturing time (2.25 and 3.00 h) did not depict any premature release (Figure 5.13). In other words, undesired premature release was only observed with completely hydrated and gelled units which provided diffusion paths for the drug molecules to diffuse out from

surrounding coat. This implies that at 30% w/w concentration of K4M in outer coat, the CCTs started to transform towards SR type from burst PR. Hence, in addition to high variability, premature release also unfit higher concentration of HPMC K4M in outer coat for developing EC based PR CCTs.

Concisely, the CCTs of higher MW HPMCs (K100LV and K4M) demonstrated comparatively higher variability in lag time than those of low MW grades (E5, E15 and E50). Further, with K4M CCTs, the variability in lag time significantly increased with increase in its concentration in the outer coat and at 30% w/w level slight premature release was also observed before the rupture of outer coat. Thus, higher concentration of HPMC K4M in the outer coat was found incompetent with regards to stated drawbacks. In nutshell, low MW HPMCs (E5, E15 and E50), which exhibited low variability in lag time (less than 10 %RSD i.e. within USP limits) and no premature release, were found to be more efficient and should be preferred for developing robust EC based PR CCTs. Hence, further development and optimization of outer coat was carried out using HPMC E5 as a hydrophilic polymer for achieving desired lag time.

5.1.3.4.4. Risk assessment by FMEA

Once all key ingredients of the formulation have been selected, further development and optimization was carried out using risk assessment by FMEA approach. The factors, which were considered critical, were assessed by FMEA as elaborated in Table 5.19. All three failure modes were ranked for each critical parameter and RPN was calculated using Eq. 5.3. The factors with RPN $\geq$ 40 were considered at high risk, RPN $\geq$ 20 but < 40 were considered at medium risk, and RPN < 20 were considered at low risk (33, 34). Here, the factors with medium risk category were evaluated using OFAT approach whereas those with high risk category were investigated using design of experiment (DoE) approach. Thus, core tablet super-disintegrant amount, core tablet hardness, and CCT hardness were investigated using OFAT approach whereas amount of HPMC in outer coat and coating weight were subjected to statistical optimization using DoE.

Table 5.19 Risk assessment by FMEA analysis to identify criticality of failure modes

Formulation/ process parameter	Failure mode	Failure Severity Potential Effects	S	Failure Occurrence Potential causes	O	Failure Detectability Method or control	D	RPN
Core tablet elements								
Concentration of super-disintegrant	Inappropriate super-disintegrant concentration	Lag time, burst release	4	Improper concentration	2	Dissolution	3	24
Core tablet hardness	Inappropriate hardness and its range	Lag time, burst release, friability	4	Improper selection, Machine failure, operator's error	3	Hardness, friability, dissolution	2	24
Coating elements								
Concentration of HPMC	Inappropriate HPMC concentration	Lag time, burst release	5	Improper concentration	4	Dissolution	3	60
Coating weight	Inappropriate coating weight	Lag time	5	Improper selection, Weight variation	5	Weight variation, Dissolution	2	50
CCT hardness	Inappropriate hardness and its range	Lag time, friability	5	Improper selection, Machine failure, operator's error	3	Hardness, friability, dissolution	2	30
Packaging and stability of final formulation	Effect of temperature and humidity	Hardness, assay, drug release	5	Improper selection of excipient, packaging material	3	Hardness, assay, drug release	2	30

5.1.3.4.4.1. Risk assessment of core elements

Since the core tablets were formulated with 3% w/w SSG and 5 kp hardness (range 4-6 kp), the risk associated with them were examined by selectively varying their levels, on both, higher as well as lower side to the target value – i.e. 2% w/w and 4% w/w SSG; and 3 kp (range 2-4 kp) and 7 kp (range 6-8 kp) hardness. For the same, initially core tablets were prepared by selectively altering SSG level while keeping all other parameters constant followed by compression coating with 240 mg of EC-HPMC E5 blend (20% w/w HPMC) to obtain the CCTs with 13 kp hardness. In a similar way, the CCTs with different core tablet hardness (i.e. 3 kp and 7 kp), were also prepared while keeping all other parameters constant. The CCTs, when evaluated for drug release testing, revealed that the selected change in either core tablet SSG or hardness did not significantly (p value >0.05) alter either lag time or burst release behaviour. Thus, it was concluded that at selected levels, the risk of failure for core tablet SSG (3% w/w) as well as core tablet hardness (4-6 kp) was low. Further, the impact of double compression on core tablets was also determined by carefully scraping out the outer coat of CCT (20% w/w HPMC) and analyzing the core tablets for thickness, hardness and drug release. The results depicted no distinguishable difference in all three parameters due to double compression. Hence, impact of compression coating on core tablet attributes was found to be low.

5.1.3.4.4.2. Risk assessment of coating elements

The risk assessment of coating elements are elucidated in Table 5.19 wherein the CCT hardness was found in medium risk category (i.e. RPN 20-40) whereas HPMC concentration and coating weight were found in high risk category (i.e. RPN >40). Hence, assessment of CCT hardness was carried out using OFAT approach by examining its effect, at both, higher as well as lower side from the target value. Here, the CCTs were prepared at two different hardness i.e. 10 kp (range 9-11 kp) and 16 kp (range 15-17 kp) with 240 mg of EC-HPMC E5 blend (20% w/w HPMC) using preformed PRS core. Both CCTs, when analyzed for drug release testing, demonstrated no significant difference (p value >0.05) on either lag time or burst release. So, it was inferred that the risk of failure for selected CCT hardness (11.5-14.5 kp) was low.

5.1.3.4.4.3. Statistical optimization

The optimization of two most critical parameters i.e. concentration of HPMC in outer coat and coating weight were carried out using circumscribed CCD (2 factor, 5 level, 13 run) as a DoE tool to obtain the desired quality traits (61). For optimization, the limits of lag time were further constrained to 4-5 h instead of 4-6 h in order to clinch better drug delivery. The levels were meticulously chosen based on the results of our preliminary screening studies.

The two most critical attributes of a PR formulation are stringent lag time and sharp burst release after completion of lag time. The later target was almost ensured by formulating fast dissolving IR core which thereafter kept constant during optimization and desired lag time was exclusively targeted by optimization of outer coat. Precisely, the aim was to obtain the HPMC concentration which would exhibit 4-5 h of lag time with 5% weight variation limit. The selected CCD with actual and coded levels for both independent variables is depicted in Table 5.20. Lag time and burst release were selected as dependent variables.

Table 5.20 Selected formulation variables and their levels for CCD

Independent variables	Actual levels	Coded levels
X_1	11.344	-1.414
HPMC concentration	13	-1
(% w/w in outer coat)	17	0
	21	1
	22.656	1.414
X_2	211.72	-1.414
Coating weight (mg)	220	-1
	240	0
	260	1
	268.28	1.414
Dependent variables	**Constrain**	
Y_1 - Lag time	4-5 h	
Y_2 - Burst release	>85% within 30 min after completion of lag time	

The experimental CCD matrix with their measured responses is displayed in Table 5.21. The experimental sequence was randomised to exclude any bias. As expected, time to reach 85% drug release after completion of lag time (Y_2) was less than 15 min for all batches; which was fairly within the desired specification of 30 min. Hence, the optimization was solely focussed for response Y_1 i.e. lag time. The statistical analysis was carried out using Minitab software (ver. 16.2.1., Minitab Inc., USA) and the model was generated as shown in Table 5.22. The resultant main effect plot, interaction plot, and residual plot are respectively shown in Figure 5.18, Figure 5.19 and Figure 5.20. The main effect plot clearly demonstrates that the lag time decreased with increase in HPMC concentration and decrease in coating weight. The interaction plot abolished the interaction possibility between selected independent variables. Residual plot reveals that residuals were normally distributed and existence of missing terms, skewness, outliers, or unidentified variables were ruled out.

Table 5.21 Experimental matrix of CCD with measured responses

Experimental Sequence	Standard order	HPMC level (X_1)	Coating level (X_2)	Lag time (h)[#] (Y_1)	Time to achieve 85% of drug release after completion of lag time (min) (Y_2)
3	1	-1.000	-1.000	4.833 ± 0.190	< 15 min
13	2	1.000	-1.000	3.917 ± 0.149	< 15 min
7	3	-1.000	1.000	5.250 ± 0.175	< 15 min
6	4	1.000	1.000	4.167 ± 0.139	< 15 min
1	5	-1.414	0.000	5.250 ± 0.139	< 15 min
5	6	1.414	0.000	3.833 ± 0.149	< 15 min
10	7	0.000	-1.414	4.250 ± 0.118	< 15 min
4	8	0.000	1.414	4.917 ± 0.105	< 15 min
12	9	0.000	0.000	4.667 ± 0.105	< 15 min
9	10	0.000	0.000	4.833 ± 0.149	< 15 min
2	11	0.000	0.000	4.583 ± 0.129	< 15 min
11	12	0.000	0.000	4.750 ± 0.149	< 15 min
8	13	0.000	0.000	4.667 ± 0.091	< 15 min

[#]mean±SD; n=6

Table 5.22 Estimated Regression Coefficients for lag time along with their p values

Regression Term	Coefficient	p value (Prob >F)
Constant	4.70000	0.000*
X_1	-0.50043	0.000*
X_2	0.20118	0.000*
X_1^2	-0.08437	0.029*
X_2^2	-0.06354	0.079
$X_1 X_2$	-0.04167	0.341

Regression coefficients are in coded value
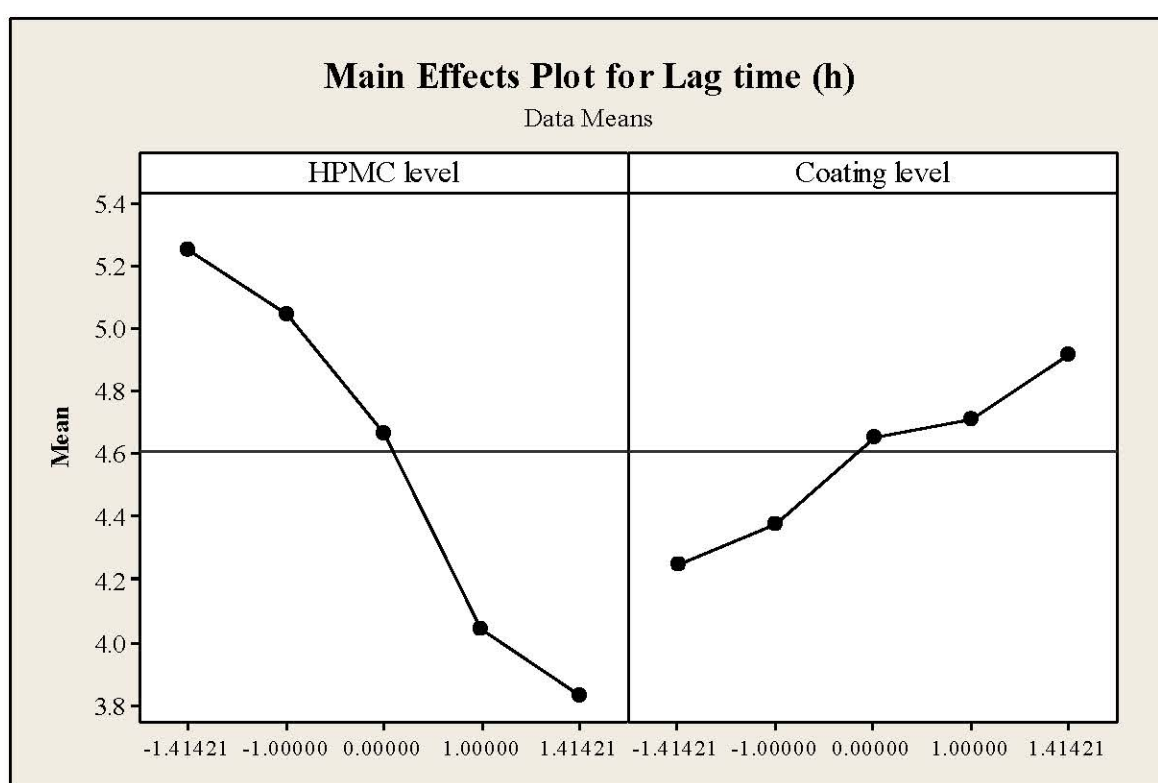
*statistically significant (p value < 0.05)

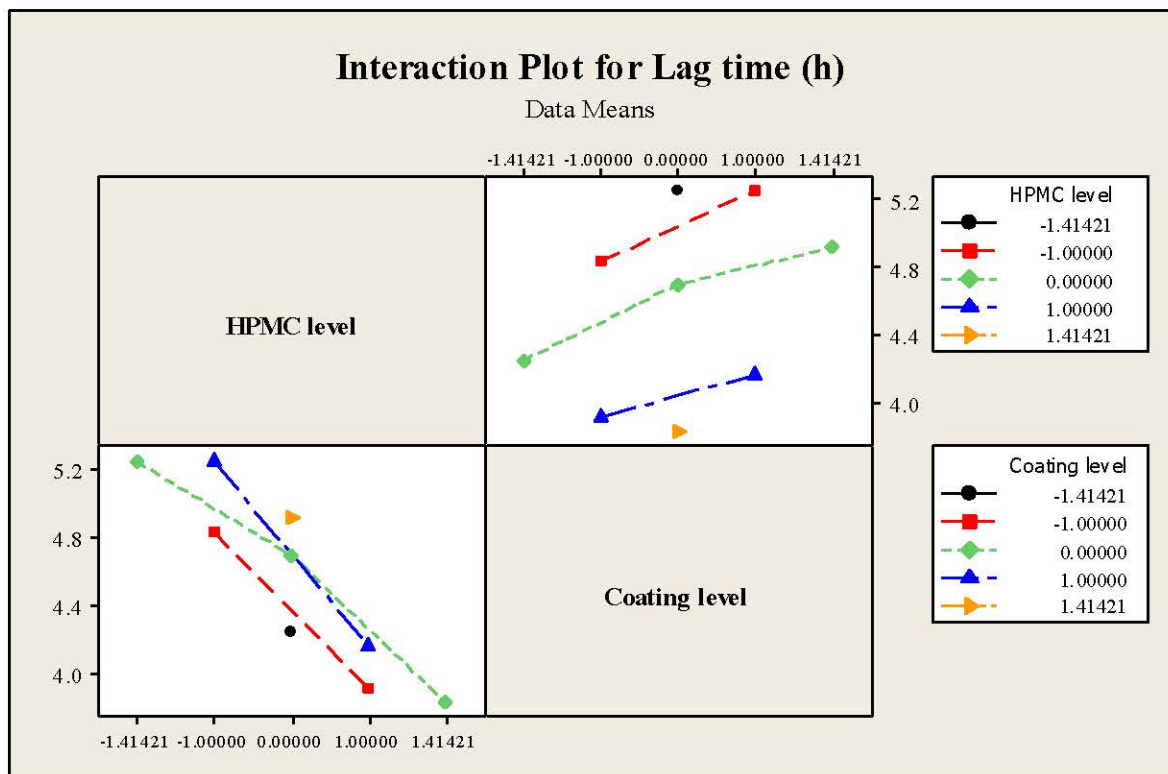Fig. 5.18 Main effect plot of lag time as a function of HPMC and Coating levels

Fig. 5.19 Interaction plot of lag time as a function of HPMC and Coating levels
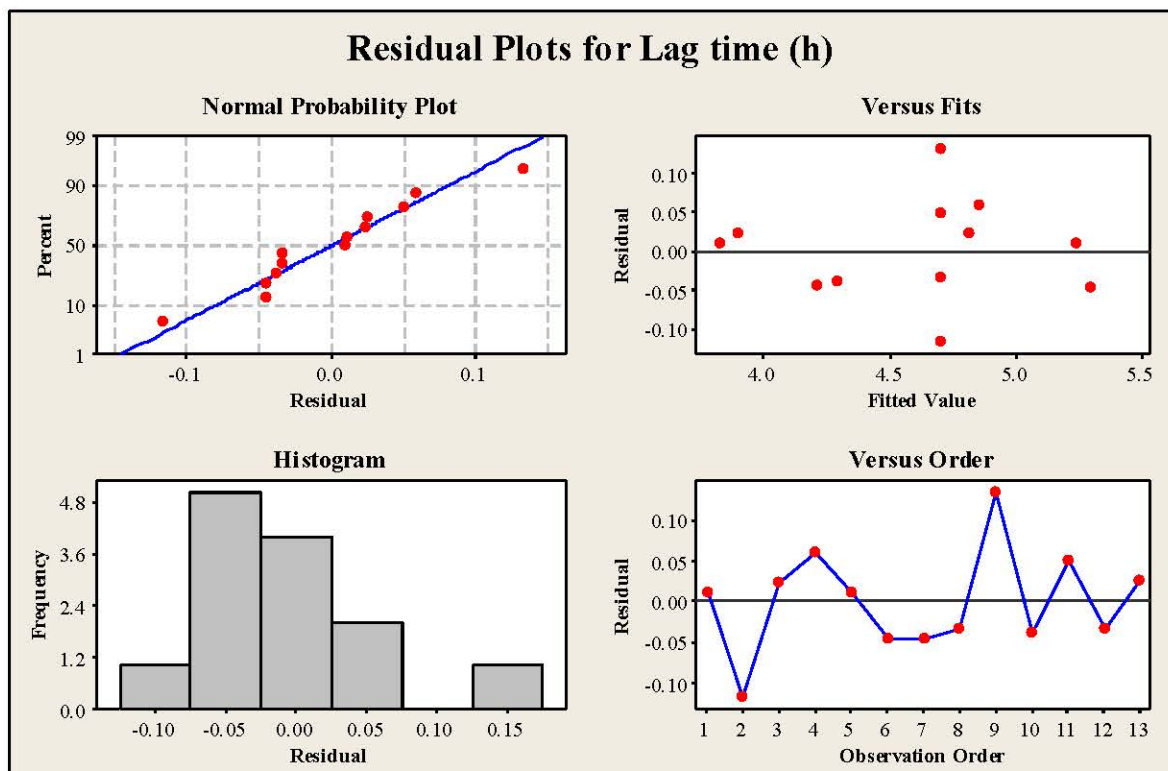

Fig. 5.20 Residual plot of lag time as a function of HPMC and Coating levels

Table 5.22 elucidate that the generated model was best fitted by Eq. 5.4 which is a full model and converted to reduced model, i.e. Eq. 5.5, by eliminating non-significant model terms (having p values >0.05).

$$Y_1 = 4.7000 - 0.5004\,X_1 + 0.2012\,X_2 - 0.0844\,X_1{}^2 - 0.0635\,X_2{}^2 - 0.0417\,X_1\,X_2 \quad (5.4)$$

$$Y_1 = 4.7000 - 0.5004\,X_1 + 0.2012\,X_2 - 0.0844\,X_1{}^2 \quad\quad\quad\quad\quad (5.5)$$

The value of R^2, predicted R^2, and adjusted R^2 were respectively found to be 0.9810, 0.9468 and 0.9675. The value of R^2 describes the amount of variation in the observed responses that is explained by the model (i.e. 98.10%); the value of predicted R^2 reflects how well the model will predict future data (i.e. 94.68%); and the value of adjusted R^2 is a modified R^2 that has been adjusted for number of terms in the model. Typically, higher values of all three parameters represent a model with good fit (33). The developed model was further examined for lack-of-fit which demonstrates the variation due to model inadequacy. As shown in Table 5.23 (ANOVA results), the p value of lack-of-fit was found to be 0.771 which is not less than 0.05 and therefore not significant. Further, the F-value of 0.38 implies the lack-of-fit is not significant relative to the pure error. There is a 77.1% chance that a 'lack-of-fit F-value' this large could occur due to noise. Hence, there is no evidence that the model does not adequately explain the variation in the responses. Thus, non-significant lack-of-fit was good and the model can be used to fit responses (62). Moreover, goodness of fit was also checked by adequate precision (Design Expert, ver. 8.0.7.1, Stat-Ease Inc., USA) which measures the signal to noise ratio. A ratio of greater than 4 is desirable (33). The value of adequate precision was found to be 26.6 that indicate an adequate signal and therefore the model can be used to navigate design space. The developed model was further cross validated using three individual experiments by varying the levels of independent variables at values other than those used to generate the model. The % bias between the experimental values and predicted values was calculated which was found to be less than 10%. Hence, it was concluded that the developed model can be efficiently used to predict the effect of chosen formulation variables on the response under study.

Table 5.23 Analysis of Variance (ANOVA) results of effect of HPMC and Coating levels on lag time

Source	DF	Seq SS	Adj SS	Adj MS	F	p value
Regression	5	2.40327	2.40327	0.48065	72.34	0.000
Linear	2	2.32727	2.32727	1.16364	175.12	0.000
X_1	1	2.00347	2.00347	2.00347	301.52	0.000
X_2	1	0.32380	0.32380	0.32380	48.73	0.000
Square	2	0.06906	0.06906	0.03453	5.20	0.041
X_1^2	1	0.04097	0.04952	0.04952	7.45	0.029
X_2^2	1	0.02809	0.02809	0.02809	4.23	0.079
Interaction	1	0.00694	0.00694	0.00694	1.05	0.341
$X_1 X_2$	1	0.00694	0.00694	0.00694	1.05	0.341
Residual Error	7	0.04651	0.04651	0.00664		
Lack-of-Fit	3	0.01040	0.01040	0.00347	0.38	0.771
Pure Error	4	0.03611	0.03611	0.00903		
Total	12	2.44979				

The developed model was employed for generation of design space using contour plot as displayed in Figure 5.21.

Contour Plot of Lag time (h) vs coating level, HPMC level
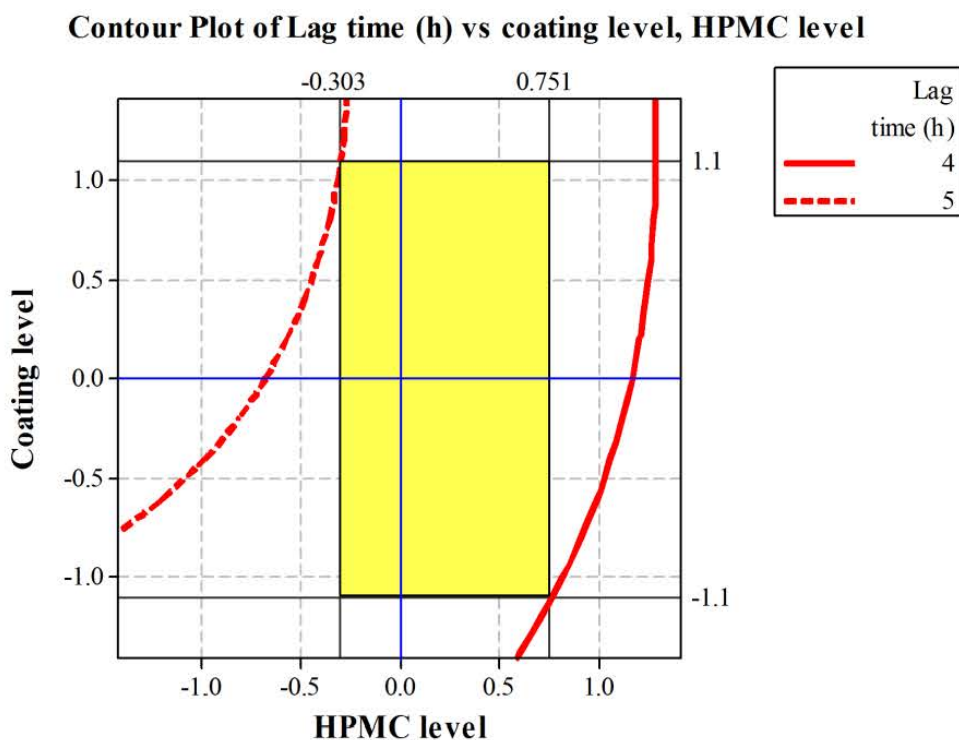
Fig. 5.21 The contour plot of lag time for selected HPMC and coating levels with corresponding design space

As shown in Figure 5.21, the middle levels (0, 0) of both independent variables reasonably fall within 4-5 h lag time. Looking at Table 5.20, the corresponding actual level for coating weight was found 240 mg; which would result in a CCT of 340 mg with an addition of 100 mg core. The 5% weight variation of 340 mg tablet is ($\pm$17) mg. However, it would also be possible to have weight variation for previously devised core tablets, i.e. ($\pm$5) mg, which may confound with the weight variation of outer coat. Hence, it would not be always possible to explicitly point out the actual weight variation occurred due to individual core and/or coat components in a final CCT. Therefore, considering a worst case scenario, the optimization was carried out with expanded weight variation limit, i.e. ($\pm$17) mg plus ($\pm$5) mg – equal to ($\pm$22) mg for final CCT. Extrapolating these limits to the coded levels depicts ($\pm$1.1) levels for coating weight; using which a rectangle was made between the contour lines of 4-5 h lag time to establish the limits for HPMC levels. The obtained HPMC levels were (-0.303) and (+0.751) in coded units (Figure 5.21), for which respective actual levels were found to be (15.8) and (20.0) % w/w. Thus, 240 mg of outer coat with 17% w/w HPMC concentration (in EC-HPMC E5 composition) was found to be suitable for obtaining 4-5 h of lag time and therefore selected as an optimized formula. Since the optimized batch convincingly exhibited the lag time within design space, the risk of associated failure turned to be low.

5.1.3.4.4.4. Evaluation of optimized PRS CCTs

The composition of optimized PRS CCT is depicted in Table 5.24.

Table 5.24 Composition of optimized PRS CCTs

Core tablet			Outer coat		
Ingredients	mg/tab	% w/w	Ingredients	mg/tab	% w/w
PRS	5.0	5.0	EC N10	196.6	81.5
MCC	38.0	38.0	HPMC E5	40.8	17.0
Lactose	53.0	53.0	Talc	2.4	1.0
SSG	3.0	3.0	SSF	1.2	0.5
Colloidal SiO$_2$	0.5	0.5	-	-	-
MgSt	0.5	0.5	-	-	-
Core weight	100.0	100.0	Coating weight	240.0	100.0
5.5 mm standard concave; 4-6 kp hardness			9 mm standard concave; 11.5-14.5 kp hardness		
Optimized CCT – 340 mg; 9 mm standard concave; 11.5-14.5 kp hardness					

The optimized PRS CCT was subjected to variegated characterizations as mentioned in section 5.1.2.9. The appearance was found to be satisfactory. The hardness was 11.5-14.5 kp, thickness was 5.9-6.0 mm and friability was less than 0.5%. The assay and weight variation results were found to be within their respective specification limits.

5.1.3.4.4.4.1. *In vitro* drug release testing (PRS CCTs)

The release profile of optimized PRS CCT is displayed in Figure 5.22 which illustrate 4-6 h of lag time followed by sharp burst release (>85%) within 15 min of outer coat rupturing.
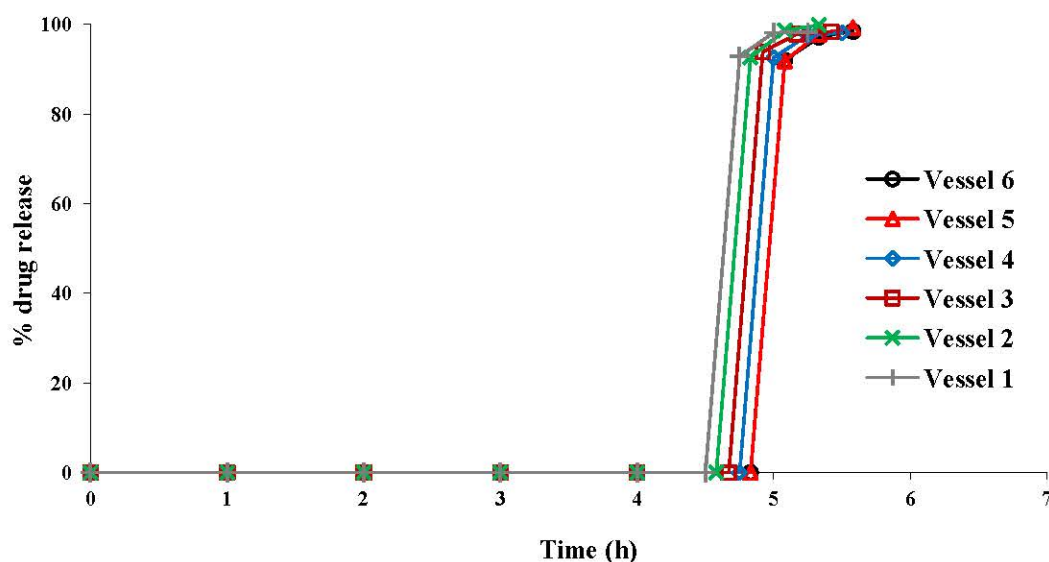
Fig. 5.22 Drug release profile of optimized PRS CCT obtained with basket apparatus; 100 rpm agitation; 0.1 N HCl for first 2 h followed by pH 6.8 buffer; 500 mL volume; 37±0.5°C temperature.

Further, the optimized formulation was subjected to variegated *in vitro* release characterizations viz. multi-media, change in apparatus, change in agitation intensity, biorelevant dissolution testing and alcohol-induced dose dumping study. The lag time results of the same are illustrated in Figure 5.23. All dissolution testing exhibited typical release behaviour i.e. stringent lag time followed by burst drug release. As shown in Figure 5.23, except alcohol-induced dose dumping study, all tested dissolution conditions (i.e. multi-media, change in apparatus, change in agitation and biorelevant media) exhibited the desired lag time with no significant difference (p value >0.05).
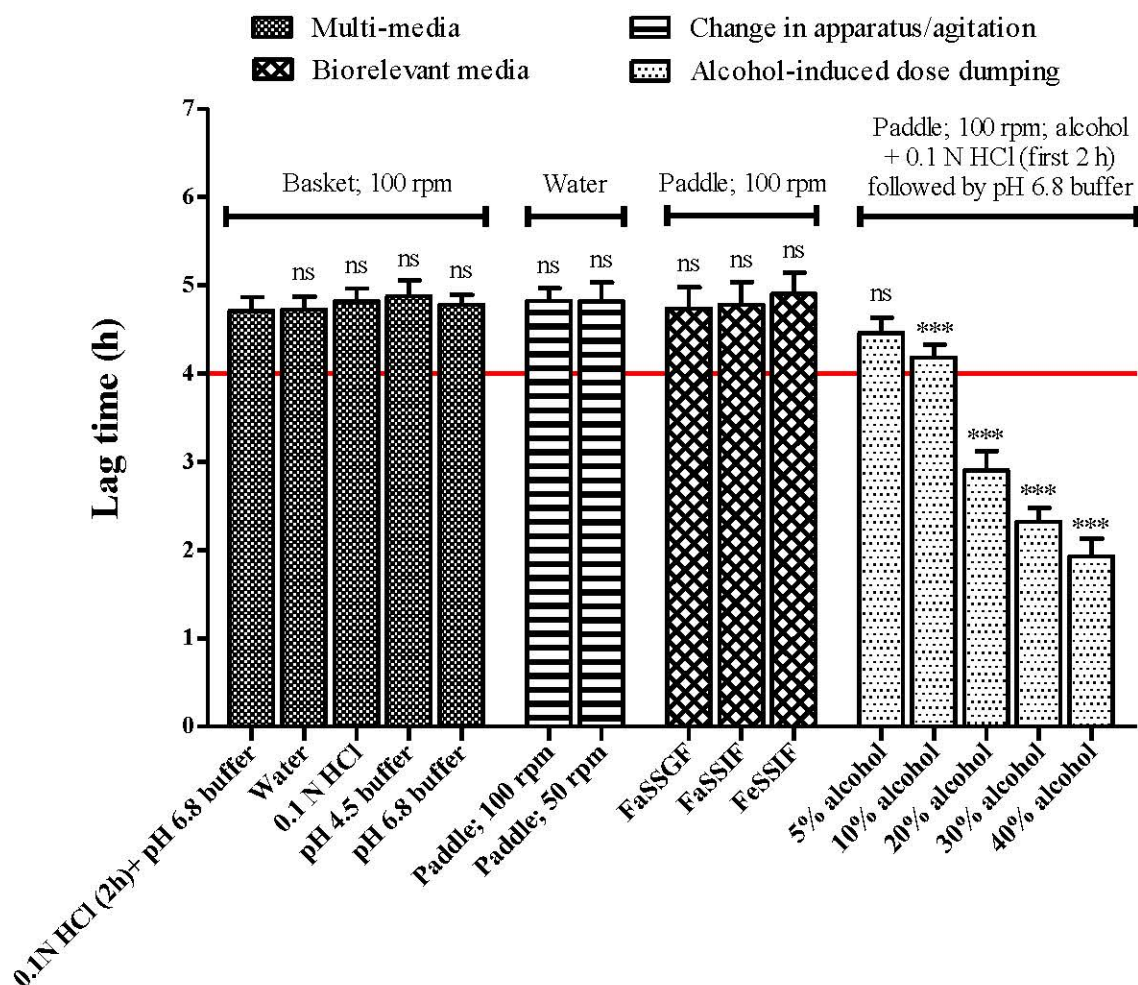
Fig. 5.23 Lag time of PRS CCTs obtained using various dissolution conditions; medium volume 500 mL; temperature $37\pm0.5°C$; [ns] p value>0.05, ***p value<0.001 (mean$\pm$SD; n=6)

The similar release profile with multi-media manifested the developed CCT as pH-independent in nature. Further, akin release behaviour with different apparatus as well as with different agitation intensity deduced that the lag time was robust enough and not influenced by change in hydrodynamics (40).

Since last some years, use of biorelevant media has been significantly increased in the assessment of solid oral dosage forms. The term biorelevant itself signifies 'biologically relevant' to *in vivo* GI fluid which can closely simulate *in vitro* release with actual or *in vivo* release. Various biorelevant media with diverse compositions are available in the literature which can be used according to the purpose (40, 63-68). In this study, three biorelevant media (FaSSGF, FaSSIF, and FeSSIF) were employed for the assessment of optimized CCT. As depicted in Figure 5.23, all three biorelevant

media exhibited desired 4-6 h of lag time followed by burst release profile. Prudently, the analogous results of biorelevant media strongly anticipate promising *in vivo* performance.

According to USFDA (69), modified release (MR) dosage forms should also be evaluated for alcohol-induced dose dumping to check the risk associated with co-administration of alcohol and to inform the patients if required. The assessment is recommended at different ethanol concentration (i.e. 5-40% v/v) in 0.1 N HCl as dissolution medium up to 2 h (70). However, in the present study, we had examined the effect of alcohol on the release profile even after 2 h by replacing the former medium with pH 6.8 phosphate buffer. The study revealed that up to 10% v/v alcohol concentration, the lag time was found within desired 4-6 h of specification limits, but with further increase in alcohol concentration, i.e. ≥20% v/v, the formulation failed to demonstrate desired lag time (Figure 5.23). The lag time progressively decreased with increase in alcohol concentration. The finding was expected and pretty in-line with the solubility of EC i.e. insoluble in water but soluble in alcohol (39) . Overall, it can be said that the developed CCT is not resistant against alcohol-induced dose dumping and associated risk has to be appropriately mentioned on the label as 'not to be co-administered along with alcohol'.

5.1.3.4.4.4.2. SEM study

The optimized PRS CCT was examined for SEM testing before and after drug release study. The SEM images (Figure 5.24) revealed that the CCT surface, which was fairly smooth before dissolution, turned rough after dissolution due to generation of pores. Thus, it was inferred that the water soluble HPMC, which was incorporated as a pore former within EC matrix, gradually dissolved out of the tablet surface upon exposure to aqueous medium. The resultant pores allowed ingress of the aqueous medium to the swellable core tablet, which in turn imparted pressure on surrounding rigid coat layer and ultimately ruptured it to cause burst drug release.
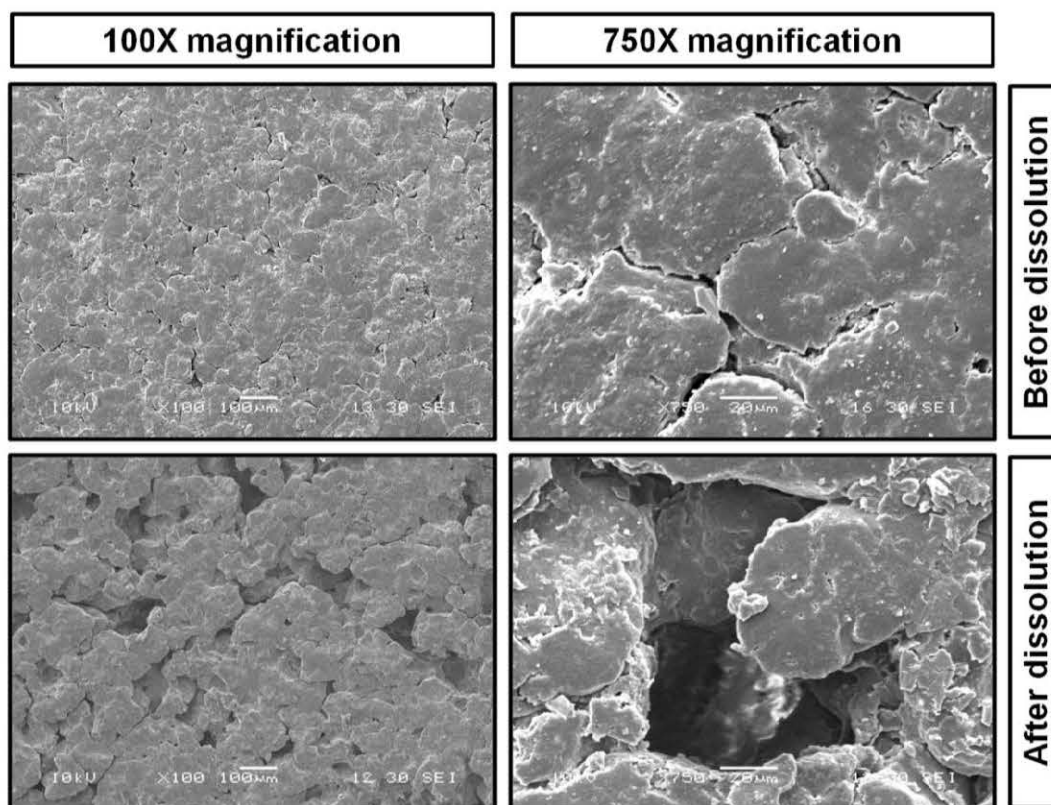
Fig. 5.24 SEM images of optimized PRS CCT before and after drug release study

5.1.3.4.4.4.3. Effect of curing (PRS CCTs)

Many times, polymer cross linking upon stability may also alter the release behaviour of a formulation (40) . Hence, the optimized CCTs were subjected to curing at 60°C for 24 h in hot air oven and subsequently analyzed for appearance, hardness, assay, and drug release. All results were found within their respective specification limits (Table 5.25) with no distinguishable difference before and after curing. Thus, no effect of curing was observed and it can be said that the outer coat polymers did not undergo internal cross-linking or became hard upon storage.

Table 5.25 Results of curing study for optimized PRS CCTs

Effect of curing	Appearance	Hardness	Assay	Lag time*	Burst release
Before curing	White colour	11.5-14.5 kp	99.6 %	4.71 ± 0.16 h	>85% in 15 min
After curing	No change	No change	99.3 %	4.76 ± 0.19 h	>85% in 15 min

*mean±SD; n=6

5.1.3.4.4.4.4. Packaging and stability (PRS CCTs)

The optimized CCTs demonstrated no detectable change for either of appearance, hardness, assay, or drug release under stated storage conditions. All results were found within their respective specification limits (Table 5.26) and hence the formulation was found stable under the selected packaging material and the risk of failure associated with the same was low.

Table 5.26 Results of stability study for optimized PRS CCTs

Storage condition	Appearance	Hardness	Assay	Lag time*	Burst release
Initial	White colour	11.5-14.5 kp	99.6 %	4.71±0.16 h	>85% in 15 min
25±2°C/60±5% RH (3M)	No change	No change	99.8 %	4.68±0.19 h	>85% in 15 min
40±2°C/75±5% RH (3M)	No change	No change	99.2 %	4.67±0.21 h	>85% in 15 min

*mean±SD; n=6

5.1.3.4.4.5. Updated risk assessment

Table 5.27 demonstrates the risk mitigation of failure modes (using FMEA) after implementation of control strategy. As shown in Table, the risk of failure for all critical parameters was found low (RPN < 20) after implementation of control strategy; the detail description of which is mentioned in their respective sections. Figure 5.25 illustrates comparative risk evaluation before and after implementation of control strategy. The final and updated risk analyses matrix for formulation variables and for unit operations after optimization are respectively depicted in Table 5.28 and Table 5.29; and respective justifications for the reduced risk are depicted in Table 5.30 and Table 5.31. The tables clearly exhibited that after optimization risk and impact of formulation variables and unit operations on drug product quality attribute falls under low category. However, it should be noted that the scalability of the process needs to be evaluated from subsequent transfer from lab scale to pilot scale and then to large commercial scale which may be possible with supplementary experience necessary for commercial lifecycle management.

Table 5.27 Risk mitigation of failure modes after implementation of control strategy

| Formulation/ process parameter	Failure mode	Failure Severity Potential Effects	S	Failure Occurrence Potential causes	O	Failure Detectability Method or control	D	RPN
Core tablet elements								
Concentration of super-disintegrant	Inappropriate super-disintegrant concentration	Lag time, burst release	2	Improper concentration	2	Dissolution	3	12
Core tablet hardness	Inappropriate hardness and its range	Lag time, burst release, friability	2	Improper selection, Machine failure, operator's error	2	Hardness, friability, dissolution	2	8
Coating elements								
Concentration of HPMC	Inappropriate HPMC concentration	Lag time, burst release	2	Improper concentration	2	Dissolution	3	12
Coating weight	Inappropriate coating weight	Lag time	2	Improper selection, Weight variation	2	Weight variation, Dissolution	2	8
CCT hardness	Inappropriate hardness and its range	Lag time, friability	2	Improper selection, Machine failure, operator's error	2	Hardness, friability, dissolution	2	8
Packaging and stability of final formulation	Effect of temperature and humidity	Hardness, assay, drug release	3	Improper selection of excipient, packaging material	2	Hardness, assay, drug release	2	12
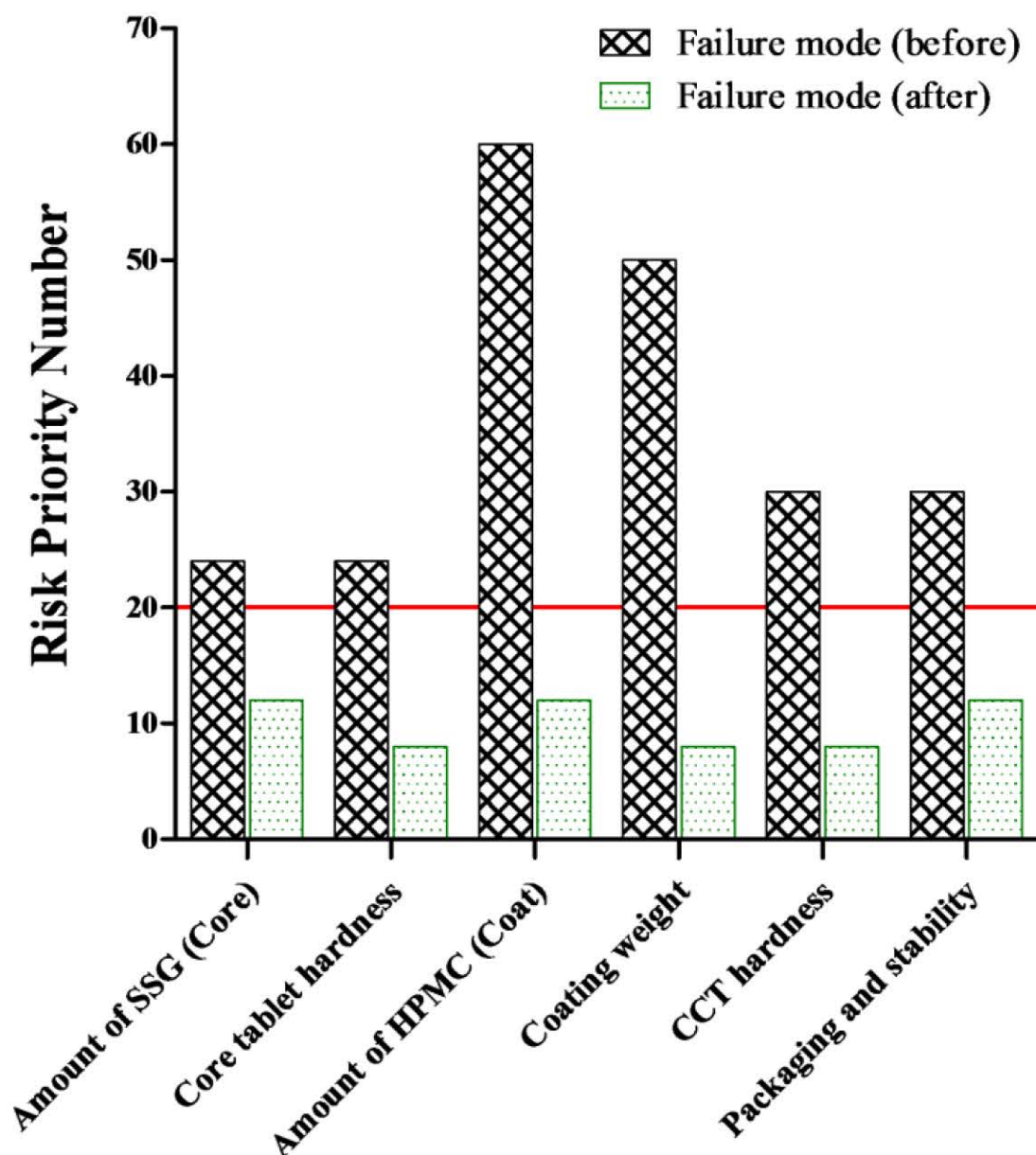
Fig. 5.25 FMEA analysis of PR formulation depicting RPN of failure modes before and after implementation of control strategy

Table 5.28 Final and updated risk analysis matrix for identification of impact of formulation ingredients on drug product attributes

Core tablet elements				
CT CQAs*	Fillers	Super-disintegrant	Glidant	Lubricant
CT Hardness	Low	Low	Low	Low
Assay	Low	Low	Low	Low
CU	Low	Low	Low	Low
CT release profile	Low	Low	Low	Low
Coating elements				
CCT CQAs#	Core tablet attributes	Hydrophilic pore former	Coating weight	Glidant	Lubricant
CCT Hardness	Low	Low	Low	Low	Low
CCT release profile	Low	Low	Low	Low	Low

CT CQAs* Core Tablet critical quality attributes; CCT CQAs# Compression-coated tablet critical quality attributes

Table 5.29 Final and updated risk analysis matrix for identification of impact of unit operations on drug product attributes

Core tablet elements				
CT CQAs*	Sifting	Blending	Compression	Compression coating
CT Hardness	Low	Low	Low	Low
Assay	Low	Low	Low	Low
CU	Low	Low	Low	Low
CT release profile	Low	Low	Low	Low
Coating elements				
CCT CQAs*	Sifting	Blending	Compression	
CCT Hardness	Low	Low	Low	
CCT release profile	Low	Low	Low	

CT CQAs* Core Tablet critical quality attributes; CCT CQAs# Compression-coated tablet critical quality attributes

Table 5.30 Justifications for updated risk assessment of formulation variables on drug product attributes

Formulation variable	Drug product CQA	Risk category	Justification for the reduced risk
Fillers (core)	CT Hardness	Low	Typically higher concentration of widely used fillers, i.e. lactose, MCC and its ratio, was found suitable for obtaining desired hardness. Risk is updated from medium to low.
Super disintegrant (core)	CT drug release profile	Low	The selected concentration of SSG exhibited >85% drug release within 15 min which is reasonably within the desired specification limits. The risk of failure turned to be low.
Lubricant (core)	CT Hardness	Low	The selected concentration (0.5% w/w) of MgSt did not exhibit any problem while achieving desired hardness as well as release profile. Associated risk turned to be low.
	CT drug release profile	Low	
Core tablet attributes	CCT drug release profile	Low	The effects of critical core attributes (i.e. SSG, hardness) were thoroughly investigated by changing their levels on lower as well as higher side. However, the lag time and burst release profile was found within their respective specification limits without any significant difference. Thus, with chosen core tablet attributes, the risk of failure for obtaining desired CCT release profile was found under low risk category.
Hydrophilic pore former (coat)	CCT drug release profile	Low	Appropriate hydrophilic additive (i.e. HPMC E5) was selected by thorough preliminary investigation and its concentration was optimized using CCD in order to get desired release profile. Since the concentration was optimized by establishing the design space, the risk of failure was shifted to low risk category.
Coating weight	CCT drug release profile	Low	In order to obtain target release profile, the coating weight was optimized using CCD and design space was generated considering in-process weight variation. The risk was updated to low risk category.
Glidant (coat)	CCT drug release profile	Low	Talc was selected as a glidant after thorough investigation. At the selected concentration (i.e. 1% w/w) of talc, the risk of failure was found to be low.
Lubricant (coat)	CCT Hardness	Low	Various lubricants were investigated for coat composition out of which SSF was found to be best suited for the stated purpose. At the selected concentration (i.e. 0.5% w/w), the risk of failure for CCT hardness as well as CCT release profile was found to be low.
	CCT drug release profile	Low	

Table 5.31 Justifications for updated risk assessment of unit operations on drug product attributes

Process variable	Drug product CQA	Risk category	Justification for the reduced risk
Blending (core)	Assay	Low	Assay and CU results exhibited that selected blending speed and time was found suitable for homogeneous mixing of blend. Further, the obtained release profile (i.e. >85% within 15 min) also ruled out the possibility of over-blending/over-lubrication with MgSt. Thus, associated risks turned to be low.
	CU	Low	
	CT drug release profile	Low	
Compression (core)	CT Hardness	Low	The compression force was suitably adjusted to achieve 4-6 kp hardness. The prepared tablets were evaluated for hardness, assay, CU and drug release profile. At selected hardness, the core tablets exhibited >85% drug release within 15 min which was reasonably under the specification limits (i.e. >85% within 30 min). Further, assay and CU results were also found within their respective specification limits. Hence, associated risks turned to be low.
	Assay	Low	
	CU	Low	
	CT drug release profile	Low	
Compression coating	CT Hardness	Low	The outer shell of the final CCT was carefully scraped out and the separated core was re-evaluated for hardness and drug release testing. Both results were found within their respective specification limits with no significant difference. Thus, CT hardness and CT release profile was not affected by compression coating and therefore associated risk of failure turned to be low.
	CT drug release profile	Low	
Compression (coat)	CCT Hardness	Low	The compression force was adjusted to achieve 11.5-14.5 kp hardness. At selected hardness, the optimized CCT demonstrated desired release profile (i.e. 4-6 h lag time followed by burst release). Further, the hardness was selectively altered on lower as well as higher side to examine its effects on release profile. The lag time as well as burst release profile remained within their respective specification limits without any significant difference. The risk of failure turned to be low.
	CCT drug release profile	Low	

5.1.4. Conclusion (PRS)

The research undertaken exemplifies comprehensive development of PR formulation of PRS employing compression coating technology. The core tablet was meant to be fast disintegrating with typical swelling excipients chosen scrupulously. The outer coat was predominantly fabricated using EC as pH-independent water insoluble excipient. Initially, variegated lubricants and glidants were explored to find the best suitable pair to be opted for further development. The study revealed that each selected glidant/lubricant i.e. colloidal SiO_2, MgSt, SSF, talc, PEG 6000, glyceryl behenate and stearic acid, even at concentration as low as 0.25% w/w, caused significant reduction in lag time as compared to unlubricated CCTs. Amongst selected glidants and lubricants, most detrimental effects were observed with most popular glidant colloidal SiO_2 and lubricant MgSt. The combined effect of colloidal SiO_2 and MgSt converted the PR formulation into IR formulation with almost complete removal of lag time, and thus the most popular glidant-lubricant combination was found unsuitable for development of EC based PR CCTs. On the other hand, less popular lubricants and glidants (i.e. talc, SSF, stearic acid, PEG 6000 and glyceryl behenate) were found to be less injurious and more worthy for development of compression-coated PR formulations. Owing to comparative less impact on lag time, talc-SSF combination was opted for further development of PR CCTs. Subsequently, several hydrophilic additives were investigated to examine their effects on lag time of EC based CCTs. Amongst various hydrophilic additives, freely water soluble hydrophilic fillers (lactose and mannitol) depicted intense reduction in lag time and therefore found inefficient in the development of compression-coated PR formulations. Amongst polymeric binders, HPMC E5 exhibited promising results in terms of lag time as well as less variability, and therefore selected as hydrophilic pore former to be used for development of PR CCTs. Further, the study was conducted to investigate the effects of HPMC MW on lag time of EC based CCTs in order to select appropriate HPMC grade. The study revealed that the CCTs of higher MW HPMCs (K100LV and K4M) demonstrated comparatively higher variability in lag time than that of low MW grades (E5, E15 and E50). With K4M CCTs, the variability in lag time significantly increased with increase in its concentration in the outer coat and at 30% w/w level slight premature release was observed before the rupture of outer coat. Thus, higher concentration of higher MW HPMC in the outer coat was found to be inappropriate with regards to stated

drawbacks. Concisely, HPMC E5 (a low MW HPMC), which exhibited low variability in lag time (less than 10 %RSD i.e. within USP limits) and no premature release, was further opted for development of PR CCTs.

Overall, the development was carried out using application of QbD principles including establishment of QTPP, identification of CQAs, risk assessment of formulation and process variables, statistical optimization using DoE, and finally risk mitigation after implementation of control strategy. Further, the risk assessment of critical formulation and process variables were also carried out using FMEA technique wherein failure modes were ranked according to the risk priorities and RPN were calculated which distributed each critical attribute into low, medium or high risk category. The attributes with medium risk category were evaluated by OFAT approach whereas those with high risk category were investigated using CCD. The CCD model generated the design space using which an optimized HPMC concentration along with 5% weight variation limits (considering a worst case scenario) was obtained. Finally, the RPNs were recalculated using the updated risk of each critical attribute which were reasonably found within low risk category after implementation of control strategy.

The developed PR CCT exhibited 4-6 h of lag time followed by burst release profile at varying dissolution conditions. The lag time was found to be explicitly pH-independent as well as unaffected by change in hydrodynamics. Further, analogous results of biorelevant dissolutions prudently anticipate promising *in vivo* performance. All of these could not be possible without implementation of the QbD tools amalgamated with risk management approaches which have inclined to divulge the degree of improvement for building quality traits inside the product.

5.2. Development of PR CCTs of Methylprednisolone (MPR)

### 5.2.1. MPR drug profile (8-10, 71-78)

MPR is a prednisolone derivative with similar anti-inflammatory and immune-modulating properties. It is a synthetic corticosteroid that inhibits the secretion of substances in the body that leads to inflammation. It has been used for the treatment of many several inflammatory states such as asthma, psoriasis, arthritis, allergic disorders, ulcerative colitis, gland (endocrine) disorders, and conditions that affect lungs, skin, eyes, nervous system, stomach, or blood cells (71).

Physicochemical characteristics (8, 9)

Molecular Formula: $C_{22}H_{30}O_5$

Chemical Name: 11β,17,21-Trihydroxy-6α-methylpregna-1,4-diene-3,20-dione.

Structure:
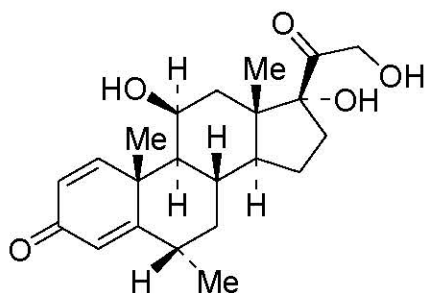
Molecular weight: 374.5 g/mol

Appearance: White or almost white, crystalline powder

Solubility: Practically insoluble in water, sparingly soluble in ethanol, slightly soluble in acetone and in methylene chloride.

Melting point: 228-237 °C

Nature: Neutral

pKa: None

Log P: 1.8

Dose: 4-48 mg

BCS class: II

Mechanism of action: Free drug enters into the cell membrane and attaches with targeted cytoplasmic receptor which leads to alteration in the mRNA transcription and ultimately inhibits the protein synthesis. The drug inhibits synthesis of various inflammatory mediators and suppresses the leucocytes infiltration and invasion at the

inflammatory response and ultimately leads to inhibition of the humoral immunity. Various other pro-inflammatory proteins like phospholipase A2, lipocortins that regulates the biosynthesis of inflammatory mediators like prostaglandins and leukotrienes, can be efficiently inhibited through the corticosteroid (78).

Pharmacokinetics (10, 72-74, 78, 79)

Absorption: Rapidly and almost completely absorbed from GIT.

Peak effect: 1-2 h

Duration of action: 1.25-1.5 days

Plasma half life: $\approx$ 3.5 h

Bioavailability: The absolute bioavailability of MPR is generally high (82% to 89%) after oral administration.

Protein binding: approximately 77% which is independent of dose.

Permeability: An apparent permeability co-efficient of 2.6×10^{-6} cm/s was reported using artificial membrane permeability assay.

Distribution: MPR exhibits linear pharmacokinetics which is independent of route of administration. Volume of distribution at steady state was found to be 91.0 L/1.73m^2.

Metabolism and Excretion: MPR is metabolized in the liver to form inactive metabolites; the major ones are 20β-hydroxymethylprednisolone and 20α-hydroxymethylprednisolone. Metabolism in the liver primarily occurs via the enzyme CYP3A4. Plasma clearance was found to be around 384 ml/min/1.73m^2 and independent of dose.

Adverse effects and contraindications: similar to PRS (76)

5.2.2. Methods (MPR)

After ensuring desired results with developed PRS CCTs, MPR was also formulated in the similar way using optimized PRS formula.

5.2.2.1. RP-HPLC method for determination of MPR

Same as PRS (section 5.1.2.1.2)

The RP-HPLC method, developed for PRS, was also employed for determination of MPR. The chromatographic conditions and various parameters are enlisted in Table 5.32.

Table 5.32 Chromatographic conditions for determination of MPR

Stationary phase:	C18, 250 mm, 4.6 mm, 5 μm
Mobile phase:	60:5:35 % v/v/v mixture of 10 mM phosphate buffer: methanol: acetonitrile
Flow rate:	1 mL/min
Detection wavelength:	240 nm
Temperature:	≈ 25°C
Injection volume:	20 μL
Retention time:	10.08±0.07 min
Asymmetry factor:	1.149±0.010
Theoretical plates:	15769±141.31

5.2.2.1.1. Preparation of standard stock solutions of MPR

Same as PRS (section 5.1.2.1.2.1)
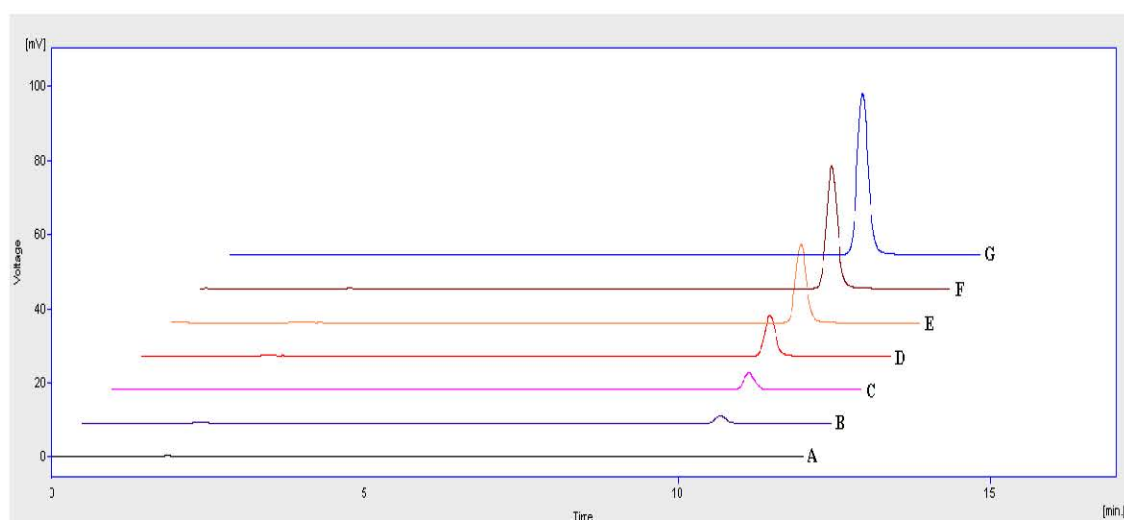
5.2.2.1.2. Preparation of calibration curve of MPR

Same as PRS (section 5.1.2.1.2.2)

The calibration curve was plotted for area vs. concentration (μg/mL) as shown in Table 5.33. The system suitability criteria complied with USP limits (26). The overlaid calibration chromatograms are depicted in Figure 5.26 and corresponding linearity curve, regression equation and correlation coefficient are depicted in Figure 5.27. Accuracy, precision and ruggedness were determined as per ICH guidelines (25) and the results are respectively depicted in Table 5.34, Table 5.35 and Table 5.36. Overall results of validation parameters are depicted in Table 5.37.

Table 5.33 Calibration curve and regression equation of MPR obtained using HPLC method

Concentration (µg/mL)	Area (mV.s) (mean±SD; n=5)
1	25.706±0.424
2	55.057±0.745
5	133.003±1.278
10	263.209±2.080
15	403.689±2.655
20	531.030±3.017
Regression equation	
Slope	0.0345±0.478
Intercept	26.632±0.137
Correlation coefficient	0.9998

Fig. 5.26 Overlain HPLC chromatograms of 1-20 µg/mL MPR; (A) blank, (B) 1 µg/mL, (C) 2 µg/mL, (D) 5 µg/mL, (E) 10 µg/mL, (F) 15 µg/mL and (G) 20 µg/mL

Methylprednisolone calibration curve - HPLC

$$y = 26.632x + 0.0345$$
$$R^2 = 0.9998$$
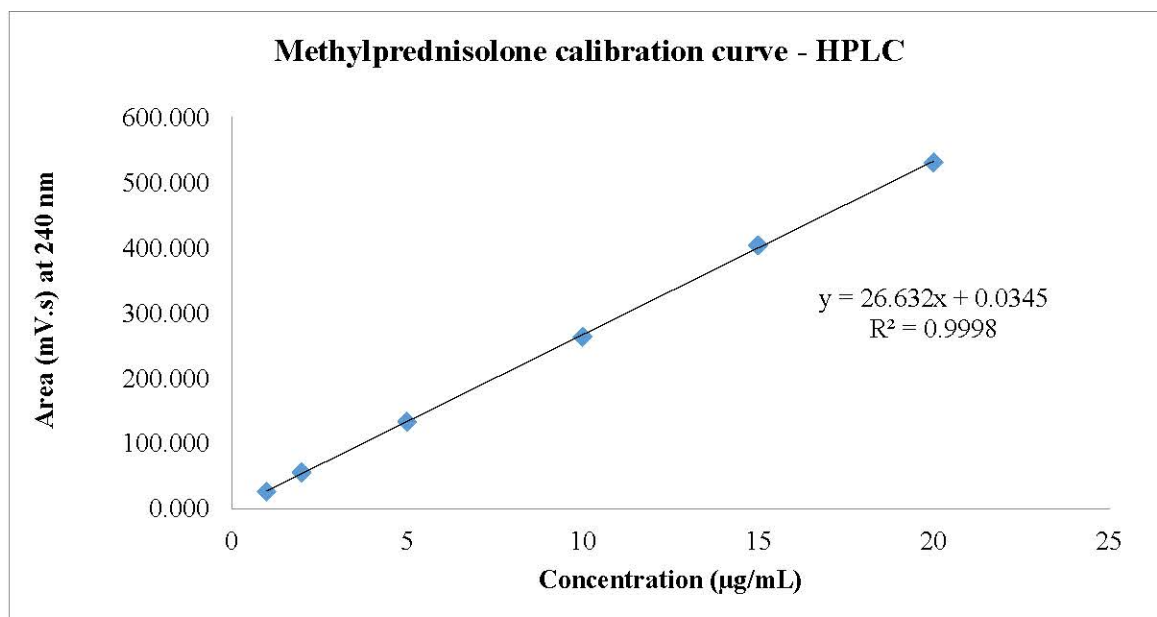
Fig. 5.27 HPLC calibration curve of MPR (1-20 µg/mL)

Table 5.34 Accuracy data of MPR obtained using HPLC method

Amount spiked (mg)	Amount recovered (mg) (mean±SD; n=3)	% recovery (mean±SD; n=3)	% recovery (range; n=3)	Average % recovery
5	5.02±0.05	100.4±0.91	99.4-101.2	
10	9.93±0.08	99.3±0.75	98.5-100.0	100.3
15	15.19±0.06	101.3±0.42	100.8-101.6	

Table 5.35 Precision data of MPR obtained using HPLC method

Concentration (µg/mL)	Repeatability (% RSD; n=3)	Intra-day (% RSD; n=3)	Inter-day (% RSD; n=3)
5	0.42	0.83	1.40
10	0.32	0.66	0.92
15	0.21	0.40	0.67

Table 5.36 Ruggedness data of MPR obtained using HPLC method

Concentration (µg/mL)	% RSD; n=2
5	1.51
10	0.93
15	0.67

Table 5.37 Summary of validation parameters of MPR HPLC method

Parameters	Results
Linearity range	1-20 µg/mL
Correlation coefficient	0.9998
Accuracy (% recovery)	98.5-101.6 %
Precision (% RSD; n=3)	
Repeatability	0.21-0.42 %
Intra-day	0.40-0.83 %
Inter-day	0.67-1.40 %
Ruggedness (% RSD; n=2)	0.67-1.51 %
LOD	0.059 µg/mL
LOQ	0.180 µg/mL

5.2.2.2. Drug-excipient compatibility

Same as section 5.1.2.5

5.2.2.3. Preparation of MPR core tablets

Same as PRS, the core tablets of MPR were prepared by direct compression method as per the composition shown in Table 5.38. The tablets were prepared at a constant average weight (100 mg) by keeping the composition as similar as possible with adjustment of just lactose quantity to compensate the dose of drug; and using the same procedure as mentioned for PRS (section 5.1.2.6.).

Table 5.38 List of ingredients and their respective concentrations employed for formulation of MPR core tablets

Ingredients	mg/tab (%w/w)
MPR	4 mg
MCC	38 mg
Lactose	54 mg
SSG	3 mg
Colloidal SiO_2	0.5 mg
MgSt	0.5 mg
Total weight	100 mg

5.2.2.4. Characterization of MPR core tablets

Same as section 5.1.2.7

5.2.2.5. Preparation of MPR CCTs

The MPR CCTs were formulated using optimized PRS outer coat composition (Table 5.24) by following same procedure as mentioned for PRS (section 5.1.2.8.).

5.2.2.6. Characterization of MPR CCTs

Same as section 5.1.2.9.

5.2.2.7. Packaging and stability study (MPR CCTs)

Same as section 5.1.2.10.

5.2.3. Results and discussion (MPR)

5.2.3.1. Evaluation of MPR core tablets

The physical appearance of core tablets was found to be satisfactory. The tablets had hardness of 4-6 kp, friability less than 0.5% and disintegration time less than 30 s. The tablet thickness was found to be 3.8-3.9 mm. The weight variation, assay and CU results were found to be within their respective specification limits. The release studies demonstrated >85% drug release within 15 min with all tested dissolution conditions and therefore the core tablets were found to be fast dissolving IR tablets (i.e. >85% release within 30 min). The dissolution profile with basket apparatus, 100 rpm, pH 6.8 phosphate buffer, 500 mL, 37±0.5°C is depicted in Figure 5.28. The impact of double compression on core tablets was determined by carefully scraping out the outer coat of CCT and analyzing the core tablets for thickness, hardness and drug release. The results depicted no distinguishable difference in all three parameters due to double compression.
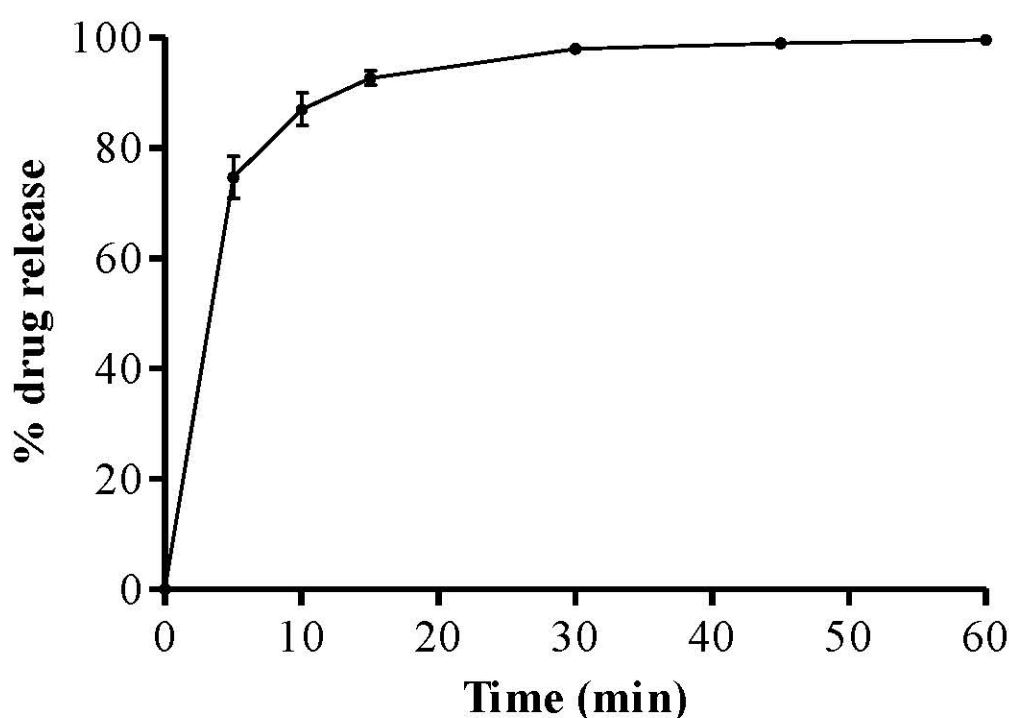

Fig. 5.28 Drug release profile of MPR core tablets in pH 6.8 phosphate buffer; basket apparatus; 100 rpm; 500 mL; 37.0±0.5°C [mean±SD; n=6]

5.2.3.2. Evaluation of MPR CCTs

The appearance was found to be satisfactory. The CCTs had hardness of 11.5-14.5 kp, thickness of 5.9-6.0 mm and friability less than 0.5%. Assay and weight variation results were found to be within their respective specification limits.

5.2.3.2.1. *In vitro* release studies (MPR CCTs)

Similar to PRS CCTs, MPR CCTs also exhibited typical 4-6 h of lag time followed by sharp burst release (>85%) within 15 min of rupturing of outer coat with all tested conditions except hydro-alcoholic media (in which the lag time did not remain confine to 4-6 h). The dissolution profile of MPR CCTs obtained with basket apparatus; 100 rpm; 0.1 N HCl followed by pH 6.8 phosphate buffer is displayed in Figure 5.29. The individual lag time results obtained with various dissolution conditions are demonstrated in Figure 5.30. As shown in Figure 5.30, no significant difference was observed between the lag times of multi-media, change in apparatus, change in agitation and biorelevant dissolution testing (p value >0.05).
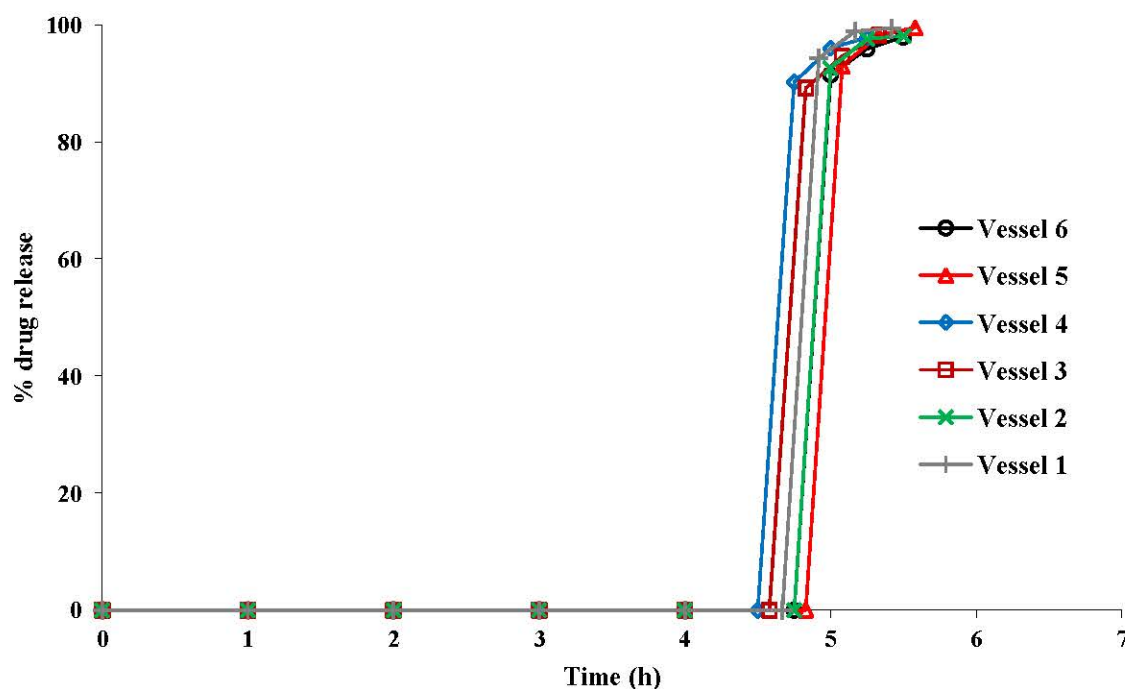

Fig. 5.29 Drug release profile of optimized MPR CCTs obtained with basket apparatus; 100 rpm agitation; 0.1 N HCl for first 2 h followed by pH 6.8 buffer; 500 mL volume; 37±0.5°C temperature.
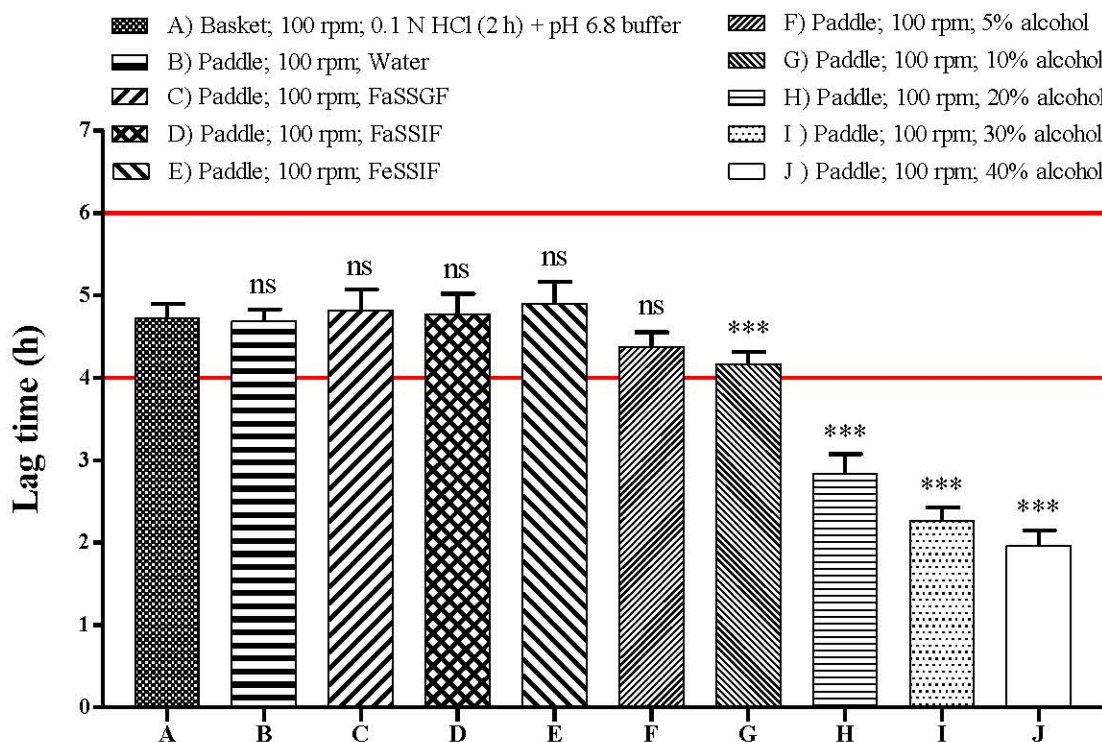
Fig. 5.30 Lag time of MPR CCTs obtained using various dissolution conditions; medium volume 500 mL; temperature $37\pm0.5°C$; [ns] p value>0.05, ***p value<0.001 (mean$\pm$SD; n=6)

Here also, similar release profile with multi-media corroborated the developed CCT as pH-independent in nature. Analogous release behaviour with different apparatus as well as agitation intensity inferred that the lag time was robust enough and not influenced by change in hydrodynamics. Further, akin release profiles with biorelevant media prudently anticipate promising *in vivo* performance. The results of alcohol-induced dose dumping study revealed that up to 10% v/v alcohol concentration, the lag time was found to be within desired 4-6 h of specification limits, whereas with further increase in alcohol concentration, i.e. $\geq$20% v/v, the formulation failed to exhibit desired lag time. Hence, the developed CCT was found to be sensitive to alcohol-induced dose dumping and therefore pertinent instruction has to be mentioned on the label. Overall, the release behaviour of MPR CCTs was found to be quite similar to PRS CCTs.

5.2.3.2.2. Effect of curing (MPR CCTs)

After exposure of 60°C for 24 h, the CCTs, when examined for appearance, hardness, assay, and drug release, exhibited all results within their respective specification limits

(Table 5.39) with no distinguishable difference before and after curing. Thus, no effect of curing was observed and it can be said that the outer coat polymers did not undergo internal cross-linking upon storage.

Table 5.39 Results of curing study for MPR CCTs

Effect of curing	Appearance	Hardness	Assay	Lag time*	Burst release
Before curing	White colour	11.5-14.5 kp	99.9 %	4.72±0.17 h	>85% in 15 min
After curing	No change	No change	99.5 %	4.78±0.20 h	>85% in 15 min

*mean±SD; n=6

5.2.3.2.3. Packaging and stability (MPR CCTs)

The CCTs demonstrated no detectable change for either of appearance, hardness, assay, or drug release under stated storage conditions. As shown in Table 5.40, all results were within their respective specification limits and hence the formulation was found to be stable under the selected packaging material and stated storage conditions.

Table 5.40 Results of stability study for MPR CCTs

Storage condition	Appearance	Hardness	Assay	Lag time*	Burst release
Initial	White colour	11.5-14.5 kp	99.9 %	4.72±0.17 h	>85% in 15 min
25±2°C/60±5% RH (3M)	No change	No change	99.7 %	4.67±0.20 h	>85% in 15 min
40±2°C/75±5% RH (3M)	No change	No change	99.3 %	4.69±0.19 h	>85% in 15 min

*mean±SD; n=6

5.2.4. Conclusion (MPR)

Same as PRS CCTs, MPR CCTs also exhibited 4-6 h of lag time followed by burst release profile at varying dissolution conditions. The lag time was found to be explicitly pH-independent as well as unaffected by change in hydrodynamics. Further, hydro-alcoholic and biorelevant dissolution results were also in-line with PRS CCTs. Thus, the change in drug candidate i.e. PRS to MPR in core tablet did not alter the desired quality traits of the developed PR CCT.

5.3. Development of PR CCTs of Diclofenac sodium (DIC)

### 5.3.1. DIC drug profile (8, 9, 80, 81)

DIC is a well-known non steroidal anti-inflammatory drug (NSAID) with analgesic, anti-inflammatory and anti-pyretic properties, which are comparable or superior to other NSAIDs. Chemically it is phenylacetic acid derivative showing preferential inhibition of the cyclooxygenase-2 enzyme. It is mainly indicated in the treatment of osteoarthritis, RA, ankylosing spondylitis and several other pains (80).

Physicochemical properties (8, 9, 80)

Molecular Formula: $C_{14}H_{10}Cl_2NNaO_2$

Chemical Name: Sodium 2-[(2,6-dichlorophenyl)amino]phenyl]acetate.

Structure:
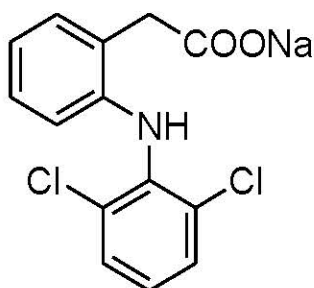
Molecular weight: 318.1 g/mol

Appearance: White crystalline powder

Solubility: Sparingly soluble in water, freely soluble in methanol, soluble in ethanol, slightly soluble in acetone.

Melting point: 283-285°C

Nature: weak acid

pKa: 3.8

Log P: 4.4

Dose: 12.5-50 mg

BCS class: II

Mechanism of action: DIC is considered to be a nonspecific COX inhibitor (COX-I and COX-II inhibitor) which results into suppression of prostaglandin synthesis and having additional potency to inhibit the leucocyte infiltration. DIC also acts on hypothalamus, resulting into dilation of the peripheral cutaneous blood vessel, increase in blood flow and subsequent heat dissemination. Prostaglandins are potent sensitizers

of pain receptors and amalgamation of all these actions leads to antipyretic as well as analgesic action of drug (81).

Pharmacokinetics (80)

Absorption: Rapidly and completely absorbed from GI tract.

Peak plasma level: 0.33-2 h

Plasma half life: ≈ 2 h

Duration of action: 6-8 h

Bioavailability: absolute bioavailability 100% following oral administration.

Protein binding: greater than 99% bound to human serum protein, primarily to albumin. However, it is pharmacokinetically insignificant as drug readily dissociates and permeates across the vascular membrane to the tissues.

Permeability: An apparent permeability co-efficient of 53.3×10^{-6} cm/s was reported using artificial membrane permeability assay.

Distribution: apparent volume of distribution is 1.4 L/kg

Metabolism and Excretion: DIC undergoes extensive metabolism in liver involving aromatic hydroxylations and conjugations. Around 65% of DIC is excreted in the urine, mainly as metabolites, and 35% in bile as conjugates of unchanged DIC and metabolites. Few amounts are eliminated in unchanged form in urine.

Contraindications: DIC is contraindicated in the patients suffering from urticarial or related allergic hypersensitive patients or patients suffering from asthma. The patients having anaphylactic reaction with aspirin like NSAIDs, might have severe allergic sensitivity with the DIC (82).

Adverse Effects: The most common adverse effects are GI symptoms mainly peptic ulcer and/or GI bleeding along with diarrhoea, indigestion, nausea, constipation, flatulence and liver test abnormalities. However, DIC has a fairly high therapeutic index as compared to other NSAIDs (82).

5.3.2. Methods (DIC)

After ensuring desired results with PRS and MPR CCTs, DIC was also formulated in the similar way using optimized PRS formula.

5.3.2.1. RP-HPLC method for determination of DIC

An RP-HPLC method was developed for determination of DIC. The chromatographic conditions and various parameters are enlisted in Table 5.41.

Table 5.41 Chromatographic conditions for determination of DIC

Stationary phase:	C18, 250 mm, 4.6 mm, 5 µm
Mobile phase:	0.1% v/v glacial acetic acid in 25:50:25 % v/v/v mixture of water: methanol: acetonitrile
Flow rate:	1 mL/min
Detection wavelength:	275 nm
Temperature:	≈ 25°C
Injection volume:	20 µL
Retention time:	8.76±0.08 min
Asymmetry factor:	1.087±0.009
Theoretical plates:	15037±129.55

5.3.2.1.1. Preparation of standard stock solutions of DIC

Accurately weighed quantity of drug (100 mg) was dissolved in 100 mL of methanol to obtain the stock solution of 1000 µg/mL. An aliquot of 10 mL of this stock solution was further diluted to 100 mL with mobile phase to obtain working standard solution of 100 µg/mL.

5.3.2.1.2. Preparation of calibration curve of DIC

Varying concentrations of drug solutions (2-30 µg/mL) were prepared from 100 µg/mL working standard solution using mobile phase as a diluent. The solutions were analyzed with Kromasil C18 column using isocratic HPLC/UV system. The samples were injected through a Rheodyne 7725 injector valve fixed with 20 µL loop. The mobile phase was vacuum filtered through 0.22 µm nylon membrane filter followed by degassing with an ultrasonicator prior to use. The detection was performed at 275 nm and calibration curve was plotted for area vs. concentration (µg/mL) as shown in Table 5.42. The system suitability criteria were in accordance with USP limits (26). The overlaid calibration chromatograms are depicted in Figure 5.31 and corresponding

linearity curve, regression equation and correlation coefficient are depicted in Figure 5.32. Accuracy, precision and ruggedness were carried out as per ICH guidelines (25) and the results are respectively depicted in Table 5.43, Table 5.44 and Table 5.45. Overall results of validation parameters are depicted in Table 5.46.

Table 5.42 Calibration curve and regression equation of DIC obtained using HPLC method

Concentration (µg/mL)	Area (mV.s) (mean±SD; n=5)
2	53.543±0.462
5	136.589±0.918
10	272.719±1.686
15	405.421±2.468
20	532.755±2.923
25	673.796±3.202
30	813.407±2.699
Regression equation	
Slope	0.3769±0.654
Intercept	26.968±0.095
Correlation coefficient	0.9998
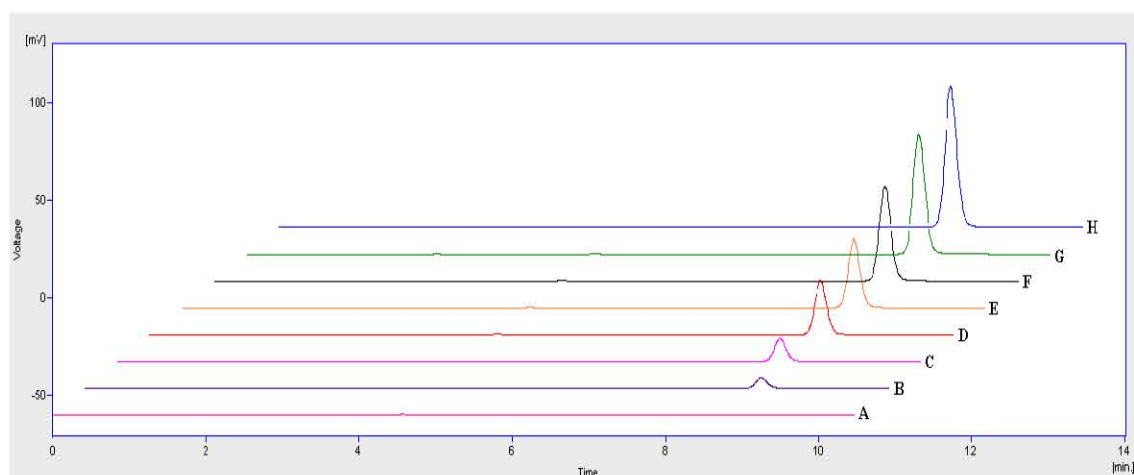
Fig. 5.31 Overlaid HPLC chromatograms of 2-30 µg/mL DIC; (A) blank, (B) 2 µg/mL, (C) 5 µg/mL, (D) 10 µg/mL, (E) 15 µg/mL, (F) 20 µg/mL, (G) 25 µg/mL and (H) 30 µg/mL
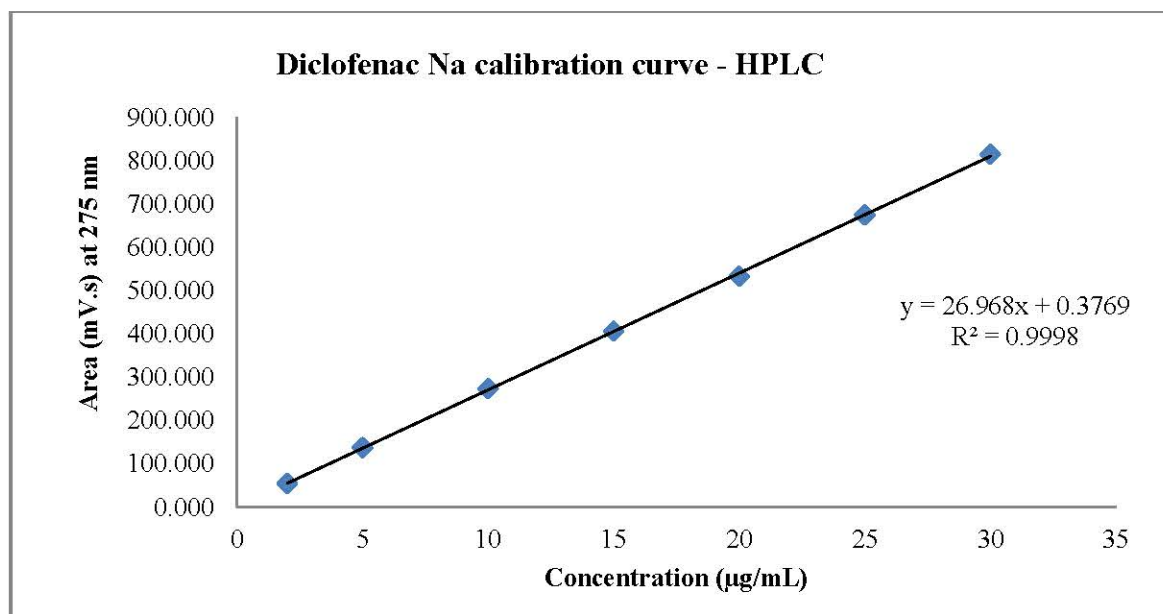
Fig. 5.32 HPLC calibration curve of DIC (2-30 µg/mL)

Table 5.43 Accuracy data of DIC obtained using HPLC method

Amount spiked (mg)	Amount recovered (mg) (mean±SD; n=3)	% recovery (mean±SD; n=3)	% recovery (range; n=3)	Average % recovery
5	5.02±0.06	100.4±1.16	99.1-101.4	
10	10.03±0.10	100.3±0.99	99.3-101.2	99.8
15	14.83±0.09	98.9±0.62	98.3-99.5	

Table 5.44 Precision data of DIC obtained using HPLC method

Concentration (µg/mL)	Repeatability (% RSD; n=3)	Intra-day (% RSD; n=3)	Inter-day (% RSD; n=3)
5	0.51	0.94	1.38
10	0.46	0.74	0.90
15	0.26	0.61	0.66

Table 5.45 Ruggedness data of DIC obtained using HPLC method

Concentration (µg/mL)	% RSD; n=2
5	1.48
10	1.17
15	0.93

Table 5.46 Summary of validation parameters of DIC HPLC method

Parameters	Results
Linearity range	2-30 µg/mL
Correlation coefficient	0.9998
Accuracy (% recovery)	98.3-101.4 %
Precision (% RSD; n=3)	
Repeatability	0.26-0.51 %
Intra-day	0.61-0.94 %
Inter-day	0.66-1.38 %
Ruggedness (% RSD; n=2)	0.93-1.48 %
LOD	0.080 µg/mL
LOQ	0.242 µg/mL

5.3.2.2. Drug-excipient compatibility

Same as section 5.1.2.5

5.3.2.3. Preparation of Active Pharmaceutical Ingredient (API) granules of DIC

The preliminary trials with DIC indicated flow issue with final compression blend. Hence, improvement of flow property was obligatory which was sought through formulating pure API granules using purified water as granulating agent. The granules were dried in oven at 60°C for 2 h and finally sifted through ASTM#40 to be employed for core tablet preparation.

5.3.2.4. Preparation of DIC core tablets

Same as PRS, the core tablets of DIC were prepared by direct compression method as per the composition shown in Table 5.47. The tablets were prepared at a constant average weight (100 mg) by keeping the composition as similar as possible with adjustment of just lactose quantity to compensate the dose of drug, using the same procedure as mentioned for PRS (section 5.1.2.6)

Table 5.47 List of ingredients and their respective concentrations employed for formulation of DIC core tablets

Ingredients	mg/tab (%w/w)
DIC API granules	25 mg
MCC	38 mg
Lactose	33 mg
SSG	3 mg
Colloidal SiO_2	0.5 mg
MgSt	0.5 mg
Total weight	100 mg

5.3.2.5. Characterization of DIC core tablets

Same as section 5.1.2.7. Additionally, the flow property of granular compression blend was evaluated in terms of Carr's index, Hausner's ratio and Angle of repose; and further compared to that of plain API compression blend.

5.3.2.6. Preparation of DIC CCTs

The DIC CCTs were formulated using optimized PRS outer coat composition (Table 5.24) by following same procedure as mentioned for PRS (section 5.1.2.8.).

5.3.2.7. Characterization of DIC CCTs

Same as section 5.1.2.9.

5.3.2.8. Packaging and stability study (DIC CCTs)

Same as section 5.1.2.10.

5.3.3. Results and discussion (DIC)

5.3.3.1. Flow property evaluation of DIC compression blends

To improve the flow, the API was converted into the granular form and blended with other ingredients to form the compression blend. The flow property of such compression blend was determined in terms three USP parameters, viz. Carr's index, Hausner's ratio, and Angle of repose (26). The comparative assessment of granular and plain API compression blends is displayed in Table 5.48 which exhibits considerable flow improvement with granular blend in comparison to as such blend. According to USP (26), the angle of repose of plain API blend fell under fair flow category (i.e. 36-40) which was shifted to good flow category (i.e. 31-35) upon formulating granular API blend. The Carr's index of plain API blend suggested it as poor flow (i.e. 26-31) which was improved to fair flow category (i.e. 16-20) with granular blend. Similarly, the Hausner's ratio of plain API blend also indicated it as poor flow (i.e. 1.35-1.45) which was shifted to fair flow category (i.e. 1.19-1.25) upon preparation of granular blend. The granular API blend did not show any issues during compression process.

Table 5.48 Flow property evaluation of DIC compression blends

Flow property parameter	Blend prepared using plain API	Blend prepared using granular API
Carr's index	26.2	16.7
Hausner's ratio	1.36	1.20
Angle of repose	37.6	31.2

5.3.3.2. Evaluation of DIC core tablets

The physical appearance of core tablets was found to be satisfactory. The tablets had hardness of 4-6 kp, friability less than 0.5% and disintegration time less than 60 s. The tablet thickness was found to be 3.8-3.9 mm. The weight variation, assay and CU results were found to be within their respective specification limits. The release studies demonstrated >85% drug release within 15 min with all tested dissolution conditions and therefore the core tablets were construed as fast dissolving IR tablets (i.e. >85% release within 30 min). The dissolution profile with basket apparatus, 100 rpm, pH 6.8 phosphate buffer, 500 mL, 37±0.5°C is depicted in Figure 5.33. The impact of double compression on core tablets was determined by carefully scraping out the outer coat of CCT and analyzing the core tablets for thickness, hardness and drug release. The results

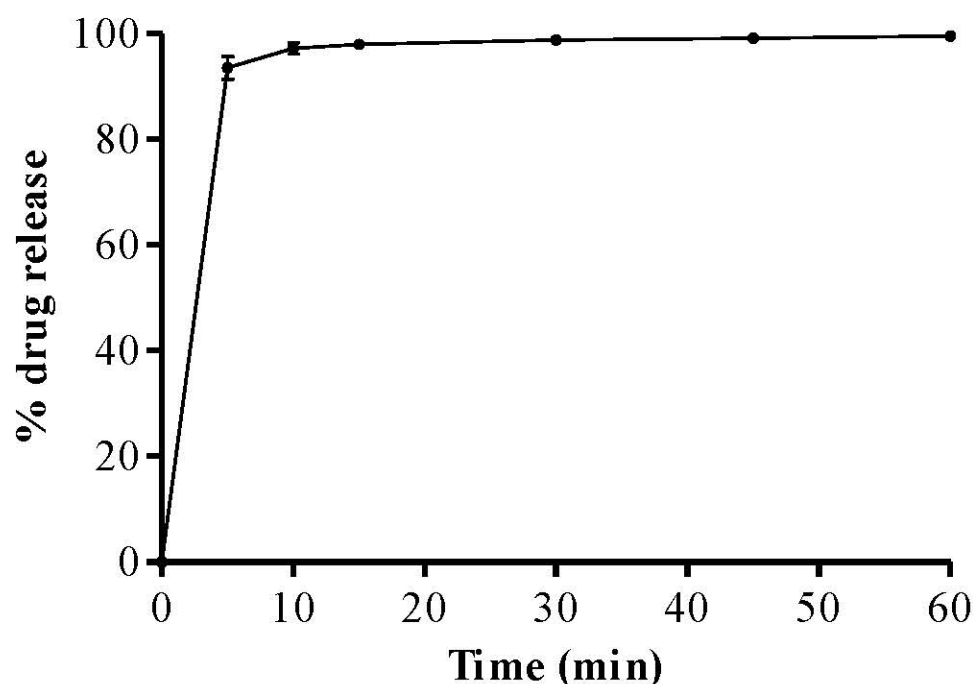depicted no distinguishable difference in all three parameters due to double compression.

Fig. 5.33 Drug release profile of DIC core tablet in pH 6.8 phosphate buffer; basket apparatus; 100 rpm; 500 mL; 37.0±0.5°C [mean±SD; n=6]

5.3.3.3. Evaluation of DIC CCTs

The CCT appearance was found to be satisfactory. The hardness was 11.5-14.5 kp, thickness was 5.9-6.0 mm and friability was less than 0.5%. The assay and weight variation results were found to be within their respective specification limits.

5.3.3.3.1. *In vitro* release studies (DIC CCTs)

The release studies exhibited typical 4-6 h of lag time followed by sharp burst release (>85%) within 15 min of outer coat rupturing with all tested conditions except hydro-alcoholic media (in which the lag time did not remain confine to 4-6 h). The dissolution profile of DIC CCTs obtained with basket apparatus; 100 rpm; 0.1 N HCl followed by pH 6.8 phosphate buffer is displayed in Figure 5.34. The individual lag time results obtained with various dissolution conditions are demonstrated in Figure 5.35. As shown in Figure 5.35, no significant difference was observed between the lag times of multi-media, change in apparatus, change in agitation and biorelevant media (p value >0.05).
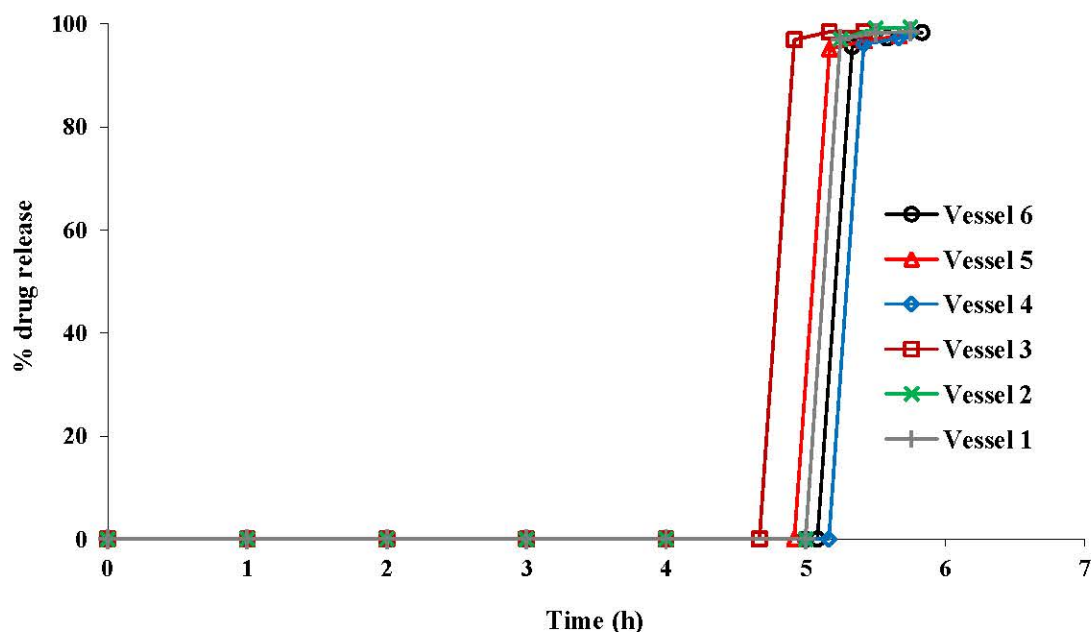
Fig. 5.34 Drug release profile of optimized DIC CCTs obtained with basket apparatus; 100 rpm agitation; 0.1 N HCl for first 2 h followed by pH 6.8 buffer; 500 mL volume; 37±0.5°C temperature.

Same as PRS CCTs, similar release profile with multi-media corroborated the developed CCT as pH-independent in nature. Analogous release behaviour with different apparatus as well as with different agitation intensity inferred that the lag time was robust enough and not influenced by change in hydrodynamics. Further, akin release profiles with biorelevant media prudently anticipate promising *in vivo* performance. The results of hydro-alcoholic media were also in-line with those of PRS/MPR CCTs, entailing pertinent instruction to be mentioned on the label.
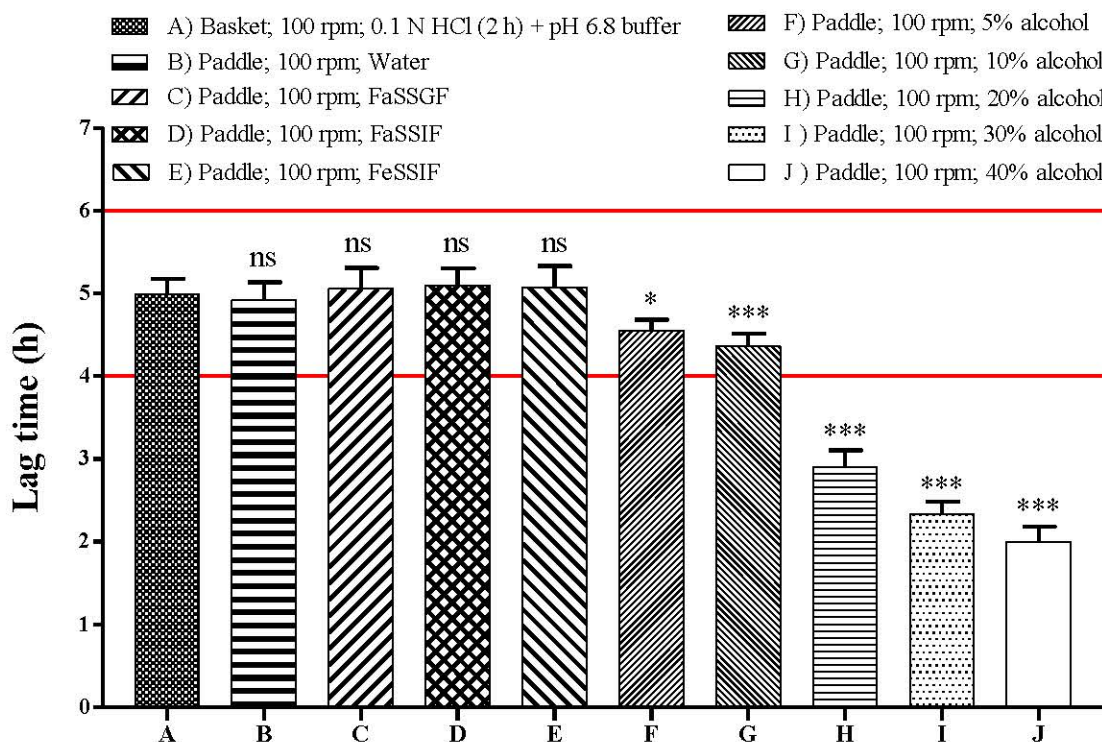
Fig. 5.35 Lag time of DIC CCTs obtained using various dissolution conditions; medium volume 500 mL; temperature $37\pm0.5°C$; [ns]p value>0.05, *p value<0.05, ***p value<0.001 (mean$\pm$SD; n=6).

5.3.3.3.2. Effect of curing (DIC CCTs)

After exposing 60°C for 24 h, DIC CCTs, when examined for appearance, assay, hardness, and drug release, exhibited all results within their respective specification limits (Table 5.49) with no distinguishable difference before and after curing. Thus, the CCTs exhibited no effect of curing.

Table 5.49 Results of curing study for DIC CCTs

Effect of curing	Appearance	Hardness	Assay	Lag time*	Burst release
Before curing	White colour	11.5-14.5 kp	100.2 %	4.99$\pm$0.19 h	>85% in 15 min
After curing	No change	No change	99.7 %	4.94$\pm$0.23 h	>85% in 15 min

*mean$\pm$SD; n=6

5.3.3.3.3. Packaging and stability (DIC CCTs)

The CCTs demonstrated no detectable change for either of appearance, hardness, assay, or drug release under stated storage conditions. Since all results were found within their respective specification limits (Table 5.50), the formulation was found to be stable under the selected packaging material and stated storage conditions.

Table 5.50 Results of stability study for DIC CCTs

Storage condition	Appearance	Hardness	Assay	Lag time*	Burst release
Initial	White colour	11.5-14.5 kp	100.2 %	4.99±0.19 h	>85% in 15 min
25±2°C/60±5% RH (3M)	No change	No change	99.6 %	4.96±0.24 h	>85% in 15 min
40±2°C/75±5% RH (3M)	No change	No change	99.8 %	4.93±0.21 h	>85% in 15 min

*mean±SD; n=6

5.3.4. Conclusion (DIC)

Same as PRS/MPR CCTs, DIC CCTs also exhibited 4-6 h of lag time followed by burst release profile at varying dissolution conditions. The lag time was found to be explicitly pH-independent as well as unaffected by change in hydrodynamics. Further, hydro-alcoholic and biorelevant dissolution results were also in-line with previous CCTs. Thus, replacement of former drug with DIC in core tablet did not alter the desired quality traits of the developed PR CCT.

5.4. Development of PR CCTs of Diltiazem hydrochloride (DIL)

5.4.1. DIL drug profile (8, 9, 83-89)

DIL belongs to the benzothiazepine class of calcium channel blocker mainly indicated for the treatment of angina pectoris and hypertension (83, 86).

Physicochemical properties (8, 9, 83-85)

Molecular Formula: $C_{22}H_{26}N_2O_4S,HCl$

Chemical Name: Hydrochloride of (2S,3S)-5-[2-(dimethylamino)ethyl]-2-(4-methoxyphenyl)-4-oxo-2,3,4,5-tetrahydro-1,5-benzothiazepin-3-yl acetate.

Structure:
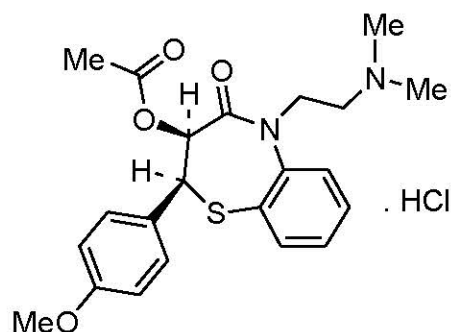
Molecular weight: 451.0 g/mol

Appearance: White or almost white, crystalline powder

Solubility: Freely soluble in water, in methanol and in methylene chloride, slightly soluble in anhydrous ethanol.

Melting point: 207.5-212°C

Nature: weak base

pKa: 7.7

Log P: 2.8

Dose: 30-120 mg

BCS class: I

Mechanism of action: Influx of extracellular calcium leads to the contractile response which is inhibited by DIL through inhibition of extracellular calcium to the myocardium and vascular smooth muscle cell membrane. The resultant suppression of the contraction of myocardial smooth muscle cells results in dilation of the coronary as well as peripheral arteries. Dilated blood vessels efficiently improve the blood flow to the arteries and fulfil the oxygen requirement (88).

Pharmacokinetics (86, 89)

Absorption: Rapidly and almost completely absorbed (about 90%) after oral dosing and exhibits dose dependent non-linear pharmacokinetics.

Peak effect: 0.5-2 h

Duration of action: ˜ 6-8 h

Plasma half life: 3-4.5 h

Bioavailability: despite of having almost complete absorption, absolute bioavailability is around 40-50% due to rapid first pass metabolism.

Protein binding: DIL is about 80 to 90% bound to plasma proteins, primarily albumin (about 35 to 40%), with the remainder bound to α-acid glycoprotein and various γ-globulins.

Distribution: It is lipophilic drug and has a large volume of distribution (3-8 L/kg).

Metabolism and Excretion: DIL is extensively metabolized, predominantly due to hepatic metabolism. The major metabolic pathways are O-desacetylation, N-demethylation and O-demethylation along with some minor pathways such as glucuronidation or sulfation. Only traces (0.1-4%) of unchanged drug are eliminated in the urine.

Adverse Effects: The principal adverse effects are oedema, headache, nausea, dizziness, rash and asthenia. The most frequent and serious side effect is atrioventricular block, which happens in about 0.2% of overall patients. Patients taking simultaneous beta-adrenoceptor antagonists might be at elevated risk of developing conduction disturbances (87).

5.4.2. Methods (DIL)

After ensuring desired results with PRS, MPR and DIC CCTs, DIL was also formulated into PR CCTs using optimized PRS formula.

5.4.2.1. RP-HPLC method for determination of DIL

An RP-HPLC method was developed for the determination of DIL as required throughput the study. The chromatographic conditions and various parameters are enlisted in Table 5.51.

Table 5.51 Chromatographic conditions for determination of DIL

Stationary phase:	C18, 250 mm, 4.6 mm, 5 μm
Mobile phase:	0.1% v/v triethylamine in 45:30:25 % v/v/v mixture of water: methanol: acetonitrile; pH adjusted to 3.0 with o-phosphoric acid
Flow rate:	1 mL/min
Detection wavelength:	236 nm
Temperature:	≈ 25°C
Injection volume:	20 μL
Retention time:	5.57±0.05 min
Asymmetry factor:	1.371±0.012
Theoretical plates:	8895±83.52

5.4.2.1.1. Preparation of standard stock solutions of DIL

Accurately weighed quantity of drug (100 mg) was dissolved in 100 mL of methanol to obtain the stock solution of 1000 μg/mL. An aliquot of 10 mL of this stock solution was further diluted to 100 mL with mobile phase to obtain working standard solution of 100 μg/mL.

5.4.2.1.2. Preparation of calibration curve of DIL

Varying concentrations of drug solutions (2-30 μg/mL) were prepared from 100 μg/mL working standard solution using mobile phase as diluent. The solutions were analyzed with Kromasil C18 column using isocratic HPLC/UV system. The samples were injected through Rheodyne 7725 injector valve fixed with 20 μL loop. The mobile phase was vacuum filtered through 0.22 μm nylon membrane filter followed by degassing with an ultrasonicator prior to use. The detection was performed at 236 nm and calibration curve was plotted for area vs. concentration (μg/mL) as shown in Table

5.52. The system suitability criteria were in accordance with USP limits (26). The overlaid calibration chromatograms are depicted in Figure 5.36 and corresponding linearity curve, regression equation and correlation coefficient are depicted in Figure 5.37. Accuracy, precision and ruggedness were carried out as per ICH guidelines (25) and the results are respectively depicted in Table 5.53, Table 5.54 and Table 5.55. Overall summary of validation results are depicted in Table 5.56.

Table 5.52 Calibration curve and regression equation of DIL obtained using HPLC method

Concentration (μg/mL)	Area (mV.s) (mean±SD; n=5)
2	76.251±0.618
5	193.449±1.255
10	393.986±3.155
15	589.391±3.760
20	786.323±5.712
25	973.525±6.138
30	1170.486±5.036
Regression equation	
Slope	0.5488±0.926
Intercept	39.061±0.191
Correlation coefficient	0.9999
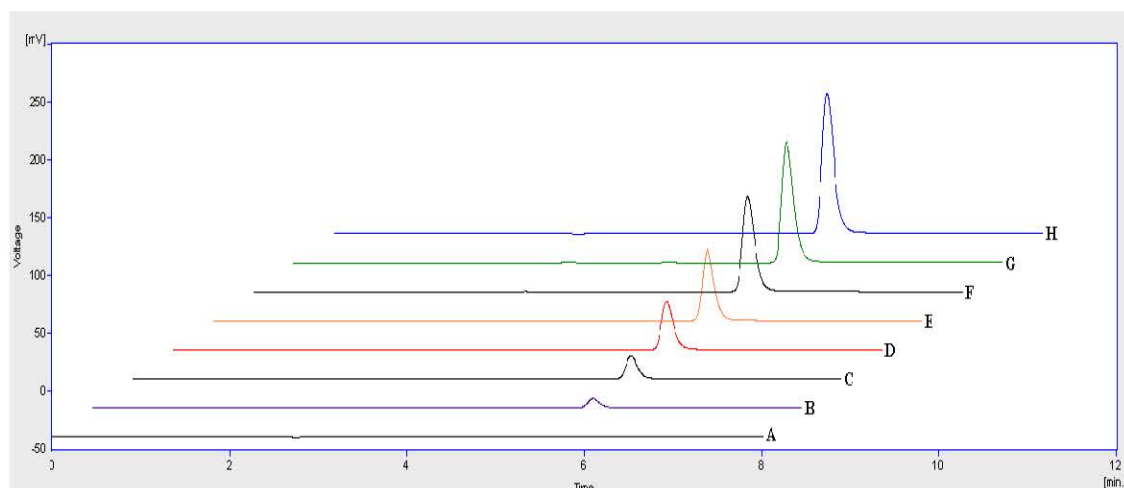
Fig. 5.36 Overlaid HPLC chromatograms of 2-30 μg/mL DIL; (A) blank, (B) 2 μg/mL, (C) 5 μg/mL, (D) 10 μg/mL, (E) 15 μg/mL, (F) 20 μg/mL, (G) 25 μg/mL and (H) 30 μg/mL

Diltiazem HCl calibration curve - HPLC

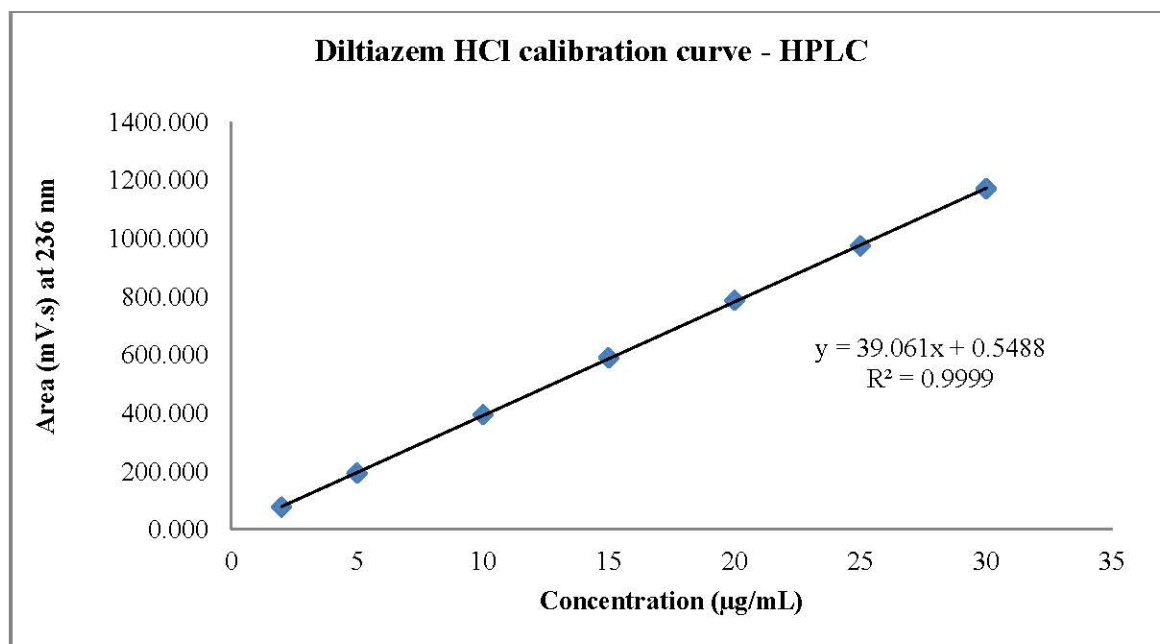$y = 39.061x + 0.5488$
$R^2 = 0.9999$

Fig. 5.37 HPLC calibration curve of DIL (2-30 µg/mL)

Table 5.53 Accuracy data of DIL obtained using HPLC method

Amount spiked (mg)	Amount recovered (mg) (mean±SD; n=3)	% recovery (mean±SD; n=3)	% recovery (range; n=3)	Average % recovery
5	4.95±0.04	98.9±0.88	98.3-99.9	
10	10.02±0.08	100.2±0.78	99.7-101.1	99.7
15	14.99±0.09	99.9±0.61	99.3-100.5	

Table 5.54 Precision data of DIL obtained using HPLC method

Concentration (µg/mL)	Repeatability (% RSD; n=3)	Intra-day (% RSD; n=3)	Inter-day (% RSD; n=3)
5	0.48	0.89	1.35
10	0.37	0.74	1.18
15	0.25	0.68	0.76

Table 5.55 Ruggedness data of DIL obtained using HPLC method

Concentration (µg/mL)	% RSD; n=2
5	1.66
10	1.27
15	0.83

Table 5.56 Summary of validation parameters of DIL HPLC method

Parameters	Results
Linearity range	2-30 µg/mL
Correlation coefficient	0.9999
Accuracy (% recovery)	98.3-101.1 %
Precision (% RSD; n=3)	
Repeatability	0.25-0.48 %
Intra-day	0.68-0.89 %
Inter-day	0.76-1.35 %
Ruggedness (% RSD; n=2)	0.83-1.66 %
LOD	0.078 µg/mL
LOQ	0.237 µg/mL

5.4.2.2. Drug-excipient compatibility

Same as section 5.1.2.5.

5.4.2.3. Preparation of API granules of DIL

Same as section 5.3.2.3.

5.4.2.4. Preparation of DIL core tablets

Same as PRS, DIL core tablets were also prepared by direct compression method as per the composition shown in Table 5.57. The tablets were prepared at a constant average weight (100 mg) by keeping the composition as similar as possible with adjustment of just lactose quantity to compensate the dose of drug, using the same procedure as mentioned for PRS (section 5.1.2.6.).

Table 5.57 List of ingredients and their respective concentrations employed for formulation of DIL core tablets

Ingredients	mg/tab (%w/w)
DIL API granules	30 mg
MCC	38 mg
Lactose	28 mg
SSG	3 mg
Colloidal SiO_2	0.5 mg
MgSt	0.5 mg
Total weight	100 mg

5.4.2.5. Characterization of DIL core tablets

Same as section 5.3.2.5.

5.4.2.6. Preparation of DIL CCTs

The DIL CCTs were formulated using optimized PRS outer coat composition (Table 5.24) following same procedure as mentioned for PRS (section 5.1.2.8.).

5.4.2.7. Characterization of DIL CCTs

Same as section 5.1.2.9.

5.4.2.8. Packaging and stability study (DIL CCTs)

Same as section 5.1.2.10.

5.4.3. Results and discussion (DIL)

5.4.3.1. Flow property evaluation of DIL compression blend

To improve the flow, the API was converted into the granular form and blended with other ingredients to form the compression blend. The flow property of such compression blend was determined in terms three USP parameters, viz. Carr's index, Hausner's ratio, and Angle of repose (26). The comparative assessment of granular and plain API compression blend is displayed in Table 5.58 which exhibits considerable flow improvement with granular blend in comparison to as such blend. According to USP, the angle of repose of plain API blend fell under passable flow category (i.e. 41-45) which was shifted to good flow category (i.e. 31-35) upon formulating granular API blend. The Carr's index of plain API blend suggested it as poor flow (i.e. 26-31) which was improved to fair flow category (i.e. 16-20) with granular blend. Similarly, the Hausner's ratio of plain API blend also indicated it as poor flow (i.e. 1.35-1.45) which was shifted to fair flow category (i.e. 1.19-1.25) upon preparation of granular blend. The granular API blend did not show any issues during compression process.

Table 5.58 Flow property evaluation of DIL compression blends

Flow property parameter	Blend prepared using plain API	Blend prepared using granular API
Carr's index	29.9	20.0
Hausner's ratio	1.43	1.25
Angle of repose	41.6	35.1

5.4.3.2. Evaluation of DIL core tablets

The physical appearance of core tablets was found to be satisfactory. The tablets had hardness of 4-6 kp, friability less than 0.5% and disintegration time less than 180 s. The tablet thickness was found to be 3.8-3.9 mm. The weight variation, assay and CU results were found within their respective specification limits. The release studies demonstrated >85% drug release within 15 min with all tested dissolution conditions and therefore the core tablets were construed as fast dissolving IR tablets (i.e. >85% release within 30 min). The dissolution profile with basket apparatus, 100 rpm, pH 6.8 phosphate buffer, 500 mL, $37\pm0.5°C$ is depicted in Figure 5.38. The impact of double compression on core tablets was determined by carefully scraping out the outer coat of CCT and analyzing the core tablets for thickness, hardness and drug release. The results

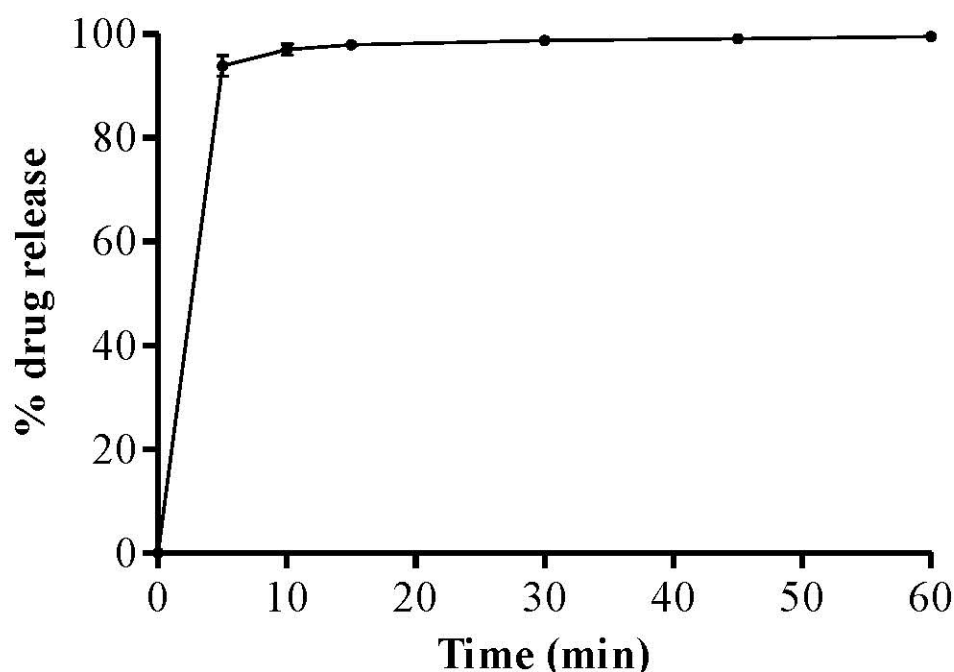depicted no distinguishable difference in all three parameters due to double compression.

Fig. 5.38 Drug release profile of DIL core tablet in pH 6.8 phosphate buffer; basket apparatus; 100 rpm; 500 mL; 37.0±0.5°C [mean±SD; n=6]

5.4.3.3. Evaluation of DIL CCTs

The appearance of CCTs was found to be satisfactory. The hardness was 11.5-14.5 kp, thickness was 5.9-6.0 mm and friability was less than 0.5%. Assay and weight variation results were found to within their respective specification limits.

5.4.3.3.1. *In vitro* release studies (DIL CCTs)

The release studies exhibited typical 4-6 h of lag time followed by sharp burst release (>85%) within 15 min of outer coat rupturing with all tested conditions except hydro-alcoholic media (in which the lag time did not remain confine to 4-6 h). The dissolution profile of DIL CCTs obtained with basket apparatus; 100 rpm; 0.1 N HCl followed by pH 6.8 phosphate buffer is displayed in Figure 5.39. The individual lag time results obtained with various dissolution conditions are demonstrated in Figure 5.40. As shown in Figure 5.40, no significant difference was observed between the lag times of multi-media, change in apparatus, change in agitation and biorelevant media (p value >0.05).
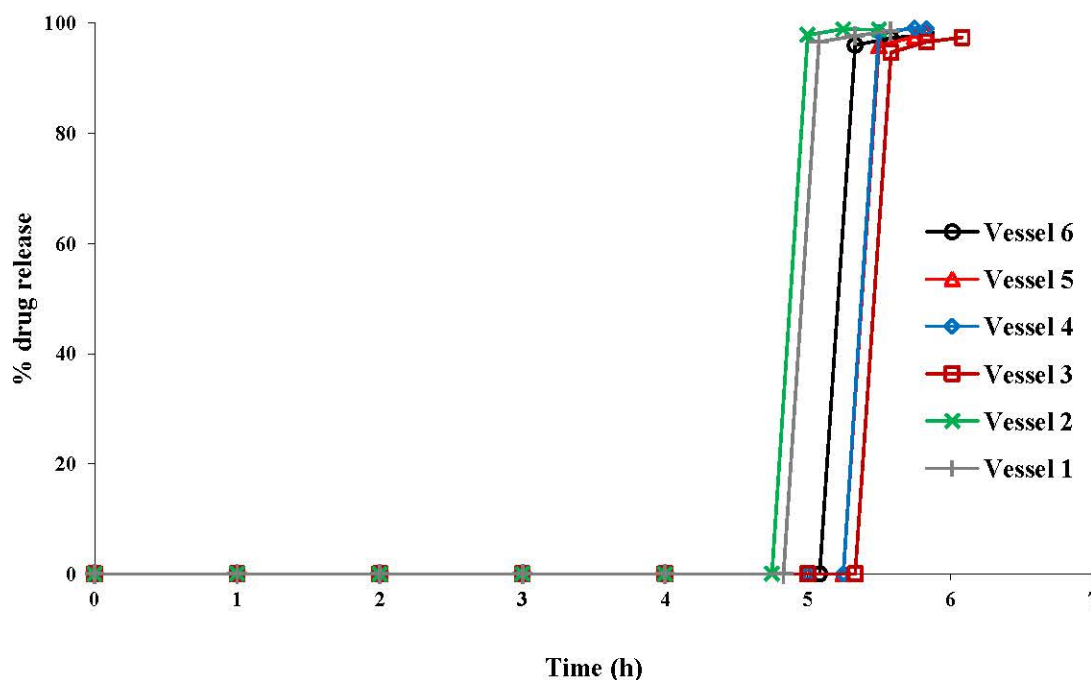
Fig. 5.39 Drug release profile of optimized DIL CCTs obtained with basket apparatus; 100 rpm agitation; 0.1 N HCl for first 2 h followed by pH 6.8 buffer; 500 mL volume; 37±0.5°C temperature.

Same as PRS, similar release profile with multi-media corroborated the developed CCT as pH-independent in nature. Analogous release behaviour with different apparatus as well as agitation intensity inferred that the lag time was robust enough and not influenced by change in hydrodynamics. Further, akin release profiles with biorelevant media prudently anticipate promising *in vivo* performance. The results of hydro-alcoholic media were also in-line with previous CCTs, entailing pertinent instruction to be mentioned on the label.
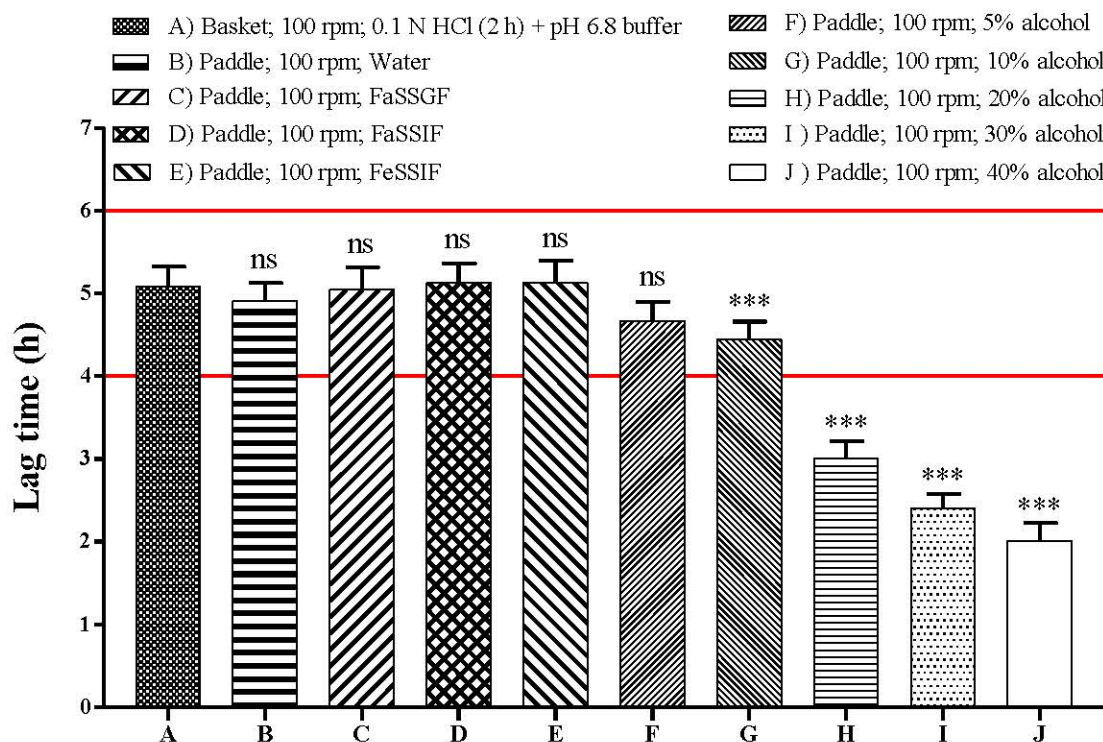
Fig. 5.40 Lag time of DIL CCTs obtained using various dissolution conditions; medium volume 500 mL; temperature $37\pm0.5°C$; [ns] p value>0.05, ***p value<0.001 (mean±SD; n=6)

5.4.3.3.2. Effect of curing (DIL CCTs)

After exposure of 60°C for 24 h, the CCTs, when examined for appearance, assay, hardness, and drug release, exhibited each result within respective specification limits (Table 5.59) with no distinguishable difference before and after curing. Thus, DIL CCTs also exhibited no effect of curing.

Table 5.59 Results of curing study for DIL CCTs

Effect of curing	Appearance	Hardness	Assay	Lag time*	Burst release
Before curing	White colour	11.5-14.5 kp	99.7 %	5.08±0.24 h	>85% in 15 min
After curing	No change	No change	99.6 %	5.10±0.21 h	>85% in 15 min

*mean±SD; n=6

5.4.3.3.3. Packaging and stability (DIL CCTs)

The CCTs demonstrated no detectable change for either of appearance, hardness, assay, or drug release under stated storage conditions. Since all results were found within their respective specification limits (Table 5.60), the formulation was found stable under the selected packaging material and stated storage conditions.

Table 5.60 Results of stability study for DIL CCTs

Storage condition	Appearance	Hardness	Assay	Lag time*	Burst release
Initial	White colour	11.5-14.5 kp	99.7 %	5.08±0.24 h	>85% in 15 min
25±2°C/60±5% RH (3M)	No change	No change	99.9 %	5.07±0.20 h	>85% in 15 min
40±2°C/75±5% RH (3M)	No change	No change	99.5 %	5.04±0.24 h	>85% in 15 min

*mean±SD; n=6

5.4.4. Conclusion (DIL)

Same as previous CCTs, DIL CCTs also exhibited 4-6 h of lag time followed by burst release profile at varying dissolution conditions. The lag time was found to be explicitly pH-independent as well as unaffected by change in hydrodynamics. Further, hydro-alcoholic and biorelevant dissolution results were also in-line with previous CCTs. Thus, replacement of former drugs with DIL in core tablet did not alter the desired quality traits of the developed compression-coated PR formulation.

5.5. Development of PR CCTs of Nifedipine (NIF)

5.5.1. NIF drug profile (8, 9, 90-92)

NIF is a dihydropyridine class calcium channel blocker indicated in the treatment of angina pectoris and hypertension. It predominantly suppresses trans-membrane calcium transport, however its affinity for vascular tissue with no myocardial depressant effect is helpful in managing conditions associated with variant angina, vascular spasm and raynaud's syndrome (90).

General Characteristics (8, 9, 90, 91)

Molecular Formula: $C_{17}H_{18}N_2O_6$

Chemical Name: Dimethyl 2,6-dimethyl-4-(2-nitrophenyl)-1,4-dihydropyridine-3,5-dicarboxylate

Structure:
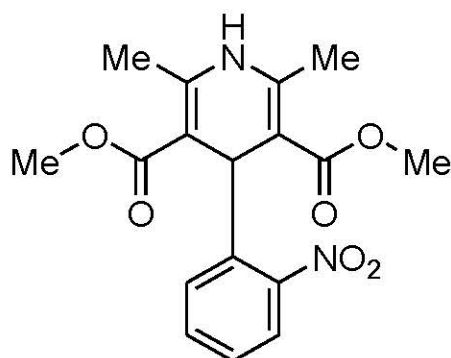
Molecular weight: 346.3 g/mol

Appearance: yellow crystalline powder

Solubility: Practically insoluble in water, freely soluble in acetone, sparingly soluble in ethanol.

Photostability: NIF is a very photosensitive molecule which degrades in the presence of UV light to produce 4-(2-nitrophenyl)-pyridine analogue, and in the presence of normal day light to produce 4-(2-nitrosophenyl)-pyridine analogue. As a result, precautions are essential to protect NIF from light while handling in the laboratory (e.g., working under dark or yellow light conditions and covering all samples, solutions and apparatus containing NIF with aluminium foil) to be protected from light.

Melting point: 171-175 °C

Nature: Weak acid

pKa$_1$: -0.9; pKa$_2$:13

Log P: 2.2

Dose: 5-20 mg

BCS class: II

Mechanism of action:

NIF is a potent L-type calcium channel blocker causing the suppression of the arterial smooth muscle contraction and ultimately restrict the vasoconstriction due to stoppage of the calcium influx. The entry of calcium ion through these channels forms calcium-calmodulin complex which acts on myosin light chain kinase (MLCK) to activate it. The activated MLCK phosphorylates the light chain subunit of the myosin which leads to muscle contraction. All this in combination, leads to calcium induced calcium release from the sarcoplasmic reticulum through ryanodine receptor. Having calcium blocking potential, NIF causes the arterial dilation leading to improved oxygen supply with diminished total peripheral resistance, decreased afterload and decreased blood pressure (93).

Pharmacokinetics (90, 92)

Absorption: Rapidly and almost completely absorbed after oral administration.

Peak effect: ~ 0.5-3 h

Duration of action: ~ 4-6 h

Plasma half life: $\approx$ 2 h

Bioavailability: The absolute bioavailability varies from 42% to 56% due to first-pass metabolism.

Protein binding: NIF is highly bound to the serum proteins, the percentage of bound drug occur between 91% and 98%.

Permeability: An apparent permeability co-efficient of 52.3×10^{-6} cm/s was reported using Caco-2 permeability assay.

Distribution: It experiences significant tissue distribution with the steady-state volume of distribution around 0.62–0.77 L/kg, more than doubled the volume of distribution of the central compartment (0.25–0.29L/kg).

Metabolism and Excretion: NIF rapidly oxidized to form nitropyridine metabolite and 70-80% of the dose is eliminated in urine largely as inactive metabolites and a minor quantity of unchanged (<0.1%) drug was found in urine. The remaining amount is

excreted in the faeces in form of metabolite resulting from biliary elimination. The total body clearance varies from 450 to 700 mL/min.

Adverse effects: The most common side effects are headache, flushing, and dizziness. Apart from that, GI disturbances (nausea, vomiting, heartburn, dyspepsia), oedema, swelling, fluid retention, burning and heat sensitivity are also reported (92).

5.5.2. Methods (NIF)

After ensuring desired results with previous CCTs, a poorly soluble drug NIF was also chosen to further challenge the robustness of optimized PR formulation. Notably, as NIF is a photosensitive drug, all experiments with NIF were performed in the dark environment throughout the study.

5.5.2.1. RP-HPLC method for determination of NIF

An RP-HPLC method was developed for the determination of NIF as required throughput the study. Chromatographic conditions and various parameters are enlisted in Table 5.61.

Table 5.61 Chromatographic conditions for determination of NIF

Stationary phase:	C18, 250 mm, 4.6 mm, 5 μm
Mobile phase:	0.1% v/v glacial acetic acid in 35:40:25 % v/v/v mixture of water: methanol: acetonitrile
Flow rate:	1 mL/min
Detection wavelength:	238 nm
Temperature:	$\approx 25°C$
Injection volume:	20 μL
Retention time:	7.06±0.06 min
Asymmetry factor:	1.122±0.010
Theoretical plates:	11261±106.07

5.5.2.1.1. Preparation of standard stock solutions of NIF

Accurately weighed quantity of drug (100 mg) was dissolved in 100 mL of methanol to obtain the stock solution of 1000 μg/mL. An aliquot of 10 mL of this stock solution was diluted to 100 mL with mobile phase to obtain 100 μg/mL working standard solution.

5.5.2.1.2. Preparation of calibration curve of NIF

Varying concentrations of drug solutions (0.25-10 μg/mL) were prepared from 100 μg/mL working standard solution using mobile phase as diluent. The solutions were analyzed with Kromasil C18 column using isocratic HPLC/UV system. The samples were injected through Rheodyne injector valve fixed with 20 μL loop. The mobile phase was vacuum filtered through 0.22 μm nylon membrane filter followed by degassing with an ultrasonicator prior to use. The detection was performed at 238 nm

and calibration curve was plotted for area vs. concentration as shown in Table 5.62. System suitability criteria complied with USP limits (26). Overlaid calibration chromatograms are depicted in Figure 5.41 and corresponding linearity curve, regression equation and correlation coefficient are depicted in Figure 5.42. Accuracy, precision and ruggedness were determined as per ICH guidelines (25) and the results are respectively depicted in Table 5.63, Table 5.64 and Table 5.65. Overall summary of validation results are depicted in Table 5.66.

Table 5.62 Calibration curve and regression equation of NIF obtained using HPLC method

Concentration (μg/mL)	Area (mV.s) (mean±SD; n=5)
0.25	11.598±0.291
0.5	23.418±0.410
1	42.576±0.663
2	87.571±1.145
4	178.207±1.566
6	268.532±2.048
8	349.566±2.327
10	442.389±3.731
Regression equation	
Slope	0.3657±0.535
Intercept	44.124±0.260
Correlation coefficient	0.9998
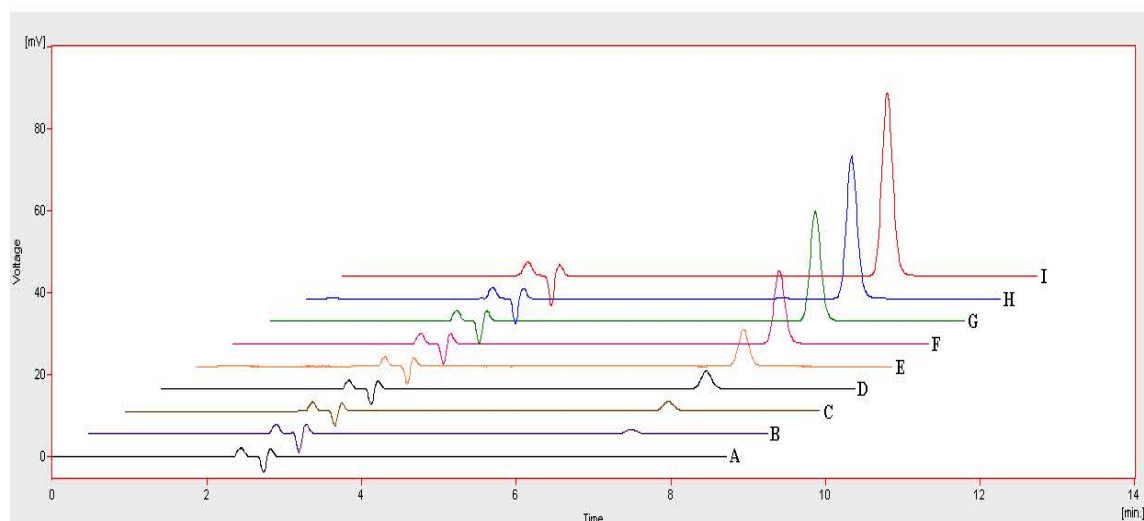
Fig. 5.41 Overlaid HPLC chromatograms of 0.25-10 μg/mL NIF; (A) blank, (B) 0.25 μg/mL, (C) 0.5 μg/mL, (D) 1 μg/mL, (E) 2 μg/mL, (F) 4 μg/mL, (G) 6 μg/mL, (H) 8 μg/mL, and (I) 10 μg/mL
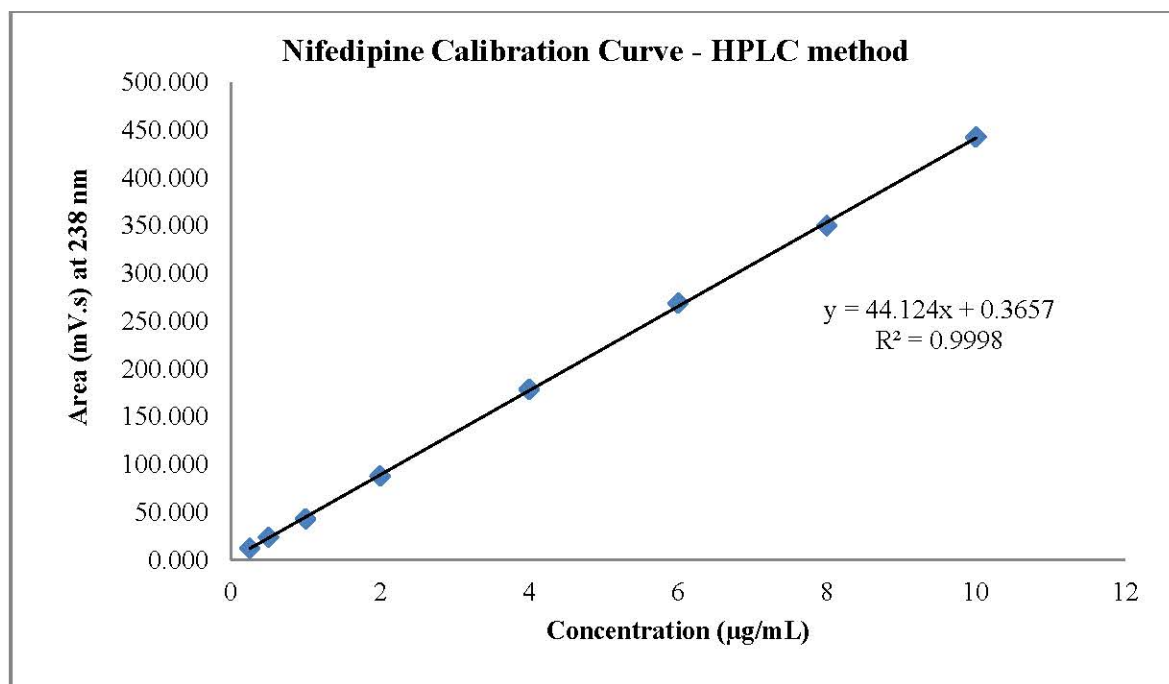
Fig. 5.42 HPLC calibration curve of NIF (0.25-10 μg/mL)

Table 5.63 Accuracy data of NIF obtained using HPLC method

Amount spiked (mg)	Amount recovered (mg) (mean±SD; n=3)	% recovery (mean±SD; n=3)	% recovery (range; n=3)	Average % recovery
4	3.96±0.03	98.9±0.77	98.3-99.8	
6	5.94±0.03	99.0±0.57	98.5-99.6	98.8
8	7.89±0.04	98.6±0.45	98.2-99.1	

Table 5.64 Precision data of NIF obtained using HPLC method

Concentration (μg/mL)	Repeatability (% RSD; n=3)	Intra-day (% RSD; n=3)	Inter-day (% RSD; n=3)
4	0.48	0.92	1.54
6	0.31	0.86	1.28
8	0.25	0.61	0.93

Table 5.65 Ruggedness data of NIF obtained using HPLC method

Concentration (μg/mL)	% RSD; n=2
4	1.81
6	1.48
8	1.31

Table 5.66 Summary of validation parameters of NIF HPLC method

Parameters	Results
Linearity range	0.25-10 µg/mL
Correlation coefficient	0.9998
Accuracy (% recovery)	98.2-99.8 %
Precision (% RSD; n=3)	
Repeatability	0.25-0.48 %
Intra-day	0.61-0.92 %
Inter-day	0.93-1.54 %
Ruggedness (% RSD; n=2)	1.31-1.81 %
LOD	0.040 µg/mL
LOQ	0.121 µg/mL

5.5.2.2. Drug-excipient compatibility

Same as section 5.1.2.5

5.5.2.3. Preparation of NIF amorphous solid dispersion (ASD)

Achieving sharp burst release after completion of lag time requires prominent solubility of drug and adequate dissolution rate of core tablet. NIF is the classical poorly soluble compound which needed enhancement of solubility before proceeding to core tablet preparation; which was strived through solid dispersion approach.

Several polymers, such as povidone K30, copovidone (COP), HPMC, PEG 6000, xylitol, mannitol etc., were investigated for preparation of NIF ASD. Optimally, NIF-COP ASD (1:2 % w/w) prepared using solvent evaporation technique was found satisfactory for preparation of NIF core tablets. Here, drug and polymer were dissolved in methanol, resultant solution was evaporated using rota evaporator (70°C; 600 mmHg) and further kept in vacuum oven (40°C; 500 mmHg) for 24 h to get a dry mass; which was then crushed using mortar-pestle and sifted through ASTM#40 to obtain free flowing powder which was finally employed for core tablet preparation.

5.5.2.4. Characterization of NIF ASD

The ASD was characterized for drug content, DSC, PXRD, FTIR and solubility studies in various aqueous media. The DSC and FTIR analysis were carried out in the same way as mentioned in section 5.1.2.5. The PXRD patterns of the pure NIF, physical mixture (PM), and ASD were investigated employing powder x-ray diffractometer using CuKa radiation of wavelength 1.54 A°, a voltage of 40 kV and a current of 40

mA. As the slide moves at an angle of theta degree, a proportional detector detects diffracted x-rays at angle of $2\theta°$ and subsequently XRD patterns were recorded. XRD patterns were recorded in the $2\theta°$ range of 5 to 60. Further, the equilibrium solubility of pure NIF, PM and ASD was determined with three aqueous media i.e. purified water, 0.1 N HCl and pH 6.8 phosphate buffer by adding excess amount of solid (150 mg) to 25 ml of aqueous medium using stoppered conical flasks which was pre-equilibrated at $37\pm0.5°C$. The flasks were placed on magnetic stirrer with heater (Remi Sales & Engineering Ltd., India) at 300 rpm. At predetermined time intervals samples were withdrawn, filtered through a 0.45 µm filter and analyzed using HPLC method. All measurements were made in triplicate.

5.5.2.5. Preparation of NIF core tablets

Same as PRS, the core tablets of NIF were also prepared by direct compression method as per the composition shown in Table 5.67. The tablets were prepared at a constant average weight (100 mg) by keeping the composition as similar as possible with adjustment of just lactose quantity as per varying dose of drug, using the same procedure as mentioned for PRS (section 5.1.2.6.).

Table 5.67 List of ingredients and their respective concentrations employed for formulation of NIF core tablets

Ingredients	mg/tab (%w/w)
NIF ASD	15 mg ($\approx$ 5 mg NIF)
MCC	38 mg
Lactose	43 mg
SSG	3 mg
Colloidal SiO_2	0.5 mg
MgSt	0.5 mg
Total weight	100 mg

5.5.2.6. Characterization of NIF core tablets

Same as section 5.1.2.7 except the release studies were carried out using 900 mL of medium volume instead of 500 mL (to adequately maintain sink condition).

5.5.2.7. Preparation of NIF CCTs

NIF CCTs were formulated using optimized PRS outer coat composition (Table 5.24) by following same procedure as mentioned for PRS (section 5.1.2.8.).

5.5.2.8. Characterization of NIF CCTs

Same as section 5.1.2.9 except the release studies were carried out using 900 mL of medium volume instead of 500 mL.

5.5.2.9. Packaging and stability study (NIF CCTs)

Same as section 5.1.2.10.

5.5.3. Results and discussion (NIF)

5.5.3.1. Evaluation of NIF ASD

Initial characterization of various binary systems was carried out using DSC analysis which typically exhibits endothermic or exothermic transitions associated with any thermodynamic event. The technique is widely used for the evaluation of crystalline or amorphous nature of a solid substance (94). The crystalline materials, in general, demonstrate sharp endotherm at its melting point whereas amorphous materials lack such transition owing to random molecular orientation. DSC thermograms of various NIF-carrier binary systems are demonstrated in Figure 5.43. The Figure clearly shows that except povidone K30 and COP, all other binary systems exhibited melting endotherm (at about 172°C) characteristic to crystalline NIF and therefore ruled out to be termed as ASD. Here, further selection was made on account of relatively higher aqueous solubility obtained with NIF-COP ASD as compared to NIF-povidone K30 ASD.
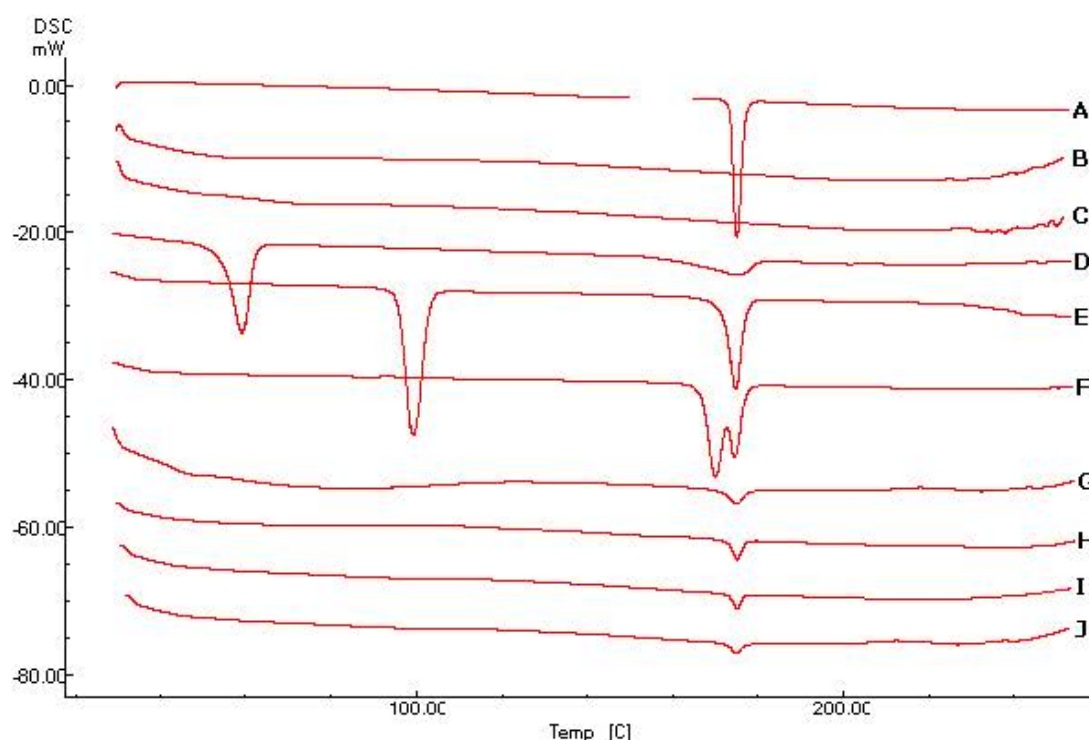

Fig. 5.43 DSC thermograms of (A) NIF, (B) NIF-COP binary system, (C) NIF-povidone K30 binary system, (D) NIF-PEG6000 binary system, (E) NIF-xylitol binary system, (F) NIF-mannitol binary system, (G) NIF-HPMC E5 binary system, (H) NIF-HPMC E15 binary system, (I) NIF-HPMC E50 binary system, (J) NIF-HPMC AS LF binary system

Figure 5.44 shows DSC thermograms of pure NIF, pure COP, NIF-COP PM, and NIF-COP ASD. As shown in Figure, pure NIF clearly exhibited crystalline nature with sharp melting endotherm at about 172°C which was slightly broadened in NIF-COP PM but completely absent in NIF-COP ASD. Hence, it was anticipated that NIF would have converted into the amorphous form and molecularly dispersed inside COP matrix. To confirm the same, the PXRD study was further carried out which can give more clear idea about crystalline and amorphous nature.
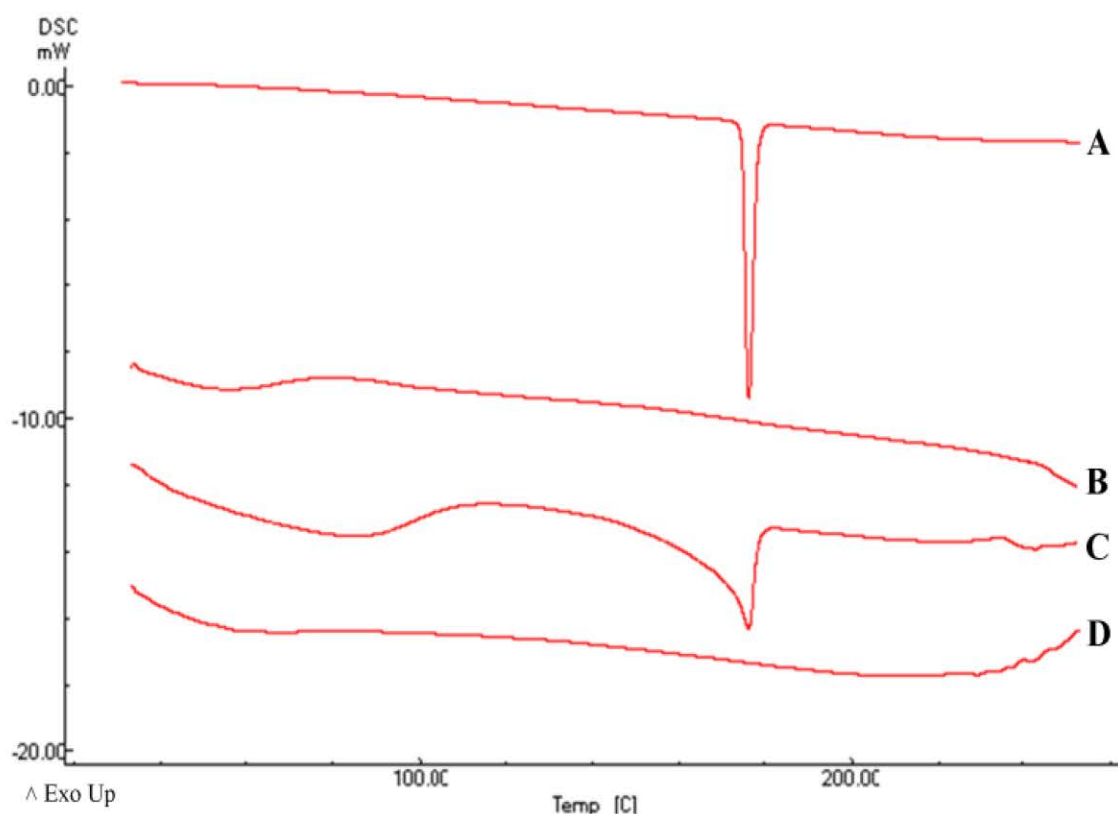

Fig.5.44 DSC thermograms of (A) NIF, (B) COP, (C) NIF-COP PM and (D) NIF-COP ASD

The results of PXRD study is demonstrated in Figure 5.45. The PXRD spectra of pure NIF demonstrated crystalline nature with 2θ peaks characteristic to NIF i.e. at 8.1, 11.7, 16.2, 19.5 and 24.6 (95). These peaks were also found present in NIF-COP PM but not in NIF-COP ASD. Hence, it was confirmed that the prepared ASD did not contain any crystalline portion and the drug molecules were molecularly dispersed throughout COP matrix. Further, FTIR study was performed to check the bonding interaction between drug and carrier.
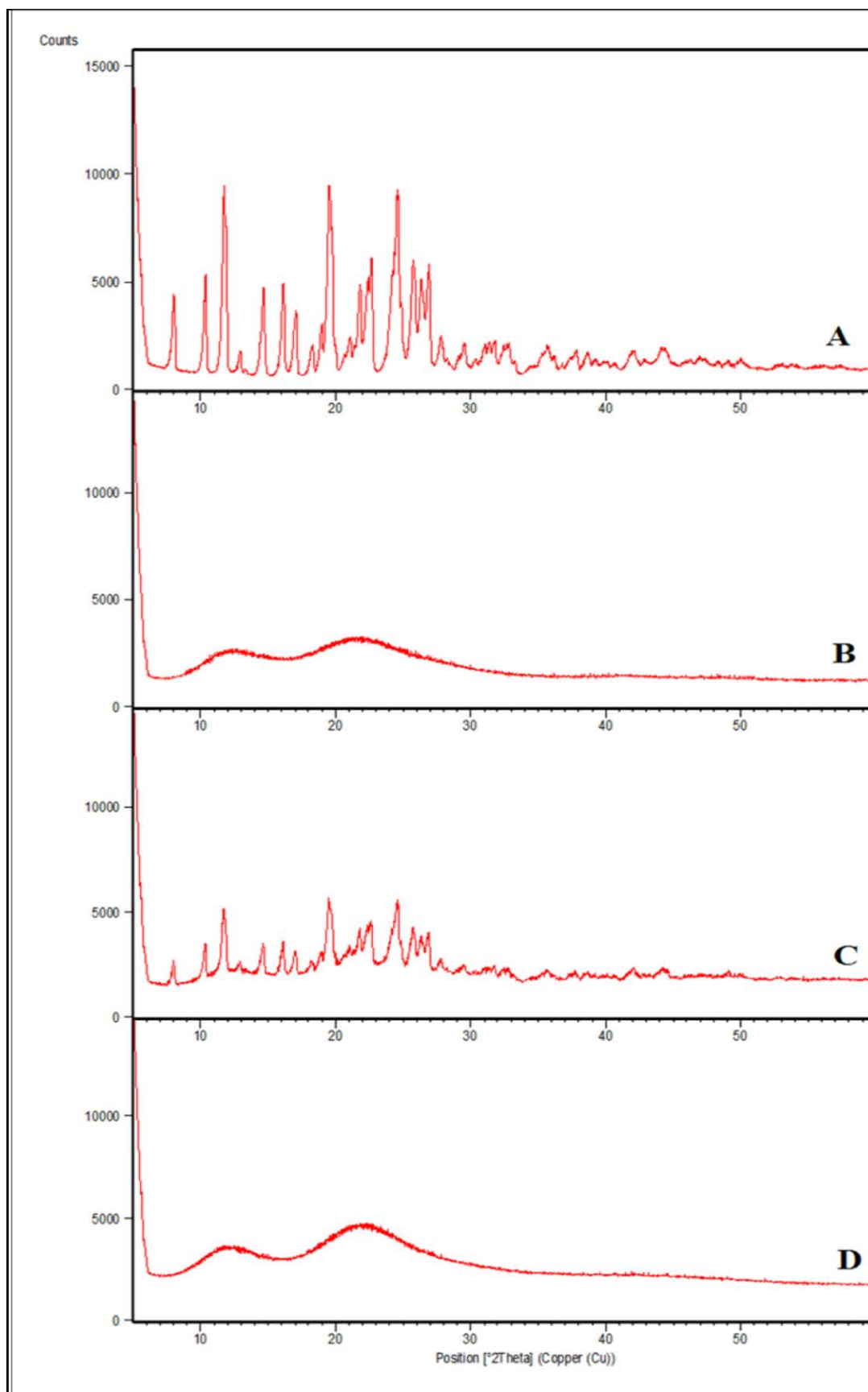
Fig. 5.45 PXRD spectra of (A) NIF, (B) COP, (C) NIF-COP PM and (D) NIF-COP ASD

The overlaid FTIR spectra of pure NIF, pure COP, NIF-COP PM, and NIF-COP ASD are displayed in Figure 5.46. The prime noticeable change was the absence of characteristic 3331 cm^{-1} band (N-H stretching vibration of NIF (95)) in the NIF-COP ASD which was found present in FTIR spectra of pure NIF as well as NIF-COP PM. The removal of this vibration frequency indicates formation of hydrogen bond between drug and carrier suggesting formulation of stable ASD (95).
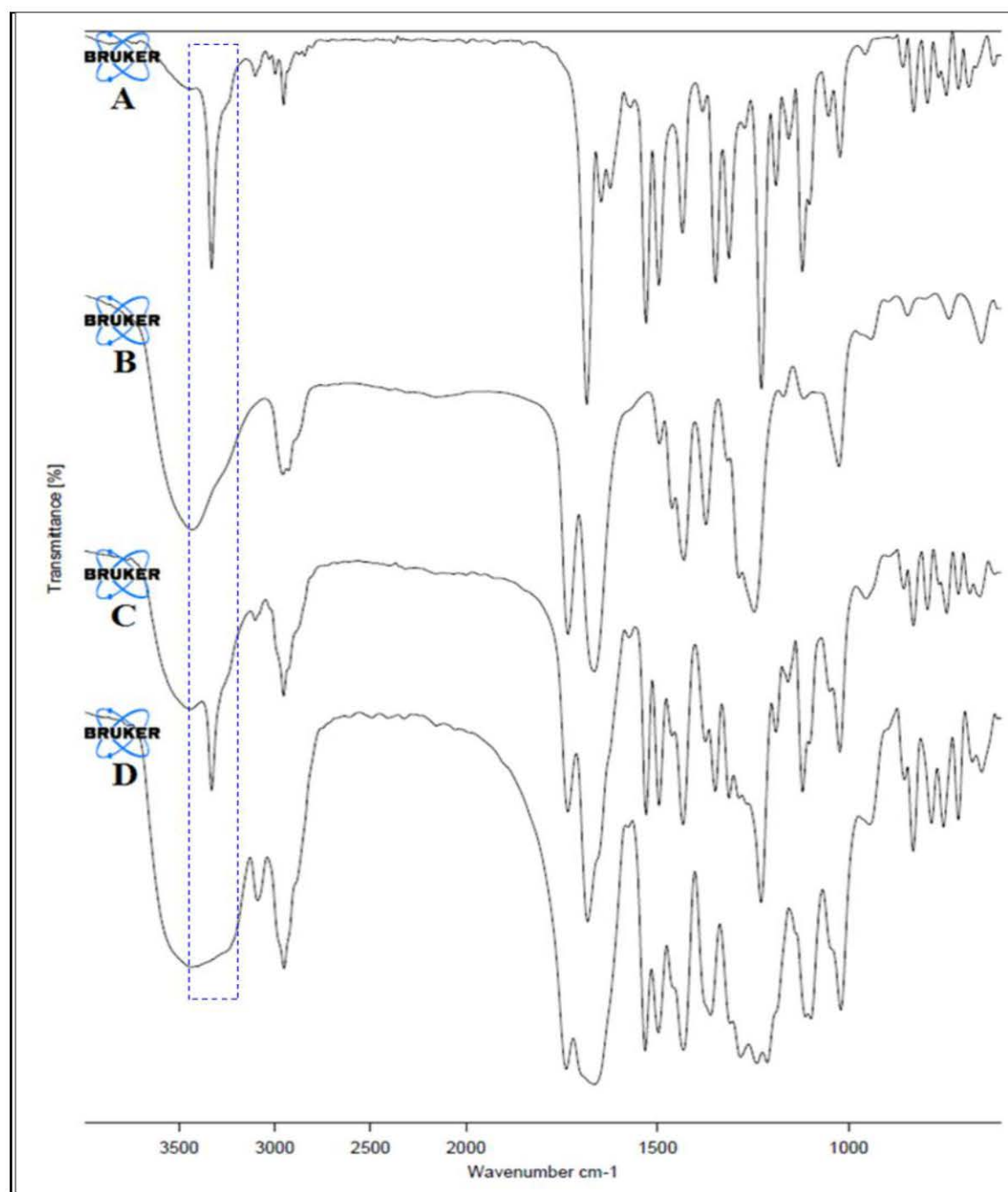

Fig. 5.46 FTIR spectra of (A) NIF, (B) COP, (C) NIF-COP PM and (D) NIF-COP ASD.

Further, the prepared NIF-COP ASD was evaluated for equilibrium solubility study; the results of which are demonstrated in Figure 5.47. In purified water, the solubility of pure NIF, NIF-COP PM, and NIF-COP ASD was respectively found to be 8.49±0.50, 12.56±0.74, and 65.58±1.13 μg/mL. Almost similar results were obtained with other medium also as shown in Figure 5.47. Hence, the prepared NIF-COP ASD, which increased the aqueous solubility about 7-8 times, was further employed for preparation of core tablets. The assay of NIF ASD was found to be 99.3% as determined using HPLC.
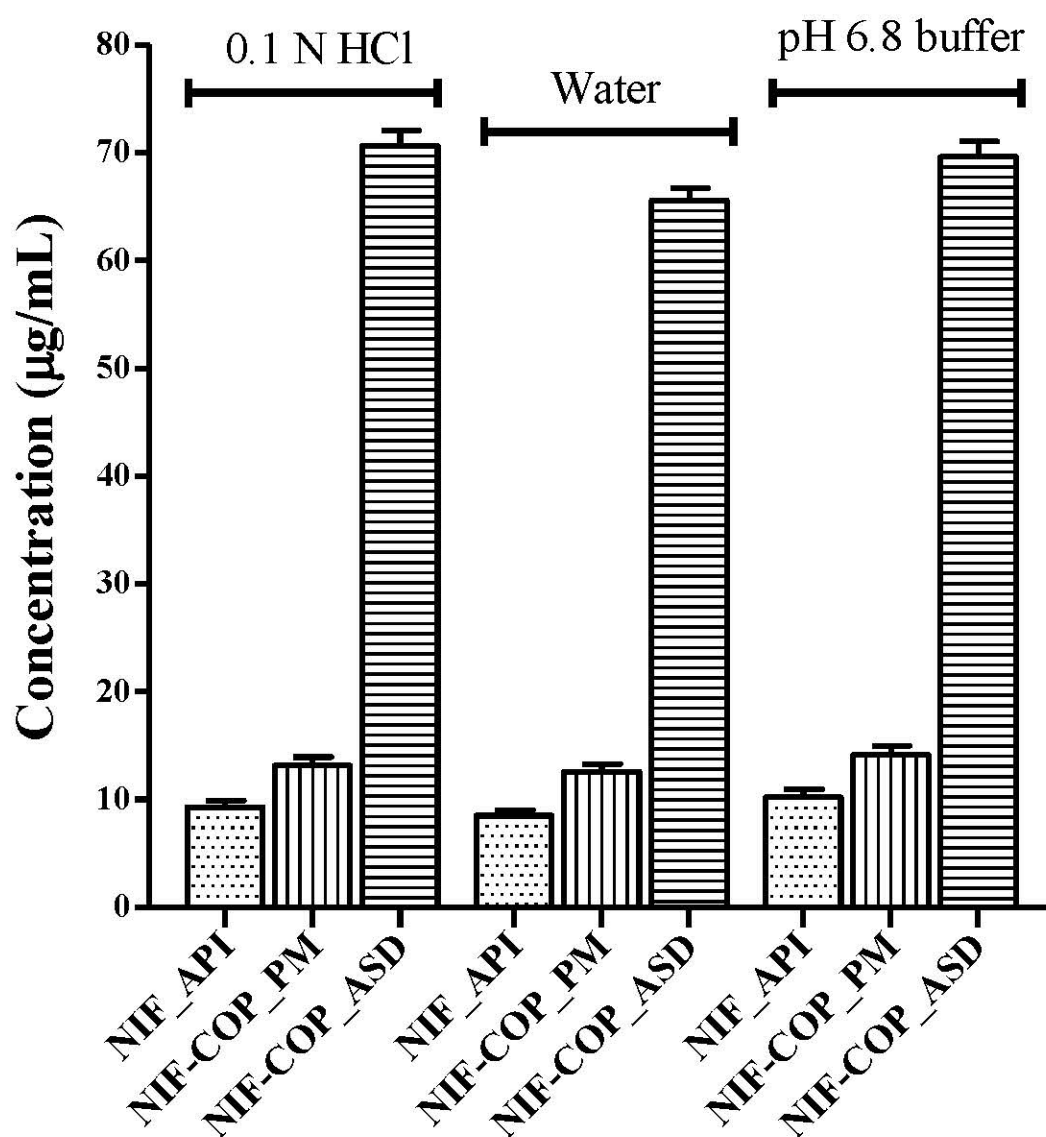

Fig. 5.47 Results of equilibrium solubility study of crystalline NIF and NIF ASD in various aqueous media (mean±SD; n=3)

5.5.3.2. Evaluation of NIF core tablets

The physical appearance of core tablets was found to be satisfactory. The tablets had hardness of 4-6 kp, friability less than 0.5% and disintegration time less than 180 s. The tablet thickness was found to be 3.8-3.9 mm. Assay, weight variation and CU results were found within their respective specification limits. The release studies demonstrated >85% drug release within 30 min with all tested dissolution conditions and therefore the core tablets were construed as fast dissolving IR tablets. The dissolution profile with basket apparatus, 100 rpm, pH 6.8 phosphate buffer/water, 900 mL, 37±0.5°C is depicted in Figure 5.48. The Figure also exemplifies comparative assessment of core tablet of NIF ASD with that of pure NIF which shows substantial enhancement of NIF dissolution rate upon formulation of ASD. Further, the impact of double compression on core tablets was determined by carefully scraping out the outer coat of CCT and analyzing the core tablets for thickness, hardness and drug release. The results depicted no distinguishable difference in all three parameters due to double compression.
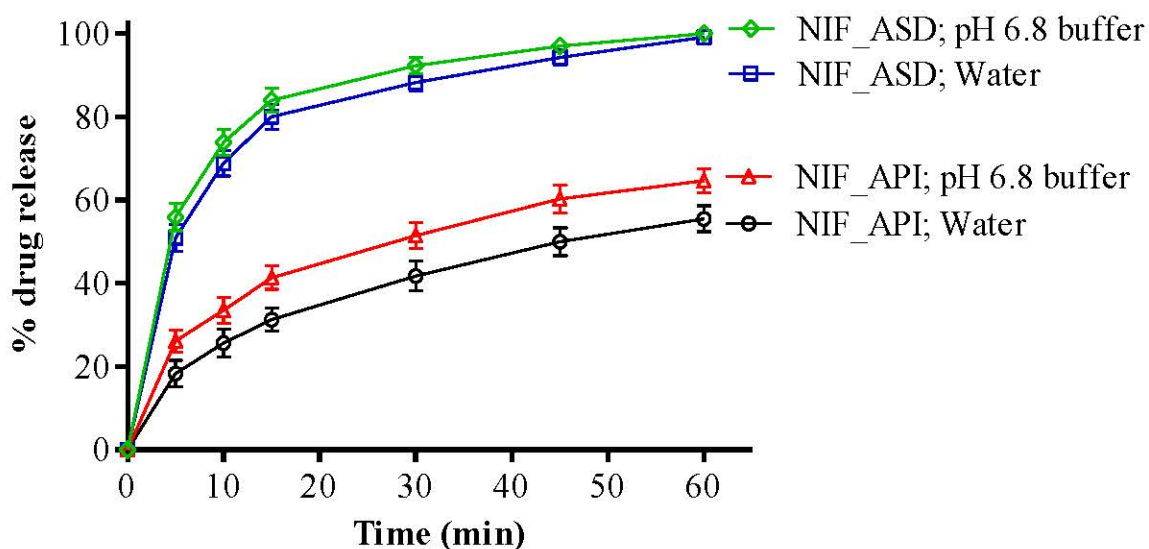

Fig. 5.48 Drug release profile of NIF core tablets prepared using ASD as well as plain API in pH 6.8 phosphate buffer/water; basket apparatus; 100 rpm; 900 mL; 37.0±0.5°C [mean±SD; n=6]

5.5.3.3. Evaluation of NIF CCTs

The appearance of the CCTs was found to be satisfactory. The hardness was 11.5-14.5 kp, thickness was 5.9-6.0 mm and friability was less than 0.5%. Assay and weight variation results were found to be within their respective specification limits.

5.5.3.3.1. *In vitro* release studies (NIF CCTs)

The release studies exhibited typical 4-6 h of lag time followed by sharp burst release (>85%) within 30 min of outer coat rupturing with all tested conditions except hydro-alcoholic media (in which the lag time did not remain confine to 4-6 h). The dissolution profile of NIF CCTs obtained with basket apparatus; 100 rpm; 0.1 N HCl followed by pH 6.8 phosphate buffer is displayed in Figure 4.49. The individual lag time results obtained with various dissolution conditions are demonstrated in Figure 5.50. As shown in Figure, no significant difference was observed between the lag times of multi-media, change in apparatus, change in agitation and biorelevant media (p value >0.05).

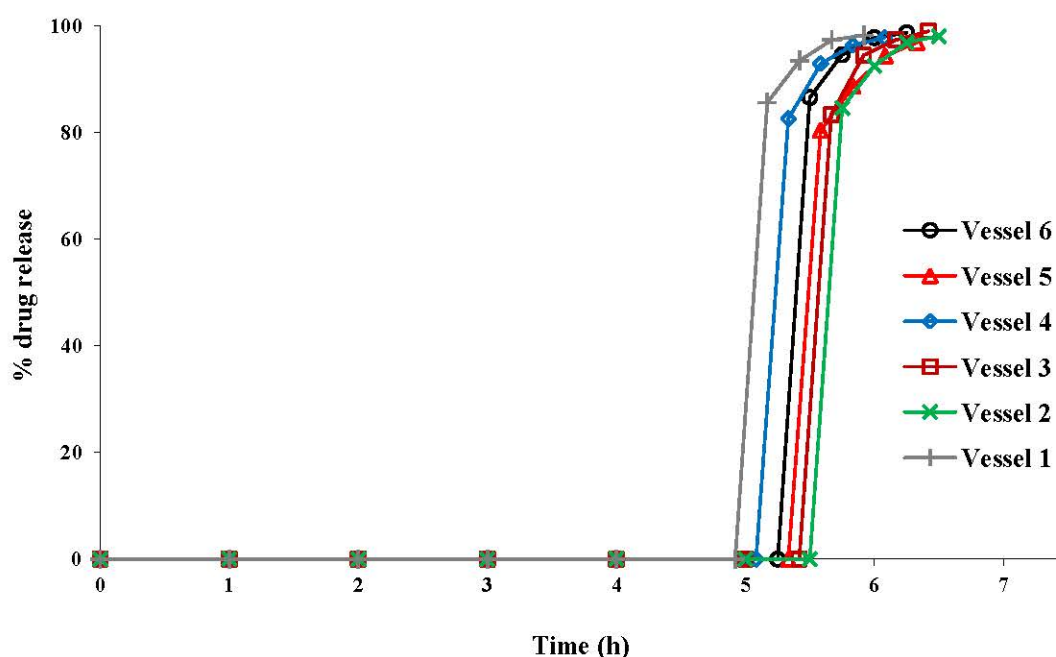Fig. 5.49 Drug release profile of optimized NIF CCTs obtained with basket apparatus; 100 rpm agitation; 0.1 N HCl for first 2 h followed by pH 6.8 buffer; 900 mL volume; 37±0.5°C temperature.

Same as PRS, similar release profile with multi-media corroborated the developed CCT as pH-independent in nature. Analogous release behaviour with different apparatus as well as with different agitation intensity inferred that the lag time

was robust enough and not influenced by change in hydrodynamics. Further, akin release profiles with biorelevant media prudently anticipate promising *in vivo* performance. The results of hydro-alcoholic media were also in-line with previous CCTs, entailing pertinent instruction ought to be mentioned on the label.

Fig. 5.50 Lag time of NIF CCT obtained using various dissolution conditions; medium volume 900 mL; temperature $37 \pm 0.5°C$; ^{ns} p value>0.05, **p value<0.01, ***p value<0.001 (mean±SD; n=6)

5.5.3.3.2. Effect of curing (NIF CCTs)

After exposure of 60°C for 24 h, NIF CCTs, when examined for appearance, hardness, assay, and drug release, exhibited each result within their respective specification limits (Table 5.68) with no distinguishable difference before and after curing. Thus, no effect of curing was observed.

Table 5.68 Results of curing study for NIF CCTs

Effect of curing	Appearance	Hardness	Assay	Lag time*	Burst release
Before curing	White colour	11.5-14.5 kp	99.4 %	5.29±0.29 h	>85% in 30 min
After curing	No change	No change	99.2 %	5.31±0.27 h	>85% in 30 min

*mean±SD; n=6

5.5.3.3.3. Packaging and stability (NIF CCTs)

The CCTs demonstrated no detectable change for either of appearance, hardness, assay, or drug release under stated storage conditions. Since all results were found within their respective specification limits (Table 5.69), the formulation was found to be stable under the selected packaging material and stated storage conditions.

Table 5.69 Results of stability study for NIF CCTs

Storage condition	Appearance	Hardness	Assay	Lag time*	Burst release
Initial	White colour	11.5-14.5 kp	99.4 %	5.29±0.29 h	>85% in 30 min
25±2°C/60±5% RH (3M)	No change	No change	99.1 %	5.26±0.24 h	>85% in 30 min
40±2°C/75±5% RH (3M)	No change	No change	99.0 %	5.28±0.26 h	>85% in 30 min

*mean±SD; n=6

5.5.4. Conclusion (NIF)

Since NIF is a poorly soluble drug, initially enhancement of solubility was carried out by formulating ASD using COP as a hydrophilic carrier; which was in turn employed for core tablet preparation and subsequently processed for compression coating using previously developed formula (PRS CCTs). Albeit, the CCTs exhibited 4-6 h of lag time followed by burst release profile at varying dissolution conditions. The lag time was found to be pH-independent as well as unaffected by change in hydrodynamics. Further, hydro-alcoholic and biorelevant dissolution results were also found similar to those of previous CCTs. Thus, replacement of former drugs with NIF (even after formulating ASD) in core tablet did not alter the desired quality traits of the developed PR CCT.

5.6. Development of PR CCTs of Lornoxicam (LOR)

5.6.1. LOR drug profile (96-101)

Lornoxicam (LOR) or chlortenoxicam is an oxicam class of NSAID having analgesic, anti-inflammatory and antipyretic properties. It is indicated in relieving pain associated with osteoarthritis, RA, ankylosing spondylitis, acute sciatica and postoperative pain. It is distinguished from other oxicams by a comparatively short elimination half-life (3 to 5 h), which is beneficial in terms of tolerability standpoint (97, 98).

General Characteristics (96, 99-101)

Molecular Formula: $C_{13}H_{10}ClN_3O_4S_2$

Chemical Name: 6-Chloro-4-hydroxy-2-methyl-N-2-pyridinyl-2H-thieno[2,3-e]-1,2-thiazine-3-carboxamide1,1-dioxide.

Structure:
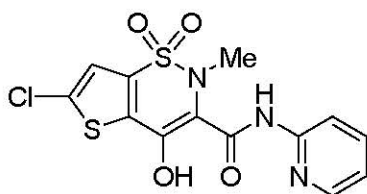
Molecular weight: 371.8 g/mol

Appearance: orange to yellow crystalline powder

Solubility: It is slightly soluble in chloroform and 0.1 M sodium hydroxide, very slightly soluble in methanol, acetonitrile and pH 7.4 phosphate buffer, and hardly soluble in water.

Melting point: 225-230°C with decomposition

Nature: Weak acid

pKa: 4.7

Log P: 1.8

Dose: 4-8 mg

BCS class: II

Mechanism of action:

LOR is a potent non-specific COX inhibitor (both COX-I and COX-II) which exert analgesic and anti-inflammatory action through inhibition of prostaglandin and thromboxane synthesis. Inspite of having non-specific COX inhibition, it also releases endogenous central acting analgesics i.e. β-endorphin and dynorphin. LOR does not

increases the production of the leukotrienes as does by other conventional NSAIDs, and shunting of arachidonic acid to the 5-lipoxygenase cascade is therefore not anticipated helping to decrease the allergic response related side effects (96, 98).

Pharmacokinetics (96-98)

Absorption: rapidly and almost completely absorbed after oral administration.

Peak effect: 1-3 h

Duration of action: ˜4-5 h

Plasma half life: 3-5 h

Bioavailability: The absolute bioavailability is 90 to 100% following oral administration.

Protein binding: LOR is highly protein bound (about 99.7%) almost exclusively to serum albumin.

Distribution: LOR exhibits low apparent volume of distribution after oral or intravenous administration i.e. 5-10 L (0.1 to 0.2 L/kg). However, it readily crosses perivascular spaces, including the synovial fluid. In patients with RA, the LOR synovial fluid: plasma AUC ratio is around 0.5 after dosing of 4 mg twice daily dose for 5 days.

Metabolism and Excretion: LOR is extensively metabolised in the liver, mainly to the inactive metabolite 5'-hydroxylornoxicam. Elimination is shared between the renal and faecal routes. 5-Hydroxylation is the major metabolic pathway, which is responsible for up to 95% of total intrinsic LOR clearance, and cytochrome P450 2C9 is reported to be the primary enzyme involved in the formation of 5-hydroxylornoxicam. The apparent oral clearance of LOR 4-8 mg twice daily dose varies from 1.5 to 3.4 L/h in healthy volunteers.

Contraindications: LOR is contraindicated in the patients who must not take other NSAIDs due to the adverse effects such as salicylate sensitivity, bleeding disorders, GI bleeding and severe impairment of heart, liver or kidney function (97).

Adverse effects: LOR has a tolerability profile characteristic of an NSAID with GI disturbances (mild dyspepsia and heartburn to ulceration, perforation and haemorrhage) being the most common adverse events. Other side effects include bronchospasms, headache and dizziness (98).

5.6.2. Methods (LOR)

After ensuring desired results with previous CCTs, LOR, a poorly soluble drug, was opted in order to challenge robustness of the optimized PR CCTs.

5.6.2.1. RP-HPLC method for determination of LOR

An RP-HPLC method was developed for the determination of LOR as required throughput the study. Chromatographic conditions and various parameters are enlisted in Table 5.70.

Table 5.70 Chromatographic conditions for determination of LOR

Stationary phase:	C18, 250 mm, 4.6 mm, 5 µm
Mobile phase:	40:30:30 % v/v/v mixture of water: methanol: acetonitrile; pH adjusted to 3.0 with o-phosphoric acid
Flow rate:	1 mL/min
Detection wavelength:	375 nm
Temperature:	≈ 25°C
Injection volume:	20 µL
Retention time:	6.50±0.06 min
Asymmetry factor:	1.222±0.011
Theoretical plates:	11857±117.21

5.6.2.1.1. Preparation of standard stock solutions of LOR

Accurately weighed quantity of drug (10 mg) was dissolved in 100 mL of acetonitrile to obtain the standard stock solution of 100 µg/mL.

5.6.2.1.2. Preparation of calibration curve of LOR

Varying concentrations of drug solutions (0.25-10 µg/mL) were prepared from 100 µg/mL standard stock solution using mobile phase as diluent. The solutions were analyzed with Kromasil C18 column using isocratic HPLC/UV system. The samples were injected through Rheodyne 7725 injector valve fixed with 20 µL loop. The mobile phase was vacuum filtered through 0.22 µm nylon membrane filter followed by degassing with an ultrasonicator prior to use. The detection was performed at 375 nm and calibration curve was plotted for area vs. concentration as shown in Table 5.71. The system suitability criteria were in accordance with USP limits (26). The overlaid calibration chromatograms are depicted in Figure 5.51 and corresponding linearity curve, regression equation and correlation coefficient are depicted in Figure 5.52.

Accuracy, precision and ruggedness were carried out as per ICH guidelines (25) and the results are respectively depicted in Table 5.72, Table 5.73 and Table 5.74. Overall summary of validation results are depicted in Table 5.75.

Table 5.71 Calibration curve and regression equation of LOR obtained using HPLC method

Concentration (µg/mL)	Area (mV.s) (mean±SD; n=5)
0.25	10.479±0.224
0.5	19.273±0.375
1	37.533±0.688
2	75.133±0.794
4	151.076±2.105
6	225.099±2.883
8	303.471±3.564
10	375.137±1.960
Regression equation	
Slope	0.4564±0.469
Intercept	37.592±0.277
Correlation coefficient	0.9999
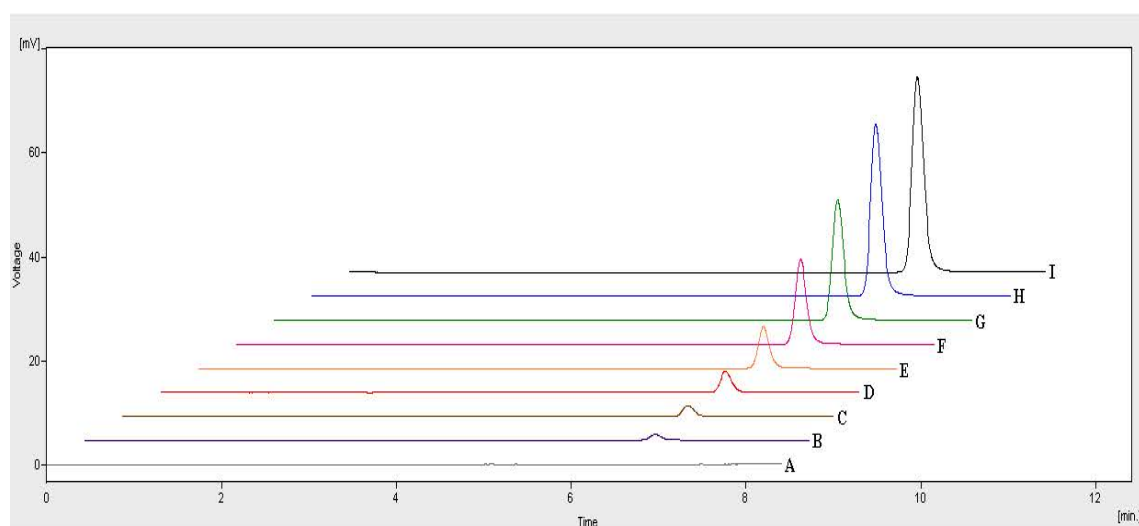
Fig. 5.51 Overlain HPLC chromatograms of 0.25-10 µg/mL LOR; (A) blank, (B) 0.25 µg/mL, (C) 0.5 µg/mL, (D) 1 µg/mL, (E) 2 µg/mL, (F) 4 µg/mL, (G) 6 µg/mL, (H) 8 µg/mL, and (I) 10 µg/mL

Lornoxicam calibration curve - HPLC

$y = 37.592x + 0.4564$
$R^2 = 0.9999$
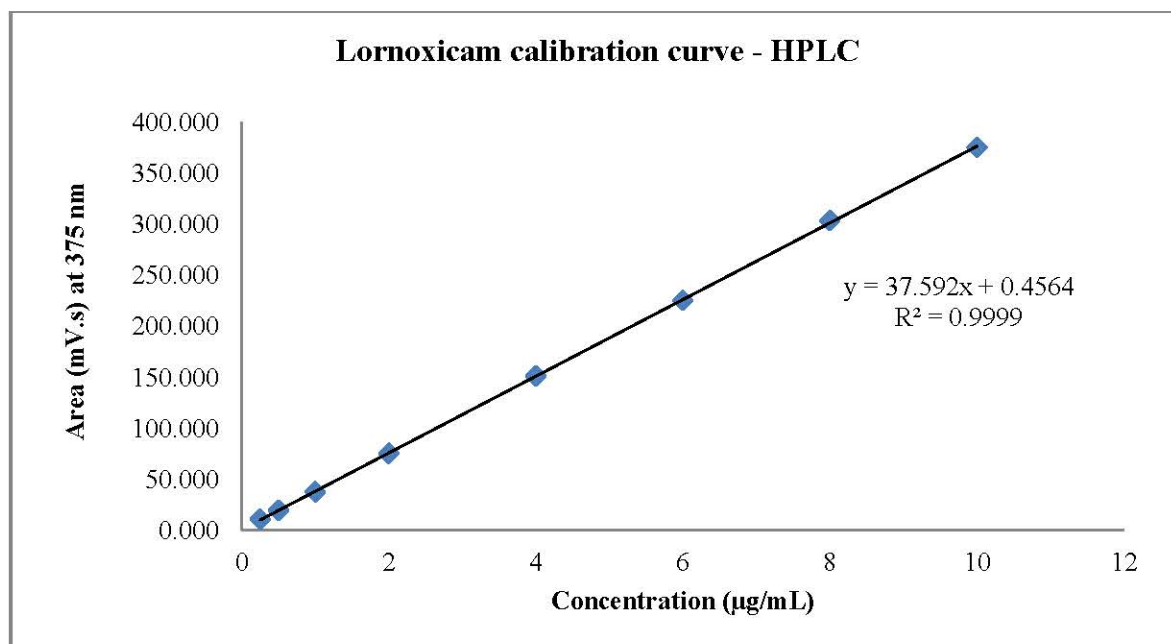
Fig. 5.52 HPLC calibration curve of LOR (0.25-10 µg/mL)

Table 5.72 Accuracy data of LOR obtained using HPLC method

Amount spiked (mg)	Amount recovered (mg) (mean±SD; n=3)	% recovery (mean±SD; n=3)	% recovery (range; n=3)	Average % recovery
2	1.98±0.02	99.1±0.90	98.3-100.1	
4	3.99±0.03	99.7±0.83	98.8-100.5	99.4
6	5.96±0.05	99.3±0.76	98.5-100.0	

Table 5.73 Precision data of LOR obtained using HPLC method

Concentration (µg/mL)	Repeatability (% RSD; n=3)	Intra-day (% RSD; n=3)	Inter-day (% RSD; n=3)
2	0.41	0.80	1.53
4	0.33	0.68	1.40
6	0.24	0.52	0.80

Table 5.74 Ruggedness data of LOR obtained using HPLC method

Concentration (µg/mL)	% RSD; n=2
2	1.62
4	1.18
6	0.79

Table 5.75 Summary of validation parameters of LOR HPLC method

Parameters	Results
Linearity range	0.25-10 µg/mL
Correlation coefficient	0.9999
Accuracy (% recovery)	98.3-100.5 %
Precision (% RSD; n=3)	
Repeatability	0.24-0.41 %
Intra-day	0.52-0.80 %
Inter-day	0.80-1.53 %
Ruggedness (% RSD; n=2)	0.79-1.62 %
LOD	0.041 µg/mL
LOQ	0.125 µg/mL

5.6.2.2. Drug-excipient compatibility

Same as section 5.1.2.5

5.6.2.3. Preparation of LOR ASD

As stated previously, achieving sharp burst release after completion of lag time necessitates prominent solubility of drug and adequate dissolution rate of core tablet. As LOR is also a poorly soluble BCS class II drug, the enhancement of solubility and thereby dissolution rate was strived through solid dispersion approach.

Since LOR is a weak acid having limited solubility in acidic pH, it was prudent and also suggested by some preliminary trials to incorporate an alkaliser for development of LOR ASD. Meglumine (MEG) was chosen as micro-environment pH modifier and trials were taken with different carriers. Optimally, ASD prepared using LOR-MEG-HPMC E5 (1:0.5:2.0 % w/w/w) ternary system was found to be suitable for preparation of LOR core tablets. LOR ASD was prepared as per following procedure: MEG, drug and polymer were sequentially dissolved in dichloromethane-methanol (1:1 % v/v) solvent mixture and the resultant solution was evaporated in rota evaporator (70°C; 600 mmHg) and further kept in vacuum oven (40°C; 500 mmHg) for 24 h to get a dry mass; which was then crushed using mortar-pestle and sifted through ASTM#40 to obtain free flowing powder which was finally employed for core tablet preparation.

5.6.2.4. Characterization of LOR ASD

Same as section 5.5.2.4

5.6.2.5. Preparation of LOR core tablets

The core tablets of LOR were prepared by direct compression method as per the composition shown in Table 5.76. Here, lactose was replaced with mannitol for preparation of core tablet since it was reviewed that there is a possibility of interaction between lactose and MEG (employed in the formulation of LOR ASD) (102). The tablets were prepared at a constant average weight (100 mg) using the same procedure as mentioned for PRS (section 5.1.2.6).

Table 5.76 List of ingredients and their respective concentrations employed for formulation of LOR core tablets

Ingredients	mg/tab (%w/w)
LOR ASD	14 mg ($\approx$ 4 mg LOR)
MCC	38 mg
Mannitol	44 mg
SSG	3 mg
Colloidal SiO$_2$	0.5 mg
MgSt	0.5 mg
Total weight	100 mg

5.6.2.6. Characterization of LOR core tablets

Same as section 5.1.2.7 except the release studies were carried out using 900 mL of medium volume instead of 500 mL (to adequately maintain sink condition).

5.6.2.7. Preparation of LOR CCTs

The LOR CCTs were formulated using optimized PRS outer coat composition (Table 5.24) by following same procedure as mentioned for PRS (section 5.1.2.8.).

5.6.2.8. Characterization of LOR CCTs

Same as section 5.1.2.9 except release studies were carried out using 900 mL of medium volume instead of 500 mL.

5.6.2.9. Packaging and stability study (LOR CCTs)

Same as section 5.1.2.10

5.6.3. Results and discussion (LOR)

5.6.3.1. Evaluation of LOR ASD

DSC thermograms of pure LOR, MEG, HPMC, LOR-MEG-HPMC PM, and LOR-MEG-HPMC ASD are displayed in Figure 5.53. As shown in Figure, pure LOR exhibited an exotherm at about 235°C due to melting with decomposition (96). The thermogram of MEG displayed a melting endotherm at 131°C whereas thermogram of HPMC did not show any sharp peak. The thermogram of LOR-MEG-HPMC PM demonstrated slight shift/broadening of melting endotherm of MEG but did not show any exotherm at 235°C which could be due to the solubilisation of LOR in already molten MEG. However, thermogram of LOR-MEG-HPMC ASD did not display any endotherm corresponding to MEG or exotherm corresponding to LOR. Hence, it was anticipated that there could be molecularly dispersed ASD of LOR-MEG-HPMC ternary system. To confirm the same, the PXRD study was carried out further.
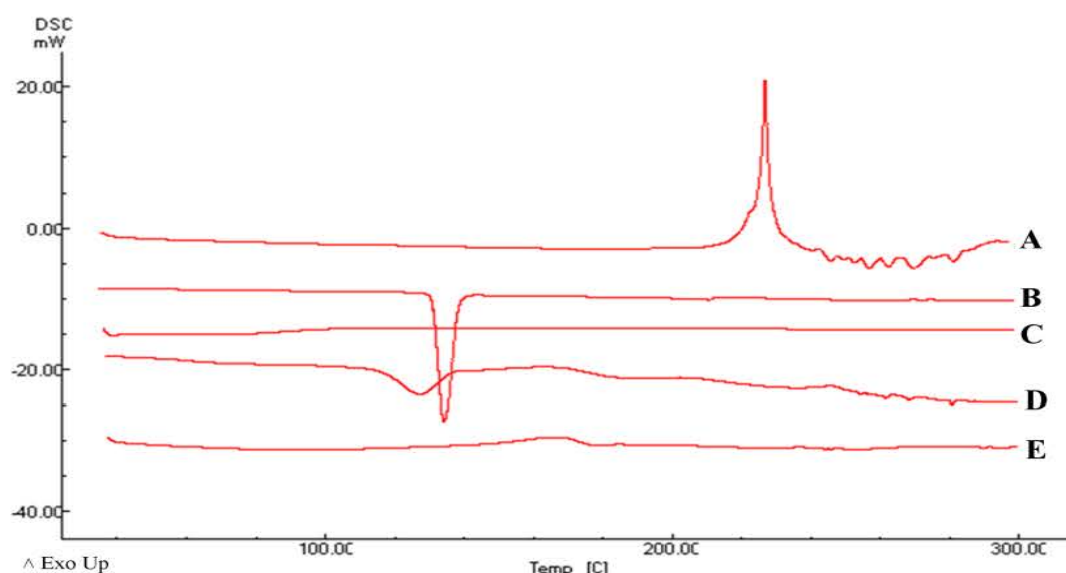
Fig. 5.53 DSC thermograms of (A) LOR, (B) MEG, (C) HPMC E5, (D) LOR-MEG-HPMC E5 PM, and (E) LOR-MEG-HPMC E5 ASD

The results of PXRD study are displayed in Figure 5.54. The Figure illustrates that pure LOR as well as MEG were evidently crystalline in nature whereas polymer HPMC was veritably amorphous. On the other hand, the spectra of LOR-MEG-HPMC PM exhibited crystalline pattern whereas that of ASD depicted amorphous nature. Hence, it was confirmed that the prepared solid dispersion was, in fact, a molecularly dispersed amorphous ternary system of LOR-MEG-HPMC E5.
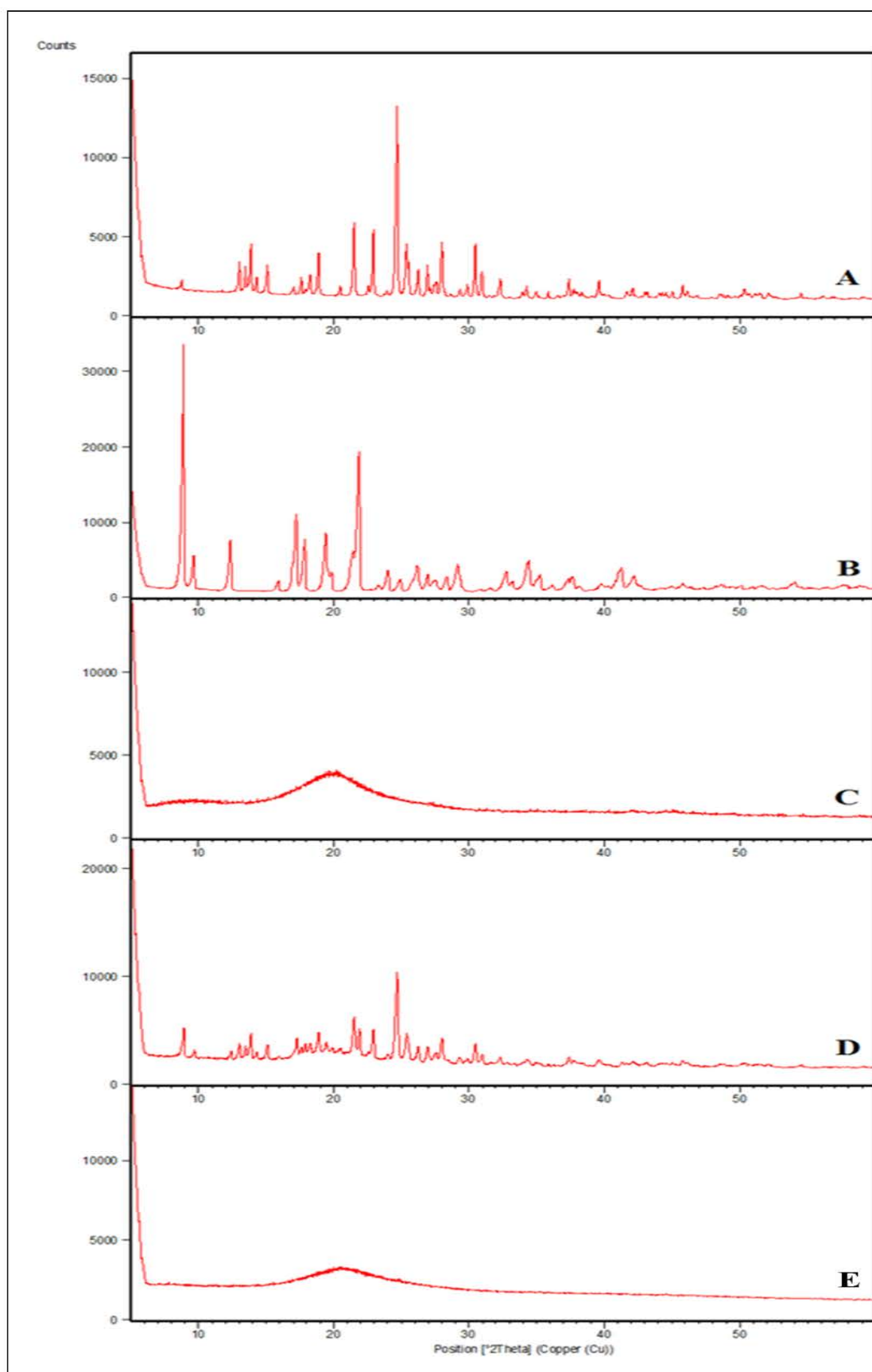
Fig. 5.54 PXRD spectra of (A) LOR, (B) MEG, (C) HPMC E5, (D) LOR-MEG-HPMC
E5 PM, and (E) LOR-MEG-HPMC E5 ASD

The overlaid FTIR spectra of pure LOR, MEG, HPMC, LOR-MEG-HPMC PM, and LOR-MEG-HPMC ASD are displayed in Figure 5.55. The FTIR spectra of pure LOR distinctly depicted the band at 3065 cm^{-1} corresponding to N-H stretching vibration of LOR (96). This band, which was absent in spectra of MEG as well as HPMC, was present in LOR-MEG-HPMC PM but not in that of ASD. Hence, same as NIF ASD, the possibility of hydrogen bonding between drug and carrier was substantiated in this case also.
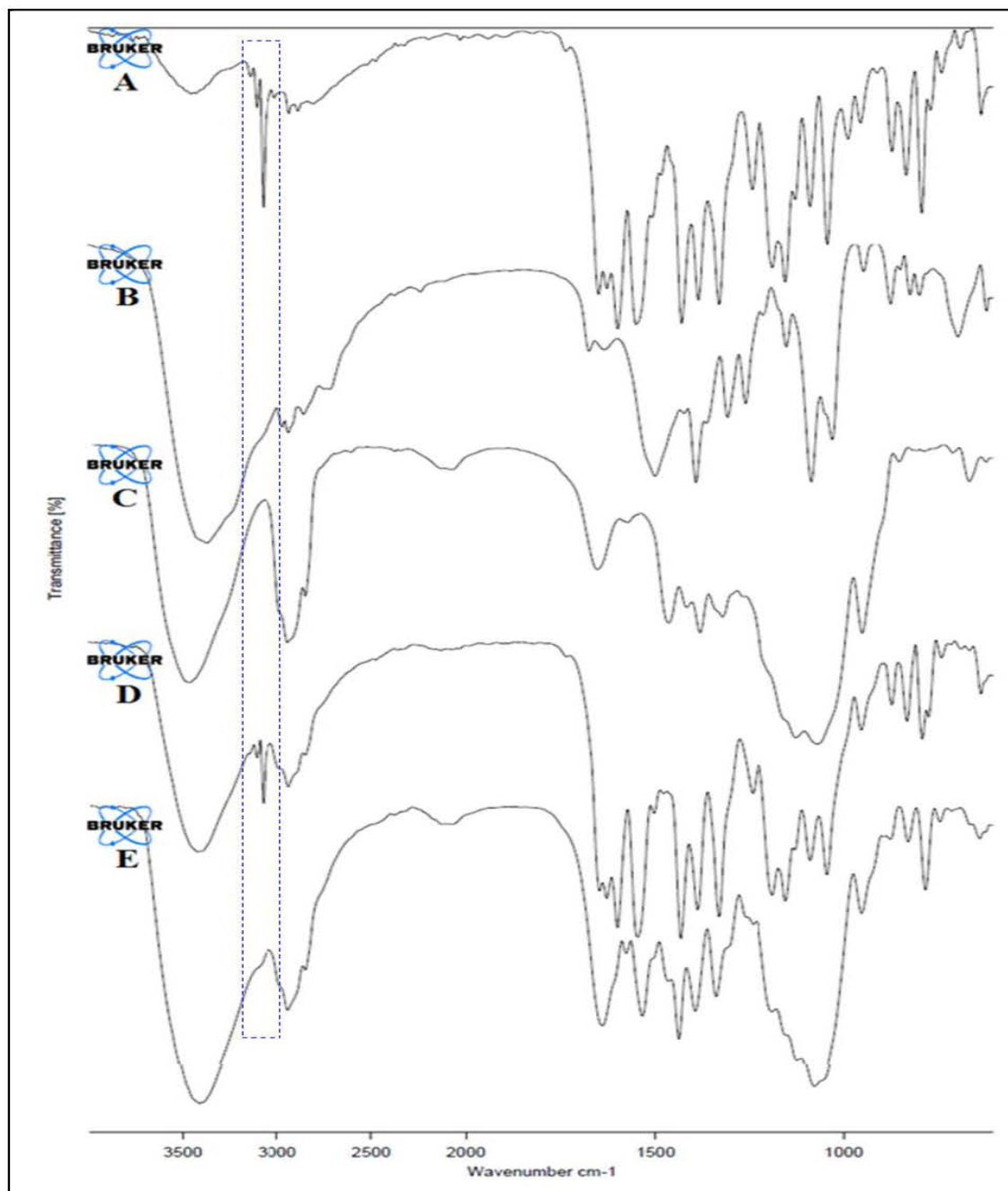
Fig. 5.55 FTIR spectra of (A) LOR, (B) MEG, (C) HPMC E5, (D) LOR-MEG-HPMC E5 PM, and (E) LOR-MEG-HPMC E5 ASD

The equilibrium solubility of crystalline LOR and LOR ASD were determined in three different aqueous media at 37±0.5°C and the results are displayed in Figure 5.56. As shown in Figure, LOR exhibited sharp pH-dependent solubility with very low in 0.1 N HCl. Hence, the focus was to improve the solubility of LOR mainly in acidic medium which would thereby solve the solubility issue with other medium also. The solubility of pure LOR, LOR-MEG-HPMC PM, and LOR-MEG-HPMC ASD in 0.1 N HCl was respectively found to be 4.08±0.19, 4.57±0.21, and 17.11±0.72 µg/mL. Thus, formulation of ternary ASD increased the solubility of LOR approx 4 fold in 0.1 N HCl. Apparently, the solubility of LOR in purified water and pH 6.8 phosphate buffer were respectively found to be 17.67±0.69 and 89.64±3.25 µg/mL, whereas the same for LOR ASD were found to be 9.65±0.18 and 10.28±0.32 mg/mL respectively. Such significant rise might be due to the increase in pH of the medium because of simultaneous solubilisation of MEG. However, with consideration of 4 fold solubility enhancement in 0.1 N HCl, the prepared ASD was further employed for preparation of core tablets. The assay of the prepared LOR ASD was found to be 99.8% as determined using HPLC.
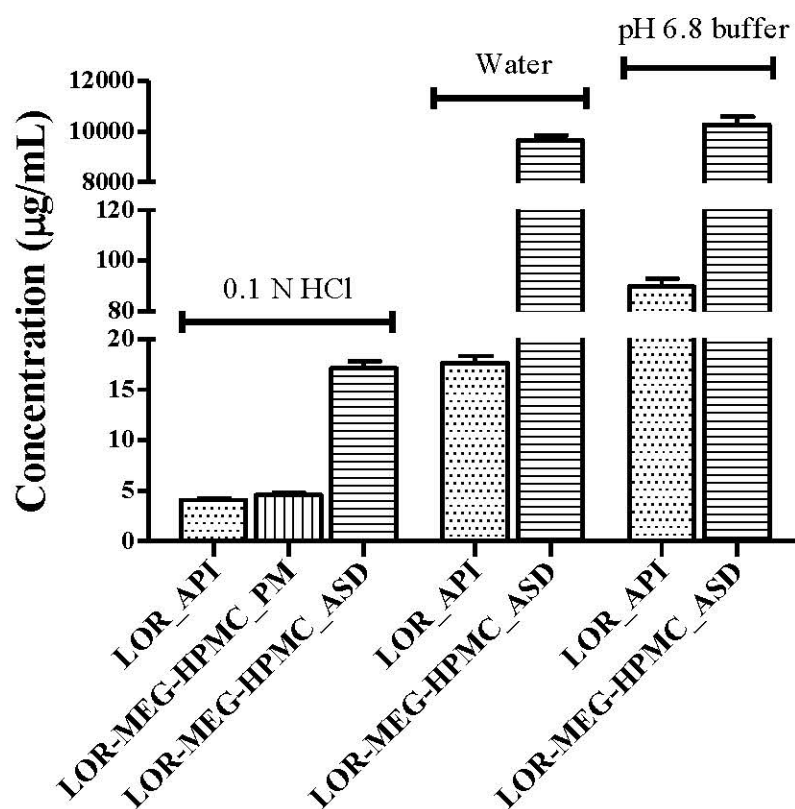
Fig. 5.56 Results of equilibrium solubility study of crystalline LOR and LOR ASD in various aqueous media (mean±SD; n=3)

5.6.3.2. Evaluation of LOR core tablets

The physical appearance of core tablets was found to be satisfactory. The tablets had hardness of 4-6 kp, friability less than 0.5% and disintegration time less than 120 s. The tablet thickness was found to be 3.8-3.9 mm. Assay, weight variation, and CU results were found to be within their respective specification limits. The release studies demonstrated >85% drug release within 15 min with all tested dissolution conditions. Since LOR had depicted the least solubility in acidic medium, the core tablets of LOR ASD were additionally examined for drug release in 0.1 N HCl as dissolution medium (900 mL; basket apparatus; 100 rpm; 37±0.5°C) – which also exhibited >85% release within 15 min. Thus, according to the release studies the core tablets were found to be fast dissolving IR tablets. The dissolution profile with basket apparatus, 100 rpm, pH 6.8 phosphate buffer/water, 900 mL, 37±0.5°C is depicted in Figure 5.57. The Figure also exemplifies comparative assessment of core tablet of LOR ASD with that of pure drug which exhibits substantial enhancement of LOR dissolution rate upon formulation of ASD. The impact of double compression on core tablets was determined by carefully scraping out the outer coat of CCT and analyzing the core tablets for thickness, hardness and drug release. The results depicted no distinguishable difference in all three parameters due to double compression.
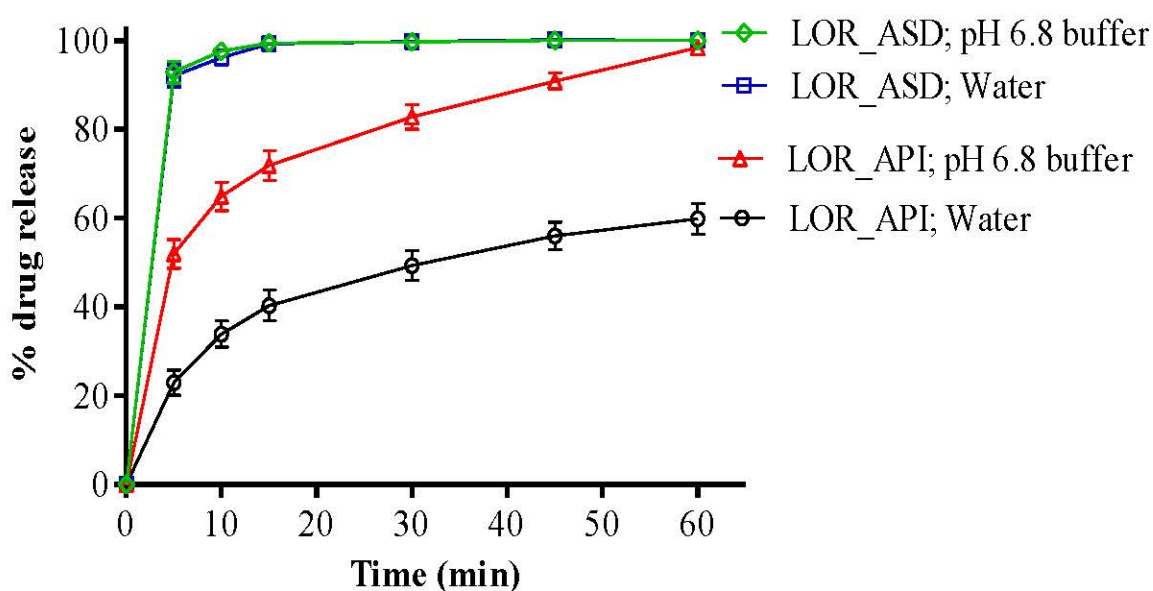
Fig. 5.57 Drug release profile of core tablets of LOR ASD as well as LOR API in pH 6.8 phosphate buffer/water; basket apparatus; 100 rpm; 900 mL; 37.0±0.5°C [mean±SD; n=6]

5.6.3.3. Evaluation of LOR CCTs

The appearance of CCTs was found to be satisfactory. The hardness was 11.5-14.5 kp, thickness was 5.9-6.0 mm and friability was less than 0.5%. Assay and weight variation results were found to be within their respective specification limits.

5.6.3.3.1. *In vitro* release studies (LOR CCTs)

The release studies exhibited typical 4-6 h of lag time followed by sharp burst release (>85%) within 15 min of outer coat rupturing with all tested conditions except hydro-alcoholic media (in which the lag time did not remain confine to 4-6 h). The dissolution profile of LOR CCTs obtained with basket apparatus; 100 rpm; 0.1 N HCl followed by pH 6.8 phosphate buffer is displayed in Figure 5.58. The individual lag time results obtained with various dissolution conditions are demonstrated in Figure 5.59. As shown in Figure, no significant difference was observed between the lag times of multi-media, change in apparatus, change in agitation intensity and biorelevant media (p value >0.05).
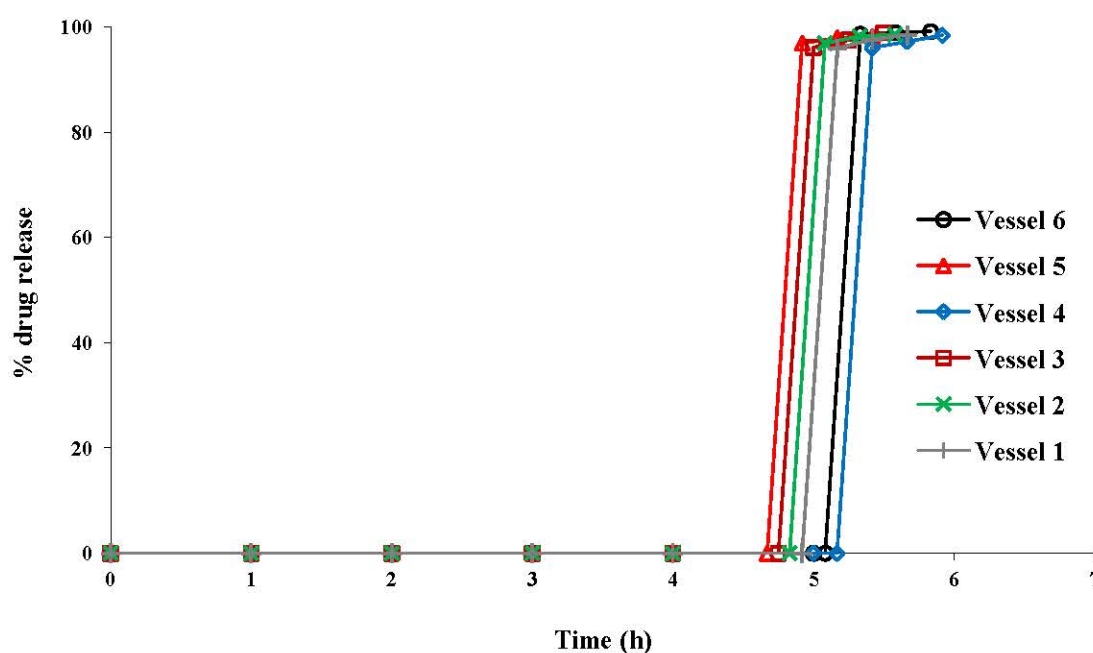
Fig. 5.58 Drug release profile of LOR CCTs obtained with basket apparatus; 100 rpm agitation; 0.1 N HCl for first 2 h followed by pH 6.8 buffer; 900 mL volume; 37±0.5°C temperature.

Same as PRS, similar release profile with multi-media dissolution corroborated the developed CCT as pH-independent in nature. Analogous release behaviour with different apparatus as well as agitation intensity inferred that the lag time was robust enough and not influenced by change in hydrodynamics. Further, akin release profiles with biorelevant media prudently anticipate promising *in vivo* performance. The results of hydro-alcoholic media were also in-line with previous CCTs, entailing pertinent instruction ought to be mentioned on the label.
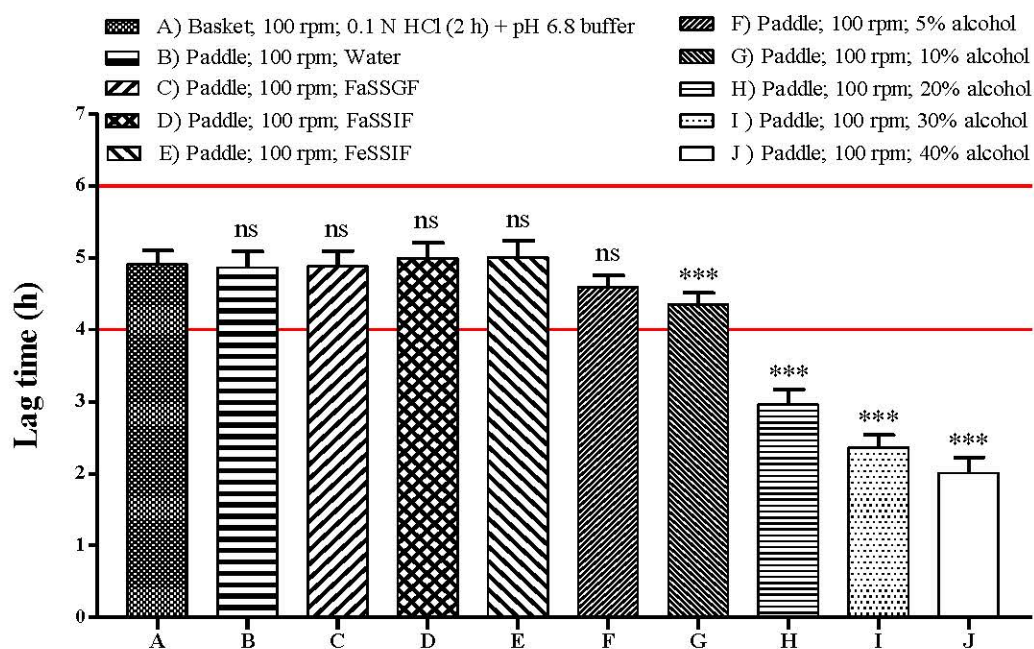
Fig. 5.59 Lag time of LOR CCTs obtained using various dissolution conditions; medium volume 900 mL; temperature $37 \pm 0.5°C$; [ns] p value>0.05, ***p value<0.001 (mean$\pm$SD; n=6)

5.6.3.3.2. Effect of curing (LOR CCTs)

After exposure of 60°C for 24 h, the CCTs, when examined for appearance, assay, hardness, and drug release, exhibited each result within their respective specification limits (Table 5.77) with no distinguishable difference before and after curing. Thus, no effect of curing was observed.

Table 5.77 Results of curing study for LOR CCTs

Effect of curing	Appearance	Hardness	Assay	Lag time*	Burst release
Before curing	White colour	11.5-14.5 kp	99.7 %	4.90 ± 0.19 h	>85% in 15 min
After curing	No change	No change	99.5 %	4.88 ± 0.24 h	>85% in 15 min

*mean$\pm$SD; n=6

5.6.3.3.3. Packaging and stability (LOR CCTs)

The CCTs demonstrated no detectable change for either of appearance, hardness, assay or drug release under stated storage conditions. Since all results were found within their respective specification limits (Table 5.78), the formulation was found to be stable under the selected packaging material and stated storage conditions.

Table 5.78 Results of stability study for LOR CCTs

Storage condition	Appearance	Hardness	Assay	Lag time*	Burst release
Initial	White colour	11.5-14.5 kp	99.7 %	4.90±0.19 h	>85% in 15 min
25±2°C/60±5% RH (3M)	No change	No change	99.4 %	4.94±0.22 h	>85% in 15 min
40±2°C/75±5% RH (3M)	No change	No change	99.2 %	4.93±0.20 h	>85% in 15 min

*mean±SD; n=6

5.6.4. Conclusion (LOR)

LOR is a poorly soluble drug which exhibits pH-dependent aqueous solubility. The solubility enhancement of LOR was achieved through formulating ASD employing MEG as a microenvironment pH-modifier and HPMC E5 as a hydrophilic carrier. The developed ASD was then employed for preparation of core tablets which was subsequently subjected to compression coating using developed CCT formula. Nonetheless, LOR CCTs also exhibited similar release behaviour as observed with previous CCTs i.e. robust and pH-independent lag time followed by burst release profile. Since all results were in-line with the previous CCTs, it was construed that replacement of former drugs with LOR (despite of formulating ASD) did not alter the desired quality traits of developed PR CCT.

5.7. Developed compression-coated PR formulation – A platform technology

The step-by-step development process of compression-coated PR formulation is illustrated in Figure 5.60. Overall, the developed PR CCT exhibited 4-6 h of lag time followed by burst release profile with six different drugs (i.e. PRS, MPR, DIC, DIL, NIF and LOR) and varying dissolution conditions (viz. multi-media, change in apparatus, change in agitation intensity and biorelevant media). The holistic outcome of the research undertaken is exemplified in Figure 5.61.

The release profile remained robust enough even after employing different formulation approaches in fabrication of varied core tablets on account of diverse drug properties. The lag time was found to be independent of change in pH as well as unaffected by change in hydrodynamics. Further, analogous results of biorelevant dissolutions prudently anticipate promising *in vivo* performance. Since the developed CCT exhibited similar profile with all six drug molecules at different dissolution conditions, it can be qualified as a time-controlled PR platform technology which can also extend its arms to several other APIs such as salbutamol (asthma), terbutaline (asthma), glucocorticoids (asthma/rheumatoid arthritis) etc. and thereby benefit patients with rather rationalised chronodelivery systems. In nutshell, the developed CCT has greater prospects and therapeutic options to be useful in the management of early morning chronological outbreaks; however human clinical trials are obligatory to prove the clinical usability of developed formulation.

Drug properties
Mol wt- 358.4
Nature- neutral,
pKa- none,
Log P 1.5,
Dose 5 mg

→ Development of compression coated PRS tablets

⇓

Establishment of QTPP

⇓

Identification of CQAs

⇓

Initial risk assessment of critical
formulation/process parameters

⇓

Excipients; MCC, lactose,
SSG, Colloidal SiO$_2$, MgSt

→ Formulation of IR core tablets → >85% release within 15 min

⇓

Development of PR CCTs

Hydrophobic polymer – EC N10

Colloidal SiO$_2$, MgSt, talc,
stearic acid, SSF, Glyceryl
behenate, PEG 6000

Selection of lubricant and glidant   [OFAT]

Glidant Talc
Lubricant SSF

PEG 4000, HPMC E5, Povidone
K30, copovidone, HPC EF,
HPC SSL, lactose, mannitol

[OFAT]   Selection of hydrophilic additives

HPMC E5

HPMC E5, E15, E50,
K100LV and K4M

Selection of HPMC MW   [OFAT]

HPMC E5

Risk assessment by FMEA

⇓

Risk mitigation of
core elements

High   High

[OFAT]   Core hardness   Core SSG   [OFAT]

Low   Low

Risk mitigation of
coating elements

High

[OFAT]   CCT hardness

Low

High   High

[CCD]   HPMC level optimization   Coating weight optimization   [CCD]

Low   Low

Optimized PRS CCT → **4-6 h lag time followed by
>85% release within 15 min**

⇓

Continue to next page

Fig. 5.60 Step-by-step development of compression-coated PR platform formulation

Optimized PRS CCTs (continue from previous page)

Development of MPR CCTs	**Development of DIC CCTs**	**Development of DIL CCTs**	**Development of NIF CCTs**	**Development of LOR CCTs**
Mol wt 374.5 Nature neutral pKa none Log P 1.8 Dose 4 mg	Mol wt 318.1 Nature weak acid pKa 3.8 Log P 4.4 Dose 25 mg	Mol wt 451.0 Nature weak base pKa 7.7 Log P 2.8 Dose 30 mg	Mol wt 346.3 Nature weak acid pKa_1 -0.9, pKa_2 13 Log P 2.2 poorly soluble Dose 5 mg	Mol wt 371.8 Nature weak acid pKa 4.7 Log P 1.8 poorly soluble Dose 4 mg
	Preparation of API granules using water as granulating agent	Preparation of API granules using water as granulating agent	Enhancement of solubility by formulating ASD employing COP as hydrophilic carrier	Enhancement of solubility by formulating ASD employing MEG as pH modifier and HPMC E5 as hydrophilic carrier

Formulation of IR core tablets

Same as PRS except adjustment of lactose quantity to compensate the dose difference	Same as PRS except granular API was used and lactose quantity was adjusted to compensate the dose difference	Same as PRS except granular API was used and lactose quantity was adjusted to compensate the dose difference	Same as PRS except ASD was used and lactose quantity was adjusted to compensate the dose difference	Same as PRS except ASD was used, lactose was replaced with mannitol, and quantity of mannitol was adjusted to compensate the dose difference
>85% release within 15 min	>85% release within 15 min	>85% release within 15 min	>85% release within 30 min	>85% release within 15 min

Fabrication of outer coat (same as PRS)

4-6 h lag time followed by >85% release within 15 min	4-6 h lag time followed by >85% release within 15 min	4-6 h lag time followed by >85% release within 15 min	4-6 h lag time followed by >85% release within 30 min	4-6 h lag time followed by >85% release within 15 min

Compression coated PR platform formulation providing 4-6 h lag time followed by burst release profile
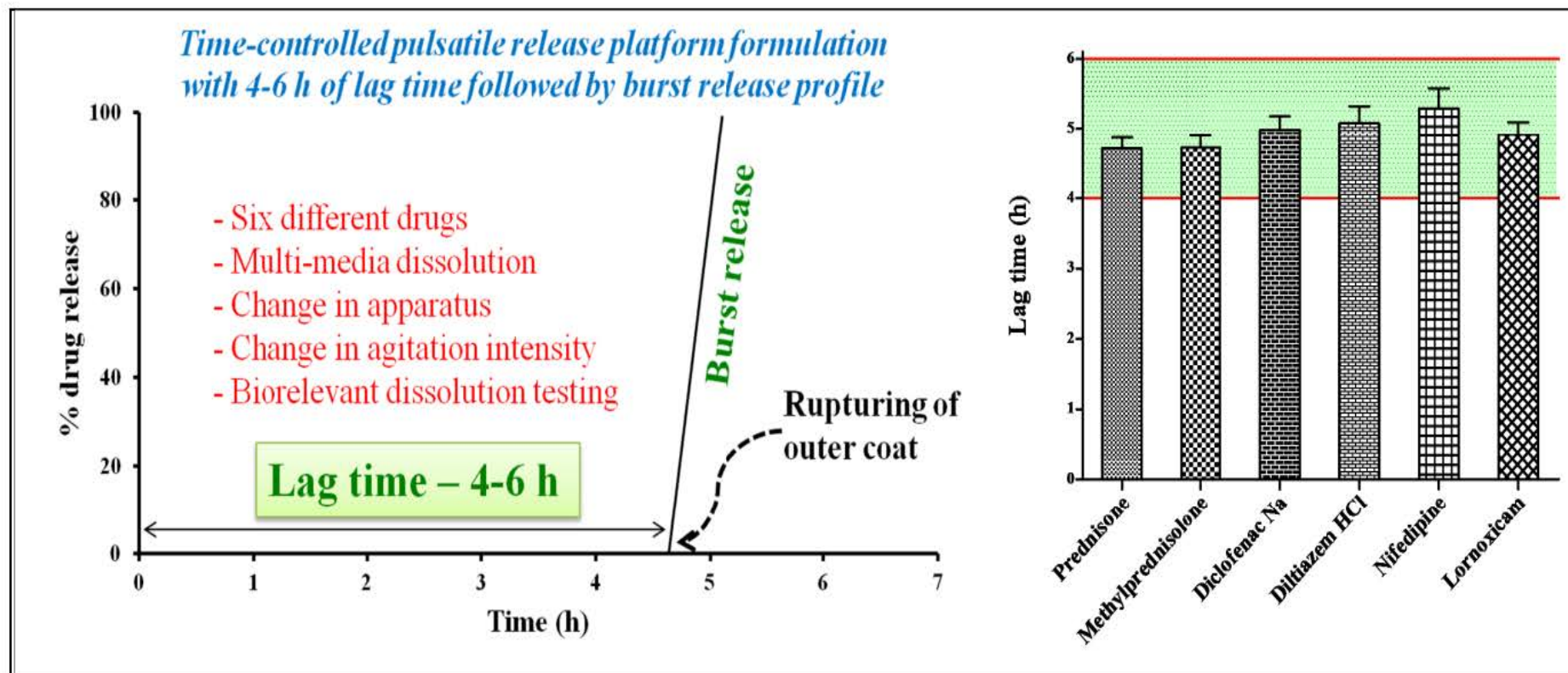
Fig. 5.61 Holistic overview of developed compression-coated PR platform formulation (error bar depicts mean with 95% CI; n=6)

References

1. Lin SY, Kawashima Y. Current status and approaches to developing press-coated chronodelivery drug systems. Journal of Controlled Release 2012;157(3):331-353.

2. Bose S, Bogner RH. Solventless pharmaceutical coating processes: a review. Pharmaceutical Development and Technology 2007;12(2):115-131.

3. Maroni A, Zema L, Cerea M, Sangalli ME. Oral pulsatile drug delivery systems. Expert Opinion on Drug Delivery 2005;2(5):855-871.

4. Maroni A, Zema L, Curto MDD, Loreti G, Gazzaniga A. Oral pulsatile delivery: Rationale and chronopharmaceutical formulations. International Journal of Pharmaceutics 2010;398(1):1-8.

5. Patil SS, Shahiwala A. Patented pulsatile drug delivery technologies for chronotherapy. Expert Opinion on Therapeutic Patents 2014;24(8):845-856.

6. Smolensky MH, Peppas NA. Chronobiology, drug delivery, and chronotherapeutics. Advanced Drug Delivery Reviews 2007;59(9):828-851.

7. Voct M, Derendorf H, Kramer J, Junginger H, Midha K, Shah V, Stavchansky S, Dressman JB, Barends DM. Biowaiver monographs for immediate release solid oral dosage forms: Prednisone. Journal of Pharmaceutical Sciences 2007;96(6):1480-1489.

8. British Pharmacopoeia. London: The stationery office on behalf of the Medicines and Healthcare products Regulatory Agency (MHRA), 2009.

9. Moffat AC, Osselton MD, Widdop B. Clarke's analysis of drugs and poisons. Third edn. London: Pharmaceutical Press, 2004.

10. Corticosteroids (Systemic): Drug Information Online Drugs.com; http://www.drugs.com/mmx/medrol.html (Accessed Feb 15, 2016).

11. Prednisone Drug Information Drugbank; http://www.drugbank.ca/drugs/DB00635 (Accessed Feb 15, 2016).

12. Prednisone - Compound Summary (CID 5865): NCBI Pubchem compound; http://pubchem.ncbi.nlm.nih.gov/summary/summary.cgi?q=all&cid=5865#ec (Accessed Feb 15, 2016).

13. Prednisone Drug Information Dailymed; http://dailymed.nlm.nih.gov/dailymed/drugInfo.cfm?setid=a784f545-f209-46d4-9350-ae64fad9e07c (Accessed Feb 15, 2016).

14. Salem M, Tainsh Jr RE, Bromberg J, Loriaux DL, Chernow B. Perioperative glucocorticoid coverage. A reassessment 42 years after emergence of a problem. Annals of Surgery 1994;219(4):416-425.

15. O'Driscoll B, Kalra S, Pickering C, Carroll K, Woodcock A, Wilson M. Double-blind trial of steroid tapering in acute asthma. The Lancet 1993;341(8841):324-327.

16. Hatton M, Vathenen A, Allen M, Davies S, Cooke N. A comparison of 'abruptly stopping'with 'tailing off'oral corticosteroids in acute asthma. Respiratory Medicine 1995;89(2):101-104.

17. Wenning G, Wiethölter H, Schnauder G, Müller P, Kanduth S, Renn W. Recovery of the hypothalamic-pituitary-adrenal axis from suppression by short-term, high-dose intravenous prednisolone therapy in patients with MS. Acta Neurologica Scandinavica 1994;89(4):270-273.

18. Busse W. Expert Panel Report-3: Guidelines for the diagnosis and management of asthma-summary report 2007. National Asthma Education and Prevention Program. The Journal of Allergy and Clinical Immunology 2007;120(5):S94-S138.

19. Jindal S, Gupta D, Aggarwal A, Agarwal R. Guidelines for management of asthma at primary and secondary levels of health care in India (2005). The Indian Journal of Chest Diseases & Allied Sciences 2005;47(4):309-343.

20. British Thoracic Society Scottish Intercollegiate Guidelines Network. British guideline on the management of asthma. Thorax 2008;63:1-121.

21. Kowanko I, Pownall R, Knapp M, Swannell A, Mahoney P. Time of day of prednisolone administration in rheumatoid arthritis. Annals of The Rheumatic Diseases 1982;41(5):447-452.

22. Reinberg A, Smolensky M, D'alonzo G, McGovern J. Chronobiology and Asthma. III. Timing corticotherapy to biological rhythms to optimize treatment goals. Journal of Asthma 1988;25(4):219-248.

23. Arvidson NG, Gudbjörnsson B, Larsson A, Hällgren R. The timing of glucocorticoid administration in rheumatoid arthritis. Annals of The Rheumatic Diseases 1997;56(1):27-31.

24. Moeller H. Chronopharmacology of hydrocortisone and 9α-fluorhydrocortisone in the treatment for congenital adrenal hyperplasia. European Journal of Pediatrics 1985;144(4):370-373.

25. ICH Q2 (R1), Validation of analytical procedures: text and methodology. ICH harmonised tripartite guideline, 2005; http://www.ich.org/fileadmin/Public_Web_Site/ICH_Products/Guidelines/Quality/ Q2_R1/Step4/Q2_R1__Guideline.pdf. (Accessed Feb 15, 2016).

26. United States Pharmacopoeia (USP37-NF32). Rockville,MD: The United States Pharmacopoeial Convention Inc, 2014.

27. Food and Drug Administration CDER, Draft guidance for industry and review staff: Target product profile-strategic development tool, 2007; http://www.fda.gov/cder/gmp/gmp2004/GMPfinalreport2004.htm (Accessed Feb 15, 2016).

28. Lionberger RA, Lee SL, Lee L, Raw A, Lawrence XY. Quality by design: concepts for ANDAs. The AAPS Journal 2008;10(2):268-276.

29. ICH Q8 (R2), Pharmaceutical development. ICH harmonised tripartite guideline, 2009; http://www.ich.org/fileadmin/Public_Web_Site/ICH_Products/Guidelines/Quality/ Q8_R1/Step4/Q8_R2_Guideline.pdf. (Accessed Feb 15, 2016).

30. Lawrence XY, Amidon G, Khan MA, Hoag SW, Polli J, Raju G, Woodcock J. Understanding pharmaceutical quality by design. The AAPS Journal 2014;16(4):771-783.

31. Food and Drug Administration, Final report on pharmaceutical cGMPs for the 21st century-A risk-based approach, 2003.

32. ICH Q9, Quality risk management. ICH harmonised tripartite guideline, 2005; http://www.ich.org/fileadmin/Public_Web_Site/ICH_Products/Guidelines/Quality/ Q9/Step4/Q9_Guideline.pdf. (Accessed Feb 15, 2016).

33. Vora C, Patadia R, Mittal K, Mashru R. Risk based approach for design and optimization of stomach specific delivery of rifampicin. International Journal of Pharmaceutics 2013;455(1):169-181.

34. Vora C, Patadia R, Mittal K, Mashru R. Risk based approach for design and optimization of site specific delivery of isoniazid. Journal of Pharmaceutical Investigation 2015;45(2):249-264.

35. Lin SY, Li MJ, Lin KH. Hydrophilic excipients modulate the time lag of time-controlled disintegrating press-coated tablets. AAPS PharmSciTech 2004;5(4):25-29.

36. Nunthanid J, Luangtana-Anan M, Sriamornsak P, Limmatvapirat S, Huanbutta K, Puttipipatkhachorn S. Use of spray-dried chitosan acetate and ethylcellulose as compression coats for colonic drug delivery: Effect of swelling on triggering in vitro drug release. European Journal of Pharmaceutics and Biopharmaceutics 2009;71(2):356-361.

37. Rane AB, Gattani SG, Kadam VD, Tekade AR. Formulation and evaluation of press coated tablets for pulsatile drug delivery using hydrophilic and hydrophobic polymers. Chemical and Pharmaceutical Bulletin 2009;57(11):1213-1217.

38. Rujivipat S, Bodmeier R. Improved drug delivery to the lower intestinal tract with tablets compression-coated with enteric/nonenteric polymer powder blends. European Journal of Pharmaceutics and Biopharmaceutics 2010;76(3):486-492.

39. Rowe RC, Sheskey PJ, Quinn ME. Handbook of pharmaceutical excipients. Sixth edn. London: Pharmaceutical press, 2009.

40. Patadia R, Vora C, Mittal K, Mashru R. Dissolution criticality in developing solid oral formulations: from inception to perception. Critical Reviews in Therapeutic Drug Carrier Systems 2013;30(6):495-534.

41. ICH Q1A (R2), Stability testing of new drug substances and products. ICH harmonised tripartite guideline, 2003; http://www.ich.org/fileadmin/Public_Web_Site/ICH_Products/Guidelines/Quality/ Q1A_R2/Step4/Q1A_R2__Guideline.pdf. (Accessed Feb 15, 2016).

42. Li J, Wu Y. Lubricants in pharmaceutical solid dosage forms. Lubricants 2014;2(1):21-43.

43. Wang J, Wen H, Desai D. Lubrication in tablet formulations. European Journal of Pharmaceutics and Biopharmaceutics 2010;75(1):1-15.

44. Augsburger LL, Shangraw RF. Effect of glidants in tableting. Journal of Pharmaceutical Sciences 1966;55(4):418-423.

45. Roberts M, Ford JL, MacLeod GS, Fell JT, Smith GW, Rowe PH, Dyas AM. Effect of lubricant type and concentration on the punch tip adherence of model ibuprofen formulations. Journal of Pharmacy and Pharmacology 2004;56(3):299-305.

46. Aly S. The resistance to compression index as a parameter to evaluate the efficacy of lubricants in pharmaceutical tabletting. Journal of Drug Delivery Science and Technology 2006;16(2):151-155.

47. Perrault M, Bertrand F, Chaouki J. An experimental investigation of the effect of the amount of lubricant on tablet properties. Drug Development and Industrial Pharmacy 2011;37(2):234-242.

48. Cabot Corporation. Technical literature. TD-169: Applications of CAB-O-SIL M-5P Fumed Silica in the Formulation and Design of Solid Dosage Forms, 2004; http://www.cabot-corp.com/wcm/download/en-us/fs/TD-169%20Applications.pdf (Accessed Feb 15, 2016).

49. Yüksel N, Türkmen B, Kurdoğlu AH, Başaran B, Erkin J, Baykara T. Lubricant efficiency of magnesium stearate in direct compressible powder mixtures comprising cellactose 80 and pyridoxine hydrochloride. FABAD Journal of Pharmaceutical Sciences 2007;32:173-183.

50. Evonik Industries. Technical Information TI 1281-1: Aerosil and Aeroperl Colloidal Silicon Dioxide for Pharmaceuticals, 2013; http://www.aerosil.com/product/aerosil/Documents/TI-1281-AEROSIL-and-AEROPERL-Colloidal-Silicon-Dioxide-for-Pharmaceuticals-EN.pdf (Accessed Feb 15, 2016).

51. Gore AY, Banker GS. Surface chemistry of colloidal silica and a possible application to stabilize aspirin in solid matrixes. Journal of Pharmaceutical Sciences 1979;68(2):197-202.

52. Monkhouse DC, Lach JL. Use of adsorbents in enhancement of drug dissolution I. Journal of Pharmaceutical Sciences 1972;61(9):1430-1435.

53. Aerde PV, Pimhatavioot P, Synave R, Severen V. Direct compression of piracetam. Drug Development and Industrial Pharmacy 1987;13(2):225-234.

54. Williams RO, McGinity JW. Compaction properties of microcrystalline cellulose and sodium sulfathiazole in combination with talc or magnesium stearate. Journal of Pharmaceutical Sciences 1989;78(12):1025-1034.

55. Patadia R, Vora C, Mittal K, Mashru R. Investigating critical effects of variegated lubricants, glidants and hydrophilic additives on lag time of press coated ethylcellulose tablets. Pharmaceutical Development and Technology 2015;21(3): 302-310.

56. Guo JH, Skinner G, Harcum W, Barnum P. Pharmaceutical applications of naturally occurring water-soluble polymers. Pharmaceutical Science & Technology Today 1998;1(6):254-261.

57. Ashland. Pharmaceutical excipients and tablet coating systems. PC-10641.2, 2011; http://www.ashland.com/Ashland/Static/Documents/ASI/PRO_250-72_Excipients_and_Tablet_Coating.pdf. (Accessed Feb 15, 2016).

58. Ashland. Product grades available. PC-11608.7, 2014; http://www.ashland.com/Ashland/Static/Documents/ASI/PC_11608_Product_Grades_Available.pdf. (Accessed Feb 15, 2016).

59. Ashland. Benecel hydrohypropyl methylcellulose for personal care: high purity, water-soluble non-ionic cellulose ethers. PC-10642.3, 2013; http://www.ashland.com/Ashland/Static/Documents/ASI/PC_10642_Benecel_HPMC.pdf. (Accessed Feb 15, 2016).

60. Katzhendler I, Hoffman A, Goldberger A, Friedman M. Modeling of drug release from erodible tablets. Journal of Pharmaceutical Sciences 1997;86(1):110-115.

61. Hao J, Wang F, Wang X, Zhang D, Bi Y, Gao Y, Zhao X, Zhang Q. Development and optimization of baicalin-loaded solid lipid nanoparticles prepared by coacervation method using central composite design. European Journal of Pharmaceutical Sciences 2012;47(2):497-505.

62. Singh B, Kumar R, Ahuja N. Optimizing drug delivery systems using systematic" design of experiments." Part I: fundamental aspects. Critical Reviews in Therapeutic Drug Carrier Systems 2005;22(1):27-105.

63. Dressman JB, Amidon GL, Reppas C, Shah VP. Dissolution testing as a prognostic tool for oral drug absorption: immediate release dosage forms. Pharmaceutical Research 1998;15(1):11-22.

64. Galia E, Nicolaides E, Hörter D, Löbenberg R, Reppas C, Dressman J. Evaluation of various dissolution media for predicting in vivo performance of class I and II drugs. Pharmaceutical Research 1998;15(5):698-705.

65. Jantratid E, Janssen N, Reppas C, Dressman JB. Dissolution media simulating conditions in the proximal human gastrointestinal tract: an update. Pharmaceutical Research 2008;25(7):1663-1676.

66. Vertzoni M, Dressman J, Butler J, Hempenstall J, Reppas C. Simulation of fasting gastric conditions and its importance for the in vivo dissolution of lipophilic compounds. European Journal of Pharmaceutics and Biopharmaceutics 2005;60(3):413-417.

67. Aburub A, Risley DS, Mishra D. A critical evaluation of fasted state simulating gastric fluid (FaSSGF) that contains sodium lauryl sulfate and proposal of a modified recipe. International Journal of Pharmaceutics 2008;347(1):16-22.

68. Reppas C, Vertzoni M. Biorelevant in-vitro performance testing of orally administered dosage forms. Journal of Pharmacy and Pharmacology 2012;64(7):919-930.

69. Individual Product Bioequivalence Recommendations: In: US FDA; http://www.fda.gov/Drugs/GuidanceComplianceRegulatoryInformation/Guidances /ucm075207.htm. (Accessed Feb 15, 2016).

70. Anand O, Lawrence XY, Conner DP, Davit BM. Dissolution testing for generic drugs: an FDA perspective. The AAPS Journal 2011;13(3):328-335.

71. Methylprednisolone Drug Information Drugs.com; http://www.drugs.com/methylprednisolone.html (Accessed Feb 15, 2016).

72. Szefler S, Ebling W, Georgitis J, Jusko W. Methylprednisolone versus prednisolone pharmacokinetics in relation to dose in adults. European Journal of Clinical Pharmacology 1986;30(3):323-329.

73. Hill MR, Szefler SJ, Ball BD, Bartoszek M, Brenner AM. Monitoring glucocorticoid therapy: a pharmacokinetic approach. Clinical Pharmacology & Therapeutics 1990;48(4):390-398.

74. Zhu C, Jiang L, Chen TM, Hwang KK. A comparative study of artificial membrane permeability assay for high throughput profiling of drug absorption potential. European Journal of Medicinal Chemistry 2002;37(5):399-407.

75. Methylprednisolone Summary report 1. The European Agency for the evaluation of the medicinal products, Committee for veterinary medicinal products, 1999; http://www.ema.europa.eu/docs/en_GB/document_library/Maximum_Residue_Li mits_-_Report/2009/11/WC500015079.pdf (Accessed Feb 15, 2016).

76. Methylprednisolone Drug Information Dailymed; http://dailymed.nlm.nih.gov/dailymed/drugInfo.cfm?setid=7bf4d3d3-3f8a-4e20-9194-061658efca61 (Accessed Feb 15, 2016).

77. Methylprednisolone compound summary (CID 6741): NCBI Pubchem compound, 2005; http://pubchem.ncbi.nlm.nih.gov/summary/summary.cgi?cid=6741#x27 (Accessed Feb 15, 2016).

78. Methylprednisolone Drug Information Drugbank; http://www.drugbank.ca/drugs/DB00959 (Accessed Feb 15, 2016).

79. Al-Habet S, Rogers HJ. Methylprednisolone pharmacokinetics after intravenous and oral administration. British Journal of Clinical Pharmacology 1989;27(3):285-290.

80. Chuasuwan B, Binjesoh V, Polli J, Zhang H, Amidon G, Junginger H, Midha KK, Shah VP, Stavchansky S, Dressman JB, Barends DM. Biowaiver monographs for immediate release solid oral dosage forms: Diclofenac sodium and diclofenac potassium. Journal of Pharmaceutical Sciences 2009;98(4):1206-1219.

81. Diclofenac Drug Information Drugbank; http://www.drugbank.ca/drugs/DB00586 (Accessed Feb 15, 2015).

82. Diclofenac sodium Information Dailymed; https://dailymed.nlm.nih.gov/dailymed/drugInfo.cfm?id=1507 (Accessed Feb 15, 2016).

83. Mazzo DJ, Obetz CL, Shuster J. Diltiazem Hydrochloride. In: Harry GB, Ed. Analytical Profiles of Drug Substances and Excipients. London: Academic Press, 1994:53-98.

84. Prabhu NB, Marathe AS, Jain S, Singh PP, Sawant K, Rao L, Amin PD. Comparison of dissolution profiles for sustained release resinates of BCS Class I drugs using USP apparatus 2 and 4: A technical note. AAPS PharmSciTech 2008;9(3):769-773.

85. Tapia C, Montezuma V, Yazdani-Pedram M. Microencapsulation by spray coagulation of diltiazem HCl in calcium alginate-coated chitosan. AAPS PharmSciTech 2008;9(4):1198-1206.

86. Buckley MM, Grant SM, Goa KL, McTavish D, Sorkin EM. Diltiazem. A reappraisal of its pharmacological properties and therapeutic use. Drugs 1990;39(5):757-806.

87. Diltiazem Drug Information Dailymed; http://dailymed.nlm.nih.gov/dailymed/drugInfo.cfm?setid=da1c1a8e-c9dd-4c20-b061-638f2d0cecda (Accessed Feb 15, 2016).

88. Diltiazem Drug Information Drugs.com; http://www.drugbank.ca/drugs/db00343 (Accessed Feb 15, 2016).

89. Scholz H. Pharmacological aspects of calcium channel blockers. Cardiovascular Drugs and Therapy 1997;10(3):869-872.

90. Gajendran J, Krämer J, Shah VP, Langguth P, Polli J, Mehta M, Groot D, Cristofoletti R, Abrahamsson B, Dressman J. Biowaiver monographs for immediate release solid oral dosage forms: Nifedipine. Journal of Pharmaceutical Sciences 2015;104(10):3289-3298.

91. Plumley C, Gorman EM, El-Gendy N, Bybee CR, Munson EJ, Berkland C. Nifedipine nanoparticle agglomeration as a dry powder aerosol formulation strategy. International Journal of Pharmaceutics 2009;369(1):136-143.

92. Sorkin EM, Clissold SP, Brogden RN. Nifedipine. A review of its pharmacodynamic and pharmacokinetic properties, and therapeutic efficacy, in ischaemic heart disease, hypertension and related cardiovascular disorders. Drugs 1985;30(3):182-274.

93. Nifedipine Drug Information Drugbank; http://www.drugbank.ca/drugs/db01115 (Accessed Feb 15, 2016).

94. Vora C, Patadia R, Mittal K, Mashru R. Preparation and characterization of dipyridamole solid dispersions for stabilization of supersaturation: effect of precipitation inhibitors type and molecular weight. Pharmaceutical Development and Technology 2015;Epub ahead of print:1-9 (DOI: 10.3109/10837450.2015.1069330).

95. Chutimaworapan S, Ritthidej G, Yonemochi E, Oguchi T, Yamamoto K. Effect of water-soluble carriers on dissolution characteristics of nifedipine solid dispersions. Drug Development and Industrial Pharmacy 2000;26(11):1141-1150.

96. Ahmed MO, Al-Badr AA. Lornoxicam. In: Harry GB, ed. Profiles of Drug Substances, Excipients and Related Methodology. London: Academic Press, 2011:205-239.

97. Skjodt NM, Davies NM. Clinical pharmacokinetics of lornoxicam: A short half-life oxicam. Clinical pharmacokinetics 1998;34(6):421-428.

98. Balfour JA, Fitton A, Barradell LB. Lornoxicam: A review of its pharmacology and therapeutic potential in the management of painful and inflammatory conditions. Drugs 1996;51(4):639-657.

99. Hamza Y, Aburahma MH. Design and in vitro evaluation of novel sustained-release matrix tablets for lornoxicam based on the combination of hydrophilic

matrix formers and basic pH-modifiers. Pharmaceutical Development and Technology 2010;15(2):139-153.

100. Shakeel F, Haq N, Alanazi FK, Alsarra IA. Solubility of anti-inflammatory drug lornoxicam in ten different green solvents at different temperatures. Journal of Molecular Liquids 2015;209:280-283.

101. Suresh K, Nangia A. Lornoxicam salts: crystal structures, conformations, and solubility. Crystal Growth & Design 2014;14(6):2945-2953.

102. Verma RK, Garg S. Selection of excipients for extended release formulations of glipizide through drug-excipient compatibility testing. Journal of Pharmaceutical and Biomedical Analysis 2005;38(4):633-644.